THESIS

DETERMINING PRIMARY DRIVERS OF RIVER BEAD FUNCTIONALITY IN MOUNTAIN HEADWATER STREAMS

Submitted by

Katherine Larkin

Department of Geosciences

In partial fulfillment of requirements

For the Degree of Master of Science

Colorado State University

Fort Collins, Colorado

Summer 2025

Master's Committee:

Advisor: Ellen Wohl

Sara Rathburn
Ryan Morrison

Copyright by Katherine Larkin 2025

All Rights Reserved

ABSTRACT

DETERMINING PRIMARY DRIVERS OF RIVER BEAD FUNCTIONALITY IN MOUNTAIN HEADWATER STREAMS

I evaluated flux attenuation potential, or functionality, in laterally extensive storage-dominated reaches known as 'beads.' Beads are disproportionately important to river corridor health. Bead functionality was evaluated as a relationship between driver variables, which directly measure or measure proxies of geomorphic and biotic system inputs, and response variables, which are proxy variables believed to most accurately reflect flux travel time and storage magnitude, assuming that functional beads contribute to higher travel times and storage magnitudes. Geomorphic driver variables include catchment and reach-scale geometry and catchment hydrology, which approximate water inputs into the stream corridor, as well as delta normalized burn index (dNBR) and catchment slope, which approximate sediment inputs into the stream corridor. Biotic driver variables include wood load, beaver modifications, and riparian vegetation. Response variables include normalized difference vegetation index (NDVI), normalized difference water index (NDWI), patch density, and total sinuosity. Driver and response variables were measured through a mixture of fieldwork and remote data for 52 beads in 27 catchments in the Colorado Front Range. Statistical analysis examined relationships between drivers and responses and also examined the effectiveness of grouping the beads in different ways (by dominant vegetation, level of disturbance, and elevation). Analyses suggest that bead functionality is most strongly linked to bead ratio, or the ratio of bead size to catchment size. Generally, functional beads have a higher ratio of bead size to catchment size. In addition,

beads can be efficiently grouped by dominant vegetation; these different types of beads display significant differences in catchment geometry, bead geometry, geomorphic inputs, and biotic inputs. Although functionality was found to be the complex result of numerous factors and may require case-by-case assessment efforts, restoration of channel-floodplain connectivity and facilitating greater retention of water will provide the biggest return on river restoration investment by increasing the width of the active floodplain. Researching drivers of functionality also provides a crucial link between system inputs, restoration action, and desired reaction, allowing plans to be tailored to address targets. In addition, certain aspects of functionality – namely position and geometry – cannot be feasibly modified, and thus the functionality framework can be used to pick a site with the greatest potential for restoration.

ACKNOWLEDGEMENTS

This research was funded by USDA Forest Service Agreement No. 23-CS-11221634-046. Additional funding was provided through a Geological Society of America Graduate Student Research Grant, a Marie Morisawa Graduate Fellowship, and a Class of 73 Scholars Award. Fieldwork was conducted in Rocky Mountain National Park via a National Park Service Research Permit. Huge thank you to Shayla Triantafillou, Owen Richardson, and Aaron Katz for their help in the field, and to Taryn Contento, Anna Cloud, Larry Dale, and Scot Barker for site-specific assistance. Thank you to my committee, Ryan Morrison and Sara Rathburn, for their valuable expertise and support. Thank you to my friends and "flamily" for being supremely talented at morale-boosting and creating distraction. I also can't give you all enough credit for sharing wisdom wherever possible - it takes a village to write a thesis (is that how the saying goes?). Extra-special thanks to my advisor, Ellen Wohl, for taking me on, nurturing my curiosity, and helping to shape me as a scientist and a person. There is no one on Earth with a mind as brilliant or a heart as huge. Infinite chocolate-covered mint Oreos for you! Endless gratitude to my parents, sister, and other loved ones for their support and kindness, and, crucially, indulging me when I rant about anything related to this project. That's what love is all about. Thank you, Mom, for your day of fieldwork with me – the stream we worked on is now known as Witiak Creek for you. Dad, if you had been able to visit when I was still doing fieldwork there would've been a Larkin Creek, I promise. Lastly, to little Katie – we did it!!!

TABLE OF CONTENTS

LIST OF TABLES

LIST OF FIGURES

1. INTRODUCTION

1.1 Beads & Strings

Rivers are complex systems, adjusting to frequently fluctuating inputs of sediment, water, and nutrients on varied spatial and temporal scales. The stream corridor, defined here as the active channels, hyporheic zone, and adjacent riparian zone and floodplains, shapes and is shaped by these inputs over time. The length of a stream corridor from source to mouth can be subdivided into sections of similar hydrology and morphology, or reaches, typically tens to hundreds of meters long. Bedrock properties, including fracture density and geometry, influence longitudinal variations in stream corridor geometry; erodible and highly fractured bedrock encourages valley widening and storage of water, supporting wetland vegetation, allowing room for channel complexity and meandering, and facilitating further storage (Ehlen & Wohl, 2022; Wohl, 2008). These relatively wide, low-gradient, storage-dominated reaches, referred to in this study as “beads”, alternate with narrow, steep, transport-dominated “strings” along mountain streams (Stanford and Ward, 1993) (Figure 1). Beads are spatially distinct portions of stream corridors due to their flat and laterally extensive geometry, which contrasts with the lateral confinement in strings. Beads store surface and subsurface water, sediment, nutrients, and organic matter, and support biodiversity, making them key to stream health (Wohl et al., 2018).

Figure 1: Aerial comparison of a bead and string on Beaver Creek, Colorado. Note differences in vegetation species (lighter green willow and marsh vegetation in bead, dark green conifers in string) and floodplain extent (wide floodplain expanse in bead, no visible floodplain in string).

A large number of studies quantify rates and volumes of storage in stream corridors (e.g., Ryan et al., 2024; Rood et al., 2006), and some literature exists on physical floodplain forms and methods of characterization (Iskin & Wohl, 2024; Thomas et al., 2015) Despite probable cause and effect between these two, very little literature has examined the feedback between flux magnitudes and modulation of these fluxes facilitated by physical floodplain forms. Flux here refers to downstream movement past a point (the end of a reach or the mouth of a catchment) of water, solutes, sediment, and particulate organic matter. I define a bead as a reach in which floodplain width is at least double bankfull channel width. Multiple factors drive bead functionality, defined here as the ability to attenuate downstream fluxes. The spatial distribution, abundance, and flux attenuation potential of the beads likely strongly influence fluxes within the entire river network. At the most fundamental level, I assume that greater spatial heterogeneity, or diversity of topography and geomorphology, as well as stronger lateral and vertical connectivity within a river bead, promote attenuation of downstream fluxes. Equally, I assume

that loss of spatial heterogeneity and connectivity can impair river flux attenuation potential and increase the risk for significant and/or lasting geomorphic and biotic change, such as transition to an alternate state of the river ecosystem, aggradation and degradation, and floodplain and/or channel abandonment.

Characterizing primary drivers of bead functionality could be widely applicable to understanding storage and transport dynamics in mountain streams from reach- to catchment-scales and to understanding factors that promote resilience to disturbances, defined here as a natural or artificial change in conditions at the reach or catchment scale that can alter fluxes into or out of the stream corridor. Some disturbances, such as debris flows, are defined events that can induce rapid and significant change in the channel and floodplain (Costa & Jarrett, 1981; Coe et al., 2014). Others, like the emplacement of dams, may have a delayed response. In addition, disturbances may act on different timescales. Natural disturbances are found in every landscape on Earth and, under normal conditions, the affected system may eventually return to conditions typical of the historical range of variability, or the diverse subset of conditions associated with spatiotemporal variations in river behavior and inputs (Morgan et al., 1994). However, artificial disturbances (dams, diversions, introduction of impervious surfaces, urban growth) that create long-term alterations may alter catchment responses by physically discouraging or preventing the system's adjustments to changes in fluxes (Furniss, 2011; Wohl, 2011). Human-induced issues such as climate change present an additional complication; the effects of climate change and human modifications in the landscape can increase the frequency of some disturbances and can decrease the resilience, or ability to adapt to change, of catchments (Furniss, 2011).

Mass impairment of catchments in the United States, combined with a lack of funding, can force environmental experts to make poorly informed decisions regarding candidates for river restoration. Restored rivers can be more resilient to disturbances, more biodiverse, and can contribute to improved water quality, among other things. The data generated from this project can improve prioritization of methods of river restoration by providing scientific background to inform decision-making. In practice, understanding of connectivity and function in rivers can be applied to select an individual site with the highest chance of widespread improvement in resilience post-restoration, maximizing the ecological and societal benefits. Producing a framework to assess bead functionality may guide process-based restoration (PBR) efforts in impaired channels by better delineating the relationships and interactions between the biosphere, geosphere, greater catchment, and reach in stream corridors. PBR utilizes understanding of stream processes to make informed engineering decisions (Beechie et al., 2010), and functionality metrics will improve this decision-making by establishing factors that can be targeted to provide the highest return on investment.

1.2 Functionality Drivers

Variables influencing stream corridor functionality (functionality drivers) can be broadly categorized as geomorphic or biotic (Figure 2). Geomorphic drivers assessed here are proxies for water and sediment inputs to the stream corridor and stream corridor geometry (ratio of floodplain/channel width). Biotic drivers assessed here are wood load, beaver modifications, and riparian vegetation.

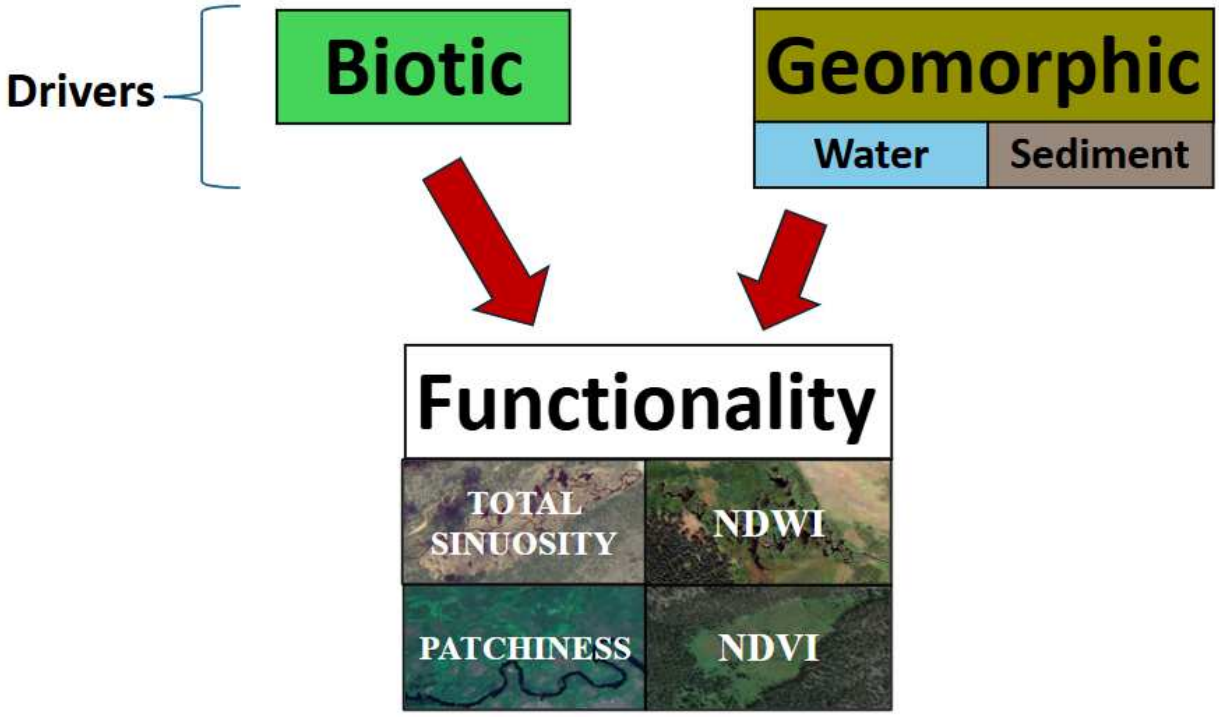

Figure 2: Figure illustrating relationship between functionality driver variables and functionality response variables. Functionality response variables and reasoning for selection are described in Section 1.3.

1.2.1 Geomorphic Drivers

The assumptions underlying the focus on geomorphic drivers are that (i) water and sediment fluxes are primary drivers of stream corridor form, (ii) increased water and sediment inputs to stream corridors during and after disturbances such as wildfire can potentially reduce bead functionality, and (iii) space available for storage, as reflected in floodplain/channel width, is a fundamental influence on fluxes and storage. Total fluxes of water and sediment into and out of each stream corridor reflect the integration of many interconnected processes, vary through time and space, and are difficult to measure accurately. In addition, these fluxes are extremely sensitive, adjusting to external factors such as drainage area and climate and to internal factors such as reach-scale geometry of the stream corridor as this enhances or limits downstream

conveyance. Fluxes vary on many temporal scales - seasonally with snowmelt, yearly with catchment- or reach-scale disturbances, and on longer timescales with climate cycles.

Human modification of catchments has fundamentally altered catchment responses to disturbances, making it increasingly difficult to capture natural response signals in a research context. Water management, such as reservoirs and diversions, places control in the hands of practitioners as primary agents of geomorphic change (Furniss, 2011; Miranda & Bettoli, 2010). Managed catchments are subject to short-term pulses of water and sediment; reservoirs in the Front Range are flushed occasionally to prevent excessive fine sedimentation (Wohl and Cenderelli, 2000). These releases can significantly impact stream corridor geometry and functionality immediately downstream of the reservoir, and the geomorphic signal associated with the increase in discharge and sediment load can propagate far downstream. Also typical are seasonal or long-term hydrograph modifications, which depend on societal and agricultural water demand. Modifications may artificially increase baseflow to maintain longitudinal connectivity or can limit peak discharge by diverting or storing excess flow during snowmelt (Wohl and Cenderelli, 2000; Wohl, 2011). Managed catchments also have modified responses to natural disturbances; human-emplaced structures and impervious surfaces, among other things, often do not effectively mimic natural ecosystems in their abilities to absorb signals and attenuate fluxes (e.g., Biron et al., 2014; Peipoch et al., 2015). Given the potentially high spatial and temporal variability and unpredictability of water and sediment fluxes, measurements of indirect factors can be used as proxies to estimate the relative magnitudes of water and sediment inputs.

Wildfires are a natural and necessary disturbance in a healthy forest – the clearing of brush and vegetation restores soil nutrients and provides room for new growth, essentially providing habitat renewal (Pausas & Keeley, 2019). However, wildfires are becoming increasingly

common due to climate-change-induced drought conditions, early snowmelt, and human interference, interrupting the once-periodic cycle of burn and growth and introducing unnecessary complications into affected landscapes (Paul et al., 2022). The effects of wildfires have been found to persist in catchments for up to five years (Paul et al., 2022), but the timelines of recovery can be varied and are difficult to predict. Severely burnt landscapes are coupled with high rates of erosion (Leonard et al., 2017) and sediment loading (Wohl et al., 2022); denudation and loss of soil cohesion leave the landscape extremely vulnerable to the effects of precipitation and hillslope processes (Moody & Martin, 2001). Additionally, the ground surface can temporarily become hydrophobic following a burn event, drastically increasing runoff to stream corridors and creating higher hydrograph peaks (Shakesby and Doerr, 2006). These increased inputs of sediment and water to post-fire waterways can cause significant floodplain-channel disconnection within a river network by facilitating increases in water velocity and consequent channel incision, as well as channel aggradation and abandonment (Wohl et. al., 2022). Following these changes, a river bead may have a diminished storage capacity and lower heterogeneity and can be in a state of disequilibrium. Impaired flux attenuation in one bead can cause a domino effect with severe consequences for ecosystems and water-users downstream.

Elevation and contributing drainage area serve as proxies for total water input to the system. Convective rainstorms do not generally occur above elevations of 2300 m in the study area, so high-elevation stream corridors are generally not subjected to flashy hydrograph responses (Jarrett, 1990; Solander et al., 2018; Kornse & Wohl, 2020) unless a catchment-scale disturbance such as wildfire has altered rainfall-runoff characteristics (Triantafillou & Wohl, 2024). Changes in rainfall-runoff relationships can initiate channel incision, sediment loading, transport and deposition of wood and logjams, and, in extreme cases, mass movements such as debris flows.

Catchments above 2300 m display peak flows in the spring and summer due to snowmelt, but these snowmelt peaks do not provide the same channel-shaping and/or bankfull velocities as precipitation events.

Sediment input was evaluated via the proxies of catchment wildfire burn severity and average catchment slope, under the assumption that burn severity and catchment steepness strongly control post-fire sediment yields (Pelletier and Orem, 2014), which are typically orders of magnitude greater than sediment yields in the Front Range under non-fire or background conditions (Ryan et al., 2024). Under this assumption, conditions in steep, severely burnt catchments are most conducive to the erosion and downslope conveyance of water and sediment and will have the highest relative sediment yields. In addition to burn severity and catchment steepness, climate also plays a significant role in determining post-fire sediment yields. Other studies have investigated the connections between topography and burn severity (Wu et. al., 2013; Lee et. al., 2009; Guo et. al, 2024; etc.). Generally, steeper high-elevation zones host more flammable vegetation and have smaller proportions of saturated/wetland soils in their basins acting as refugia zones. In addition, steeper slopes are known to increase fire spreading rates, although this depends on density and characteristics of vegetation (Butler et al., 2007; McArthur, 1968). With the increase in wildfire frequency and magnitude, the post-fire disturbance cascade has received increased attention from river scientists and practitioners (Wohl, 2024).

1.2.2 Biotic Drivers

The assumption underlying the focus on biotic drivers is that the presence of large wood, beaver modifications, and riparian vegetation increases hydraulic resistance and spatial heterogeneity of river beads and therefore increases the potential for beads to attenuate downstream fluxes of material.

In-channel woody material, such as logjams, can reduce local velocity and can facilitate localized deposition and scour, depending on the wood positioning (Manner et al., 2007). Logjams can also act as hydraulic obstacles, diverting flow, trapping fine sediment and organic matter, and raising water level. River wood load is highly dynamic – there are typically 'stick points' in a channel where entrapment of wood is commonly (or constantly) found, even though high flow has the capacity to move or alter the configuration of channel wood, changing the way in which it interacts with the channel bed and banks (Iskin & Wohl, 2022). Movement of wood is contingent on discharge, as well as jam/piece configuration and proportion of the wood piece(s) in the active channel. Wood load tends to be less dynamic in smaller channels, where the narrower dimensions limit mobility and encourage entrapment (Gurnell et al., 2002). However, snowmelt peak flows and other high flow events produce opportunities for reconfiguration and transport. Fallen wood that remains in the floodplain or is 'ramped' from the bank to the channel can act as roughness elements during high flows.

Beaver modifications also enhance floodplain-channel connectivity by slowing water velocity, trapping fine sediment, raising water level, and promoting infiltration into the channel banks and from overbank flows (Larsen et al., 2021; Wohl, 2021). Beaver modifications of the stream corridor can also create laterally extensive ponding, or beaver meadows, in adjacent floodplains. Despite historic losses of beaver population, these structures linger in fluvial corridors and can have a lasting impact on flux attenuation, channel morphology, and spatial heterogeneity (Polvi and Wohl, 2012; Wohl, 2021). Beaver-modified landscapes are also associated with riparian buffer health. Ample riparian buffers provide bank stability, decrease in-channel and overbank velocity and promote deposition of sediment (Griffin et al., 2005), and with adequate willow populations can also support and encourage beaver presence (Rosell et al.,

2005). Strong channel-floodplain connectivity is associated with higher riparian wetness values and proportion of floodplain wetlands, which create a fire-resistant buffer zone bounding stream corridors (Fairfax & Whittle, 2020).

Beaver modification is also associated with higher vegetation species richness and increased landscape patchiness; creation of ponds, dams, berms, and wetlands provides diverse conditions that support a variety of plants (Wright et al., 2002). Distinctions can be made between berms and dams; berms are inactive dams (typically covered in vegetation and breached) and dams are active, intact, and unvegetated. However, I will henceforth refer to any dam structure, active or relict, as a berm. Where necessary, identifiers such as “active”, “relict”, or “breached” will be used to provide further context.

Vegetation type and extent in the floodplain and riparian zones can strongly influence hydraulic roughness and erosional resistance of stream banks and floodplain, modifying flux attenuation within beads (Barinas et al., 2024). Vegetation can also be indicative of floodplain-channel connectivity. Connected beads typically have higher soil moisture and abundant hydrophytic vegetation, including but not limited to willow, sedges, rushes, and other wetland species. Disconnected beads typically have lower soil moisture and support grasses and conifers. Distribution and size of vegetation patches can help delineate the extent of connectivity.

Reach-scale land use changes in the stream corridor were treated as a driver in this study. Contemporary and historic land use changes can directly alter stream corridor morphology and vegetation, indirectly altering water and sediment fluxes. Land use changes often aim to increase floodplain homogeneity for development or agriculture, reduce channel lateral mobility, and reduce channel sinuosity for more efficient conveyance of water and sediment (Rak et al., 2016).

The resultant elimination of inherent channel behavior and loss of bead heterogeneity can alter bead flux attenuation potential on varied timescales.

1.3 Functionality Responses

Functionality response indicators (Figure 2) are based on proxy variables that might reflect greater storage of water or greater travel times for water entering the stream corridor. I characterized these indicators using a combination of remotely sensed and field-assessed stream corridor characteristics. The assumptions underlying the selection of these responses are that (i) functional stream corridors are laterally and vertically connected, (ii) functional stream corridors promote the attenuation of fluxes and the dampening of disturbance signals, and (iii) increases in each of these response metrics are associated with increases in functionality.

Normalized Difference Vegetation Index (NDVI) and Normalized Difference Water Index (NDWI) can be used as proxies for floodplain greenness and wetness, respectively, both of which are indicators of floodplain-channel connectivity and bead functionality (Fairfax & Whittle; Thomas et. al., 2015) and serve as a proxy for increased storage in beads. Presence of green vegetation unstressed by water limitations can be used as a proxy for water table position; grasses and other vegetation with a preference for drier soils tend to have different color signatures than the bright green marshy vegetation and willows found in wet, well-connected beads. Standing water (e.g., ponds) and presence of wetlands in the floodplain can provide similar information. Disturbed systems frequently undergo periods of incision and sedimentation, which can disconnect the channel from the floodplain and cause localized lowering of the water table; high rates of sedimentation may also fill existing ponds or wetlands (Fitzpatrick et al., 2009).

Spatial heterogeneity, or patchiness, relates to the variety of vegetation type, elevation, sediment characteristics, form, and function in a stream corridor (Iskin & Wohl, 2023). Patchiness serves as a proxy for slower travel times of fluxes, given that greater variability within a floodplain increases roughness, slowing water and amplifying its ability to store and take up materials. Increased patchiness is believed to alter river response to disturbance and improve attenuation of fluxes (Iskin & Wohl, 2023). Pulses of water and sediment entering a stream corridor with geomorphic and biotic diversity and topographic complexity are more likely to be attenuated or retained as a result of the increased hydraulic roughness.

Total sinuosity, or the ratio of primary and secondary channel length to valley length, can be used as an indicator of bead attenuation potential. Sinuous and complex channel systems facilitate slowing of water and deposition of entrained sediment; straight channel reaches do not slow/vary water velocity or encourage retention of materials as readily (Wohl & Iskin, 2022). Channel sinuosity is reflective of the ability of flows to erode the underlying substrate, distribution of stresses in the channel, discharge regime, and riparian vegetation (e.g., Lazarus and Constantine, 2013). Sinuosity can differentiate between strings and beads; smaller floodplain-channel width ratios decrease lateral channel mobility, and thus these reaches generally have lower channel sinuosity than beads. In addition to the sinuosity of the active channel, rivers with high rates of lateral mobility will carve and abandon channels over time; these relict channels create topographic relief in the floodplain and increase patchiness. Highly sinuous channels may also create additional floodplain heterogeneity, when chutes and small passages erode paths of lesser resistance between large bends.

2. OBJECTIVES

My primary objective is to evaluate whether metrics of bead functionality correlate with metrics of potential drivers. This objective can be subdivided into the objectives of (i) delineating beads on streams in the study area, (ii) quantifying bead functionality via response variables, and (iii) assessing correlations between driver and response variables. The dataset developed for this research allowed me to assess the abundance, location, and condition of beads throughout the study area. I also explored the possibility of subdividing beads into different categories (natural/modified/restored, montane/subalpine elevation zones, beaver meadow/elk grassland/forested) to evaluate whether bead functionality and characteristics differ within the dataset based on these assigned identifiers. In addition to the exploration of interactions between drivers and responses, interactions between driver variables were also investigated (Figure 3).

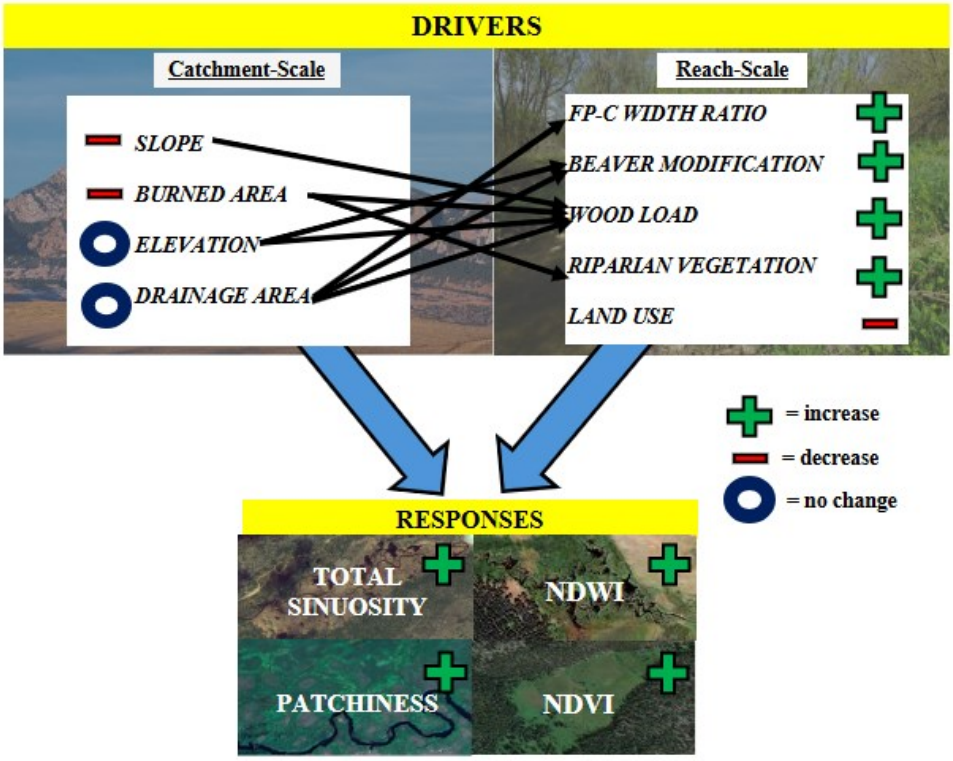

Figure 3: Conceptual model illustrating potential relationships between functionality drivers and functionality responses, as well as interactions between catchment-scale and reach-scale variables.

3. HYPOTHESES

Hypothesis 1: River bead functionality will be strongly correlated with bead categories.

The delineation of river beads serves, in practice, as a basic physical template for patterns of longitudinal variation in stream corridor geometry that are manifested as process domains. The combined effects of current and historical land uses, disturbance history, and system inputs modify this template, altering the form of beads and the biotic and geomorphic processes within them. I categorize beads by type (beaver meadow, elk grassland, forested), status (natural, impaired, restored) and elevation zone (subalpine/montane). Categories are not necessarily mutually exclusive; in particular, elk grasslands are a subset of impaired beads. I propose that

dataset divisions based on resultant vegetation cover and ecological function will show statistically significant differences in functionality.

Hypothesis 2: River bead functionality cannot be reliably defined by one metric and instead correlates with multiple driver variables.

Rivers in their entirety facilitate the downstream transport of water, sediment, and nutrients, but a river's potential to attenuate both anomalous and typical fluxes of these materials is equally important. Flux attenuation is disproportionately related to the presence of beads within the catchment. The nature of transport and storage in stream corridors is defined by numerous factors – lateral, vertical, and longitudinal contributions, climate, lithology, anthropogenic activity, and biota, among other things. Despite operating on varying scales and timeframes, these aspects are interconnected. Thus, I propose that there may not be a single driver variable that strongly correlates with metrics of bead functionality. Instead, bead functionality will correlate most strongly with a statistical model that includes multiple variables. Simple linear regression (SLR) models may, however, be used to test and eliminate variables with little influence on functionality indicator variables.

Hypothesis 3: There is a progressive relationship between bead functionality and bead size.

Bead size can be defined by both surface area and floodplain-channel width ratio. Beads with greater spatial extent and wider floodplains have greater potential for spatial and temporal heterogeneity and can store greater volumes of water and sediment. I propose that the data will illustrate a progressive relationship between bead functionality, wherein beads with higher surface areas and floodplain-channel width are more functional. A progressive relationship only implies positive coefficients and does not describe the nature of the increase; this relationship may or may not be linear. Bead surface area might or might not increase progressively with

increasing drainage area. To remove this complicating factor, I use the ratio of bead surface area to catchment area in analyses.

4. BACKGROUND

4.1 Front Range Catchments

The Cache la Poudre River, Big Thompson River, and North St. Vrain Creek serve as primary catchments containing studied subcatchments (Figure 3). All three waterways have origins high in the Rocky Mountains east of the Continental Divide and are tributaries of the South Platte River. The St. Vrain River begins at the confluence of North St. Vrain and South St. Vrain Creeks. One small subcatchment, Phantom Creek in Rocky Mountain National Park, is located west of the Continental Divide and is part of the Colorado River catchment. This subcatchment was considered under the same protocol as all others.

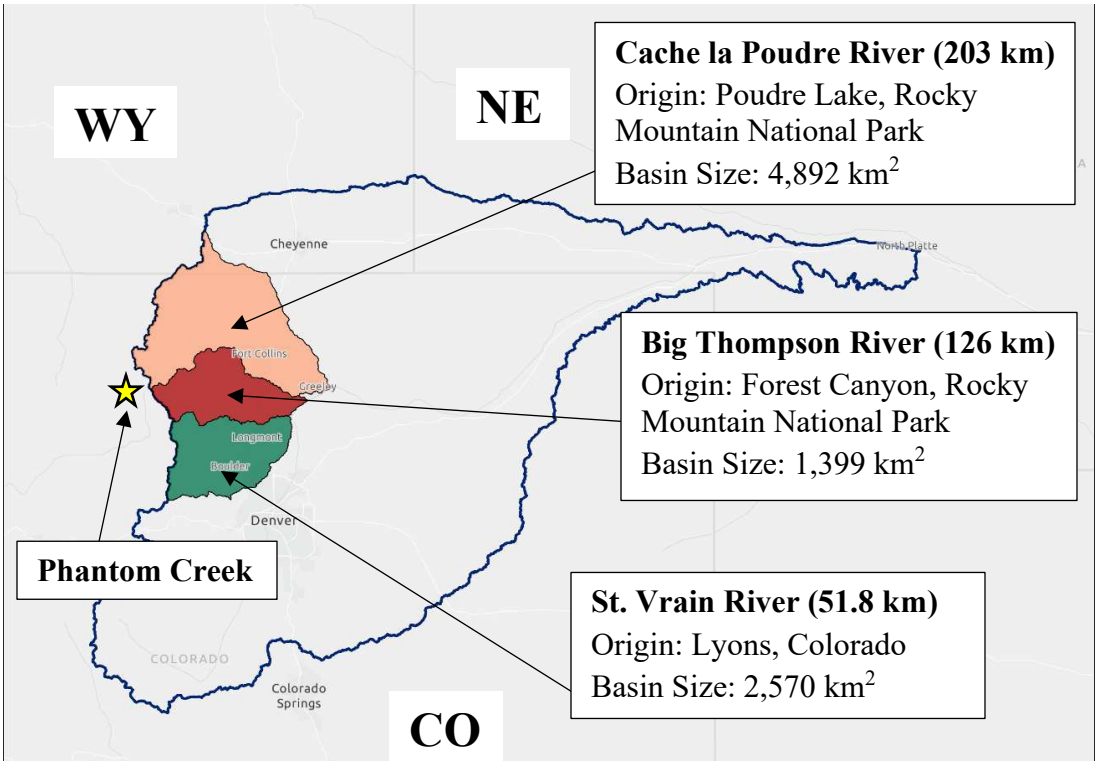

Figure 4: Flow length, flow origin, and catchment area statistics for primary study catchments and Phantom Creek. Also shown is the South Platte River catchment (outlined in navy blue), which contains all but Phantom.

The Cache la Poudre, Big Thompson, and St. Vrain are significant sources of drinking water for residents of the northern Front Range urban corridor, serving hundreds of thousands of customers. These waterways are marked with periodic diversions and dams that serve agricultural and societal needs; these features are active on a seasonal basis and typically divert peak snowmelt flow in the late spring and summer. Primary catchments have endured high degrees of human modification, but many smaller tributaries feeding into them remain unmodified. All three catchments are popular for outdoor recreation and contain coveted land parcels; as a result, they experience heavy foot traffic from hikers, bikers, rafters, residents, and others. The Big Thompson and Cache la Poudre Rivers have carved large canyons over time, in which heavily engineered roadways have been emplaced. Large floods, particularly in Big Thompson Canyon in 1976 and both canyons in 2013, caused millions of dollars in damage and

necessitated increases in flood-aware modifications, including building retaining walls and rerouting the road (McCain & Shroba, 1979; Stewart et al., 2018). In the lower segments of all catchments, rapid population growth in the Front Range urban corridor has increased the proportion of occupied land and road crossings, impacting flood response, acreage of unmodified floodplain, vegetation coverage, and water quality; all study catchments are located upstream of these heavily-modified zones, but river corridor health in the uplands can alter flux magnitudes and water quality downstream.

The Front Range is complex geologically, tectonically, and structurally and creates diversity of flow and channel geometry in the rivers that drain it. Study catchments flow through numerous geologic units, including Pre-Cambrian felsic crystalline igneous and metamorphic units in the mountainous and canyon reaches and sedimentary units through the hogbacks and onto the Great Plains (Tweto, 1979). Drainage morphologies for all catchments are dendritic. In the mountains, snowpack accumulation starts in autumn and ends in late spring as the weather warms, and the melted snow feeds nearby river networks. The nature and extent of snowpack varies year-to-year but is generally decreasing, and earlier arrivals of warmer temperatures alter hydrograph morphology into a constrained high-magnitude peak earlier in the spring and reduced peak flow in late spring and early summer (Rood et al., 2008).

The Front Range of Colorado has a semiarid climate, but the wide range of elevations found in this region contribute to spatially varied climates and biomes (Table 1). Changes in slope, lithology, climate, soil moisture, and elevation create biotically diverse zones, known as ecoregions (Figure 4). Front Range catchments with origins in the alpine zones (3,500 m +) of the Rockies flow through several ecoregions before eventually joining larger catchments in the semi-arid steppes (below 1,550 m). Study catchments are located in the montane zone and the

subalpine zones. The montane zone (1,750 – 2,850 m) refers to cool upland mountain slopes vegetated with aspen (*Populus tremuloides*), ponderosa pine (*Pinus ponderosa*), Douglas-fir (*Pseudotsuga menziesii*), lodgepole pine (*Pinus contorta*), and limber pine (*Pinus flexilis*) (Chapman et al., 2006). The subalpine zone (2,850 – 3,500 m) refers to a transitional ecoregion between montane and alpine zones, just below timberline, with distinct ecological and biological hallmarks including Engelmann spruce (*Picea engelmannii*), subalpine fir (*Abies lasiocarpa),* aspen (*Populus tremuloides*), and lodgepole pine (*Pinus contorta*) (Chapman et al., 2006). In both zones, understory and bead vegetation species vary with elevation, soil moisture, sun exposure, and other factors.

Table 1: Elevation, annual precipitation, and annual temperature ranges and bolded averages for all three study catchments, subset of study subcatchments, and study beads. Catchment and subcatchment elevation data provided from ArcGIS Online 1-degree DEM, bead elevations from USGS 3DEP 1-m DEM, precipitation from StreamStats & ArcGIS Online, and temperature from PRISM 30 yr averages (1981-2010).

	Elevation (m)	Precipitation (mm)	Temperature (°C)
Cache la Poudre River	1,402 – 4,084 **(2,146)**	330.2 – 1,346.2 **(474.0)**	-11.1 – 17.8 **(6.52)**
Big Thompson River	1,425 – 4,346 **(2,220)**	330.2 – 1,295.4 **(529.1)**	-11.1 – 17.8 **(6.74)**
St. Vrain River	1,447 – 4,328 **(2,196)**	330.2 – 1,346.2 **(545.3)**	-11.1 – 17.8 **(7.41)**
Study Subcatchments	1,505 – 4,346 **(3,142)**	427.8 – 1,144.3 **(670.9)**	-11.1 – 17.8 **(1.24)**
Study Beads	2,365 – 3,192 (**2,778**)	NA	NA

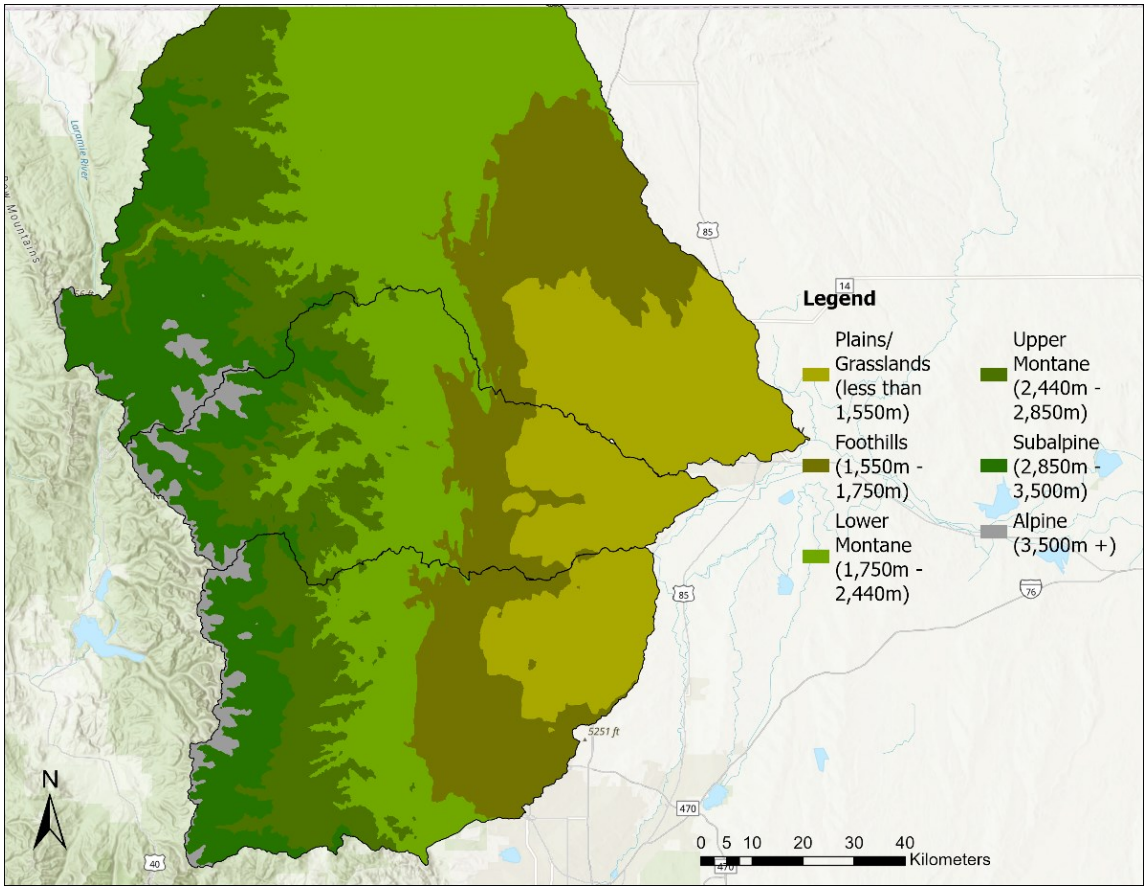

Figure 5: Study catchments color-coded for elevation-derived ecoregions (from Veblen and Donnegan, 2006), not including a small portion of the Cache la Poudre catchment that is in Wyoming and was not considered in the study. Elevation zones visualized on 1-degree digital elevation model (DEM) sourced from ArcGIS Pro Online.

4.2 Study Sites

A total of 52 beads in 27 different subcatchments were identified, delineated, and evaluated for biotic and geomorphic functionality drivers (input variables), and functionality indicators (response variables). Although this study concentrated on river beads in the Front Range, the dataset aimed to capture the varied fluvial conditions hosted in this topographically and lithologically complex region. Forty beads are in the montane zone; 12 are in the subalpine zone. Of the 40 montane beads, six are located in the lower montane zone (1,750 m – 2,440 m) and 34 are located in the upper montane zone (2,440 m – 2,850 m); however, the montane

category was not further subdivided in order to avoid overcategorization of the data and due to the small sample size of the lower montane zone.

Western Colorado been episodically glaciated, most recently during the Pinedale glaciation; evidence supports the start of this period around 29,000 years ago (Madole, 1976) and boulder surface exposure ages suggest a retreat beginning around 16,800 years ago (Benson et al., 2005). Glacial activity in the Rocky Mountains and Front Range has altered catchment morphology, carving U-shaped valleys and resulting in expansive and flat beads with wide and sinuous channels and few bedrock constrictions (Livers & Wohl, 2015). Glacial activity is also known to create unique small- and large-scale geomorphological features upon both advancement and retreat. In particular, moraines, large bars of unconsolidated sediment deposited adjacent to the glacier (lateral) or at its end (terminal) can act as hydrologic and geomorphologic controls (Arp et al., 2007). Several beads in Rocky Mountain National Park are situated above the Pleistocene glacial terminal moraine (~2430 m) deposited during the Pinedale glaciation (Wohl et al., 2004), and the headwaters of all three of the primary study catchments were glaciated during this period (Figure 6). Apart from U-shaped valleys, beads were also observed in glacier-carved depressions, primarily cirques and possibly kettles.

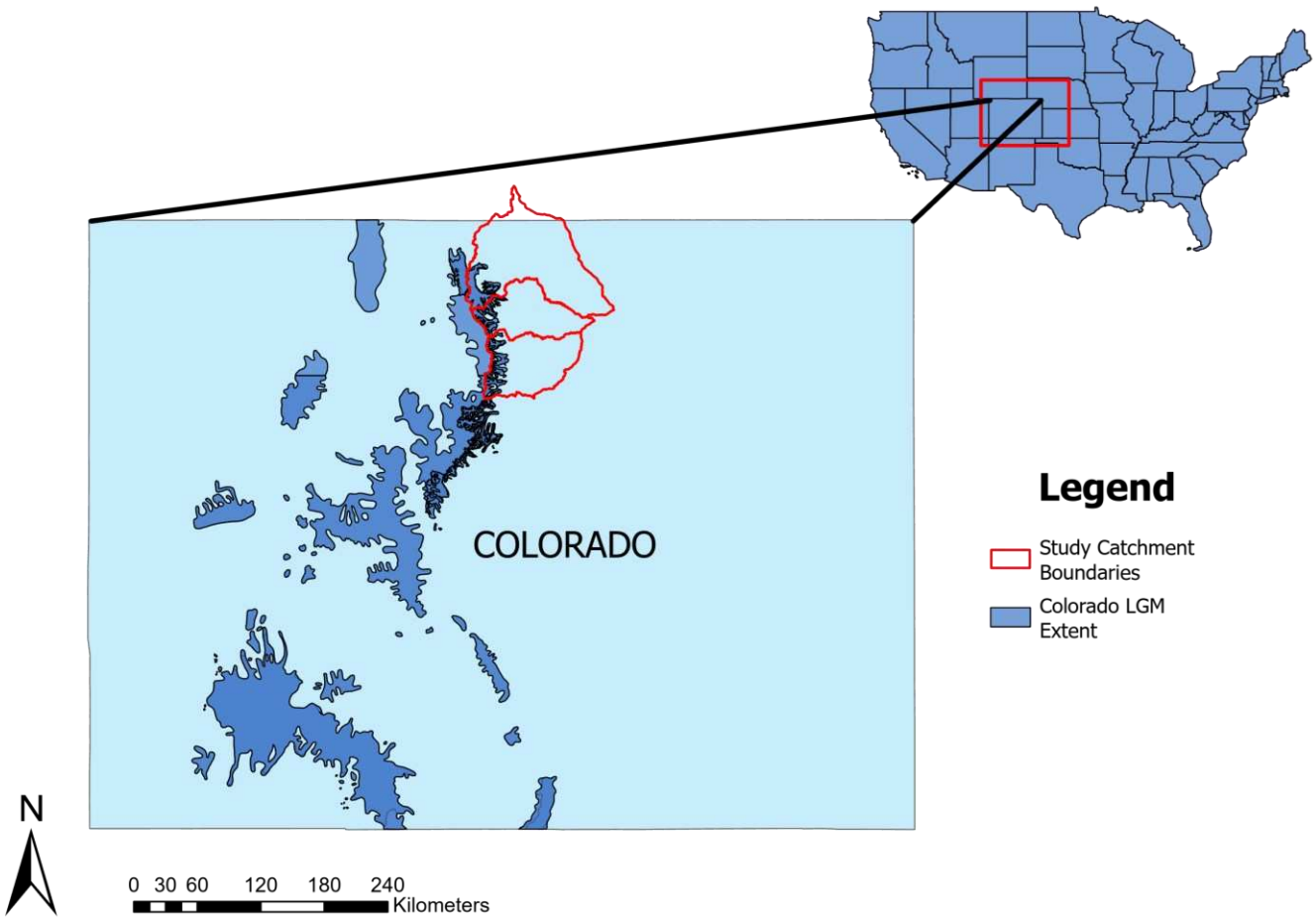

Figure 6: Colorado last glacial maximum (LGM) extent compared to study catchments. LGM data sourced from Dahms (2004) and VanSistine et al. (2022).

The 2020 Cameron Peak wildfire, the largest in Colorado history at the time of writing, burnt approximately 88,634 hectares (Swayze et al., 2021) from August 13 until December 2, 2020, and caused significant damage to land and personal property. Up to 60% of the forested uplands of the Cache la Poudre River catchment (Thurman et al., 2023) burned at varying levels of severity (Figure 5). The post-wildfire cascade here has been linked to poor downstream water quality (including blackwater events and a severe debris flow), fish kill, and increased rates of sedimentation (Kean et al., 2022). Numerous subcatchments have already received, or are planned to receive, low-tech process-based river restoration efforts, and multiple local and state

organizations are involved with improving conditions in the post-fire landscape and building resilience to future disturbances.

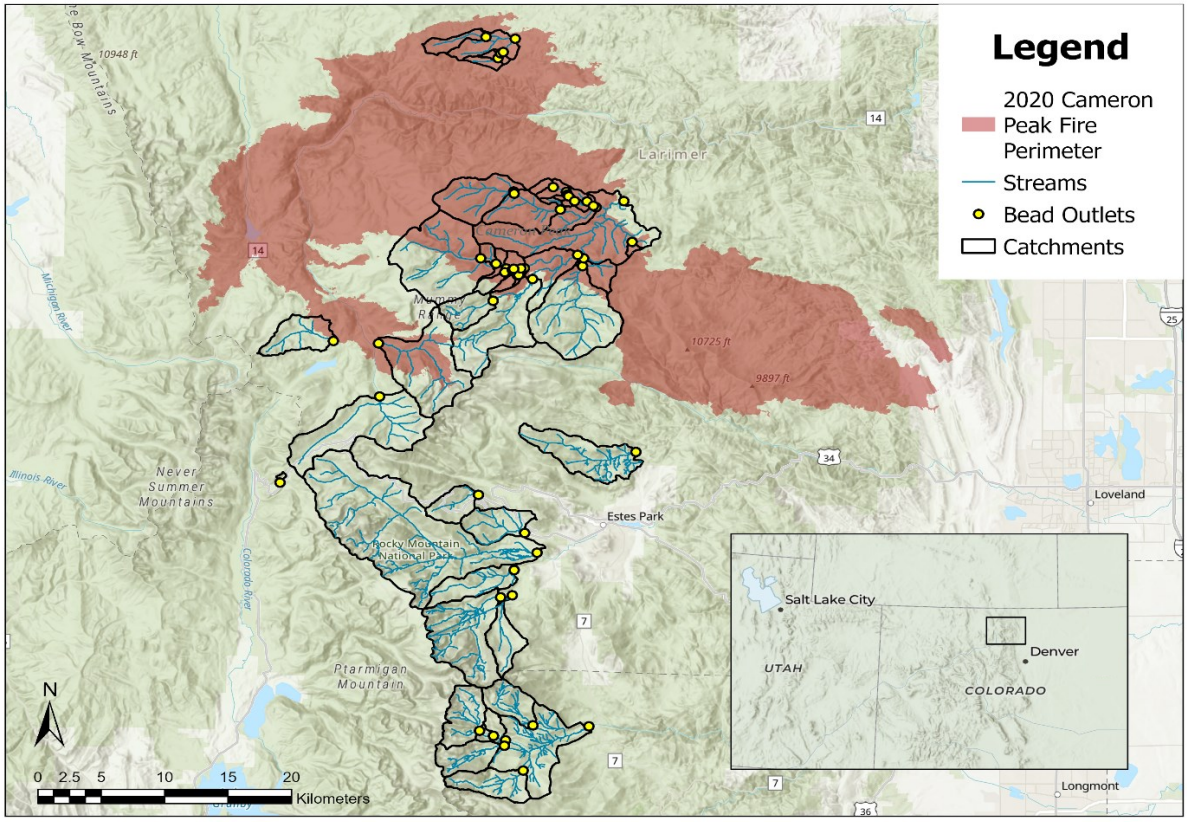

Figure 7: Study subcatchments, river networks, and bead outlet points marked in yellow, underlaid by the 2020 Cameron Peak burn extent. Wildfires are a natural disturbance affecting the Front Range, but changes in their frequency and magnitude caused by both climate change and human activity have made them especially detrimental in this region. (Other, less recent wildfires in the region not shown in this figure because they did not directly affect the study sites.)

Riparian vegetation is spatially varied both within beads and between beads. Localized stands of certain species create patch heterogeneity and are indicative of subsurface conditions, including soil type and moisture. Beaver meadows are generally dominated by willows (*Salix* spp.). Although subspecies varies with elevation, slope, and sun exposure, willows generally prefer saturated soil and full sun, and the open, flat, and wet expanses associated with beaver

activity provide optimal growing conditions for obligate phreatophytes such as willows (Hallock et al. 1986). Willow presence can be used as an indicator of active or relict beaver activity, as well as a sign of floodplain-channel connectivity within beads. Beyond willow, vegetation in beads depends on slope, soil moisture, and history of natural and anthropogenic disturbances.

A minimum of 5 beads are used as the threshold for robust representation of each category. River restoration projects are increasing in number each year with the growing visibility of river science and ecosystem management, but there are still few completely restored beads in the Colorado Front Range, placing a limit on the size of this category. My dataset includes five restored beads (Cow Creek, Elkhorn 1, South Fork Poudre 2, South Fork Poudre Tributary 2, and Beaver Brook).

5. METHODS

5.1 Bead Dimensions and Characteristics

All fieldwork was completed in Summer 2024 and analysis was completed between Fall 2024 and Spring 2025. Fieldwork was completed with the objective of documenting conditions, verifying bead geometry, and assessing wood volume and beaver modification where present. Five beads (Cony Creek, Hunters Creek, North St Vrain 1, North St Vrain 2, and Ouzel Creek) towards the southern end of the study extent were characterized using the dataset of Bridget Livers (Livers, 2016). These five beads had already been characterized extensively by Livers and were not visited as part of this investigation; all necessary data about these sites were extracted remotely or sourced from Livers' dataset.

All 47 beads visited in the field were initially measured for active channel width to assess the general geometry of the fluvial corridor. If the start of the bead was not visited, bankfull channel width and water depth at time of field visit were measured at the highest upstream

segment visited. Width of smaller channels was measured with a handheld tape measure, and larger channels were measured with a laser rangefinder. Average bankfull channel width was assumed to change minimally over the length of each bead. Three measurements of water depth (maximum depth, minimum depth, and perceived average depth) were taken to account for the presence of bedforms and variations in bed topography.

Channel substrate was also documented visually at bead start or upstream, and any significant changes in dominant size, angularity, or lithology were noted. Important features, such as sand waves, fine sediment deposits, bank collapses, and high-water marks were also identified and photographed where necessary to provide geomorphic and historical context. Sediment sources were identified when possible. Some beads with narrower floodplain widths and/or bedrock constrictions were noted to receive large boulders and angular clasts as lateral hillslope inputs; others have retained large sediment bars and deposits from snowmelt peak flows or floods. Identifying sources helped to constrain the nature and timing of inputs into the system, as well as identify possible evidence of wildfire-initiated changes in rainfall-runoff relationships.

Table 2: Catchment and bead geometry and characteristics, methods of characterization, and use in statistical analyses.

	Variable	**Method**	**Statistical variable?**
Catchment Geometry			
	Contributing drainage area (km²)	Measured remotely using StreamStats	Y
	Average catchment slope	Catchment elevations from 1-m USGS 3DEP DEMs averaged in ArcGIS Pro	Y
	Average catchment elevation (m)	Catchment elevations from 1-m USGS 3DEP DEMs averaged in ArcGIS Pro	Y
	Mixed forest (%)	Measured remotely using StreamStats	Y
	Elevation maximum (m)	Measured remotely using StreamStats	N
Bead Geometry & Characteristics			

	Bead Size (km²)	Field verification, 1-m USGS 3DEP DEMs, and remote imagery used to delineate beads in ArcGIS Pro	Y
	Bead Slope	Bead inlet and outlet elevations extracted from 1-m USGS 3DEP DEMs, used to calculate slope	Y
	Bead Inlet/Outlet Elevation (m)	Measured remotely using StreamStats	N
	Channel substrate	Characterized visually in the field	N
	Channel width (m)	Collected in the field with measuring tape or laser rangefinder	N
	Flow depth (cm)	Collected in the field with measuring tape	N
	Floodplain-channel ratio	Google Earth Pro satellite imagery used to estimate average floodplain width; divided by channel width	Y
	Bead ratio	Bead size divided by size of contributing drainage area	Y

USGS 3DEP 1-meter digital elevation models (DEMs) were sourced from OpenTopography for elevation data. DEMs were operated with a projected coordinate system (PCS) of NAD 1983 UTM Zone 13N and a geographic coordinate system (GCS) of NAD 1983. The vertical coordinate system (VCS) was set to NAD88 height (meters) in accordance with 3DEP standards. Elevations were extracted from bead inlets and outlets, and the difference between the two was divided by the total length of the valley to give average bead slope. Average slope was calculated for each catchment in ArcGIS Pro.

Dimensions of beads were documented both in the field and remotely (Figure 6). Bead starting points ("inlets") and ending points ("outlets") were collected as GPS points in the field. Beads inlets or outlets that were not field-confirmed were estimated in Google Earth Pro. DEMs, satellite imagery, and field knowledge were used to delineate boundaries of beads. Vegetation contrasts (Figure 7) between uplands commonly created clear boundaries between meadows and uplands. In incised systems, total valley width may not be reflective of active floodplain width,

and DEMs assisted in revealing topographic differences between active and inactive floodplain terraces.

Bead polygons were visualized and analyzed in ArcGIS Pro. Bead polygons were used to calculate floodplain-channel width ratio, a metric that compares fluvial corridor width to the width of available floodplain. Minimum, maximum, and estimated median floodplain widths were extracted for each bead in Google Earth Pro to account for variations in lateral confinement due to vegetation and structural elements such as bedrock outcrops. These three widths were averaged and then divided by channel width at the head of the bead to give floodplain-channel width ratio.

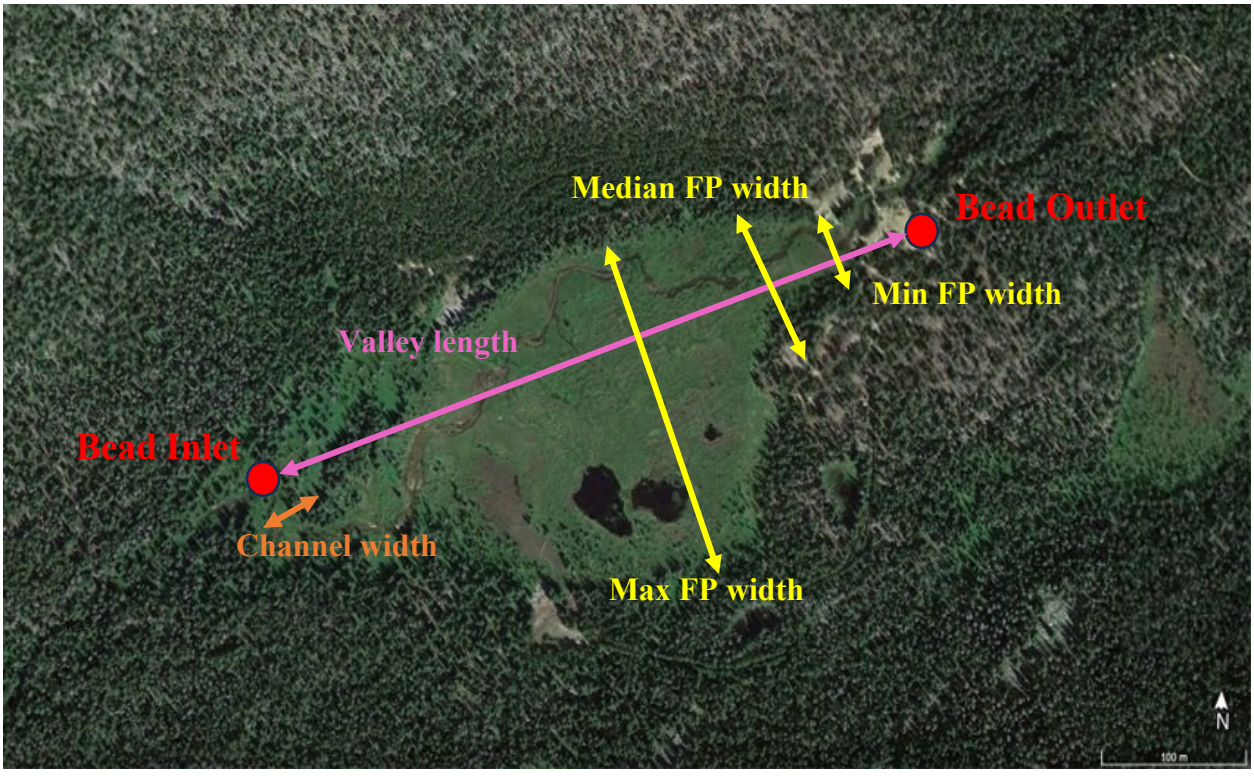

Figure 8: Measured bead dimensions visualized for Fall Creek. Satellite imagery courtesy of Google Earth Pro.

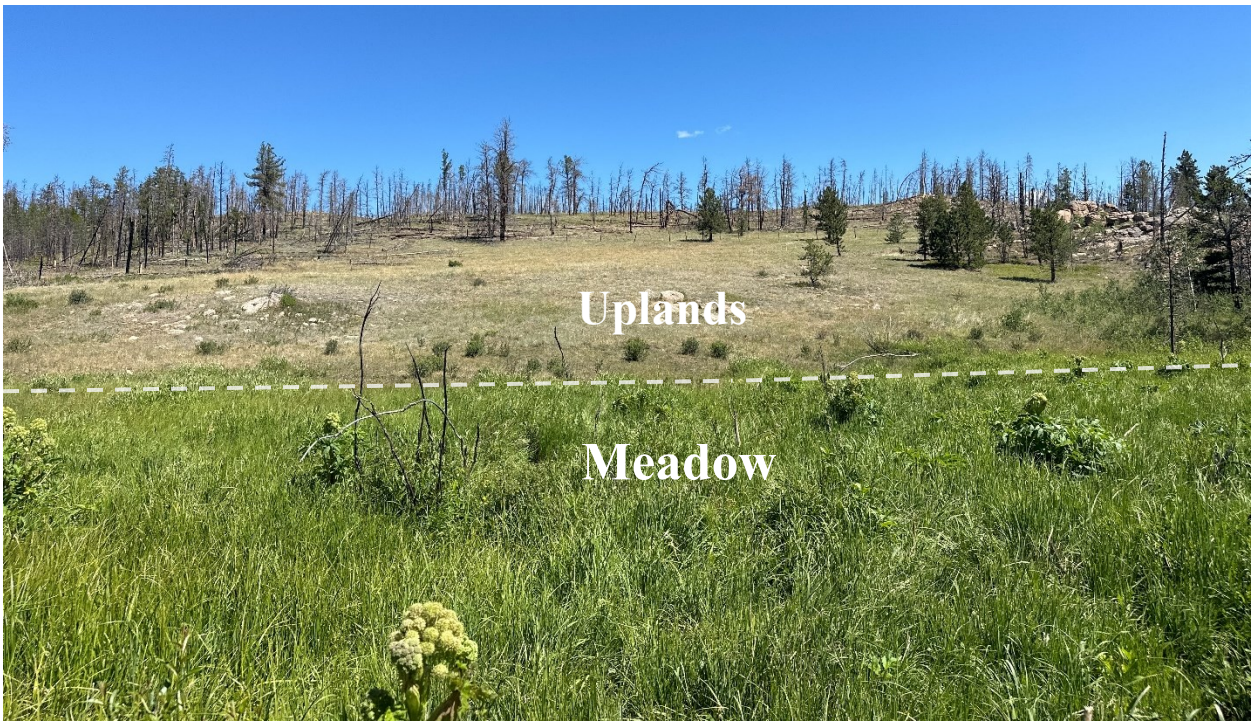

Figure 9: Vegetation contrast between meadow and uplands at Elkhorn Creek illustrated with white dashed line.

5.2 Functionality Drivers – Biotic

Biotic drivers of interest were large wood (LW), active or relict beaver modification, and riparian vegetation, all of which were measured or characterized in the field and processed remotely.

Table 3: Biotic drivers, methods of characterization, and use in statistical analyses.

Variable	Method	Statistical variable?
Large Wood Count	Measured in the field during wood surveys, extrapolated to fit total bead size where necessary	N
Wood Density (LW/km)	Large wood count in the field plus volume of larger jams divided by total channel length	Y
Wood Characteristics	Characterized in the field	N
Minimum Berm Count	Measured in the field during berm surveys, extrapolated to fit total bead size where necessary	Y
Berm Density (berms/km)	Total number of berms divided by primary channel length	Y
Riparian buffer	Remote data and field visits used to confirm and define vegetation type and longitudinal extent	Y

5.2.1 Large Wood

Wood presence enhances spatial heterogeneity, or patchiness, within a channel and is a key habitat former (Wohl, 2017). Designation as large wood (LW) requires a length of at least 1 m and a diameter of at least 10 cm (Wohl et al., 2010), and logjams are a cluster of three or more pieces of large wood (Wohl & Iskin, 2022). Wood of smaller lengths and/or widths was considered coarse particulate organic matter (CPOM) and was not formally evaluated as part of this study, although CPOM can play an important role in both flux attenuation and nutrient dynamics in rivers (e.g., Tank et al., 2010). Floodplain wood volume was not included in this study, although floodplain wood can attenuate fluxes by enhancing hydraulic roughness and hyporheic exchange flows (Wohl, 2013). Thus, all wood surveyed was in-channel or adjacent to the channel, aside from some channel-spanning and ramped pieces that rest partially or mostly on the floodplain.

LW presence was surveyed in the field and used to calculate wood load, or the volume of wood per unit area in a river. Of the 52 total beads, 45 were surveyed from beginning to end and have a fully documented wood volume. The seven remaining beads (Big Thompson River at Moraine Park, South Fork Poudre River at CSU Mountain Campus, North St Vrain Creek at Wild Basin, Poudre River, Beaver Brook, Stumble Creek at headwaters, Hague Creek, and Corral Creek) were not surveyed in entirety due to their length. However, bead geometry at all seven sites indicated homogeneity and longitudinal continuity of conditions. Field exploration confirmed continuity; a representative subset of the bead, ranging from 7% to 57% of total bead length, was selected and surveyed. Measurements from these sections were then extrapolated to fit the size of the bead from start to finish.

Each logjam or piece of wood was given a configuration descriptor and a GPS location; in addition, each log within the jam was assigned a length, diameter, azimuthal direction, decay level, and complexity level. Configuration descriptors summarize the nature of the logjam or piece, giving an idea of transport history (fluvial transportation or floodplain recruitment) and geomorphic role (whether the piece facilitates deposition, erosion, or both) (Figure 8).

Figure 10: Wood configuration examples and definitions. Bridged, unattached, and buried logs are on Beaver Creek; ramped log is on Pennock Creek, pinned logs are on Little Beaver Creek. Ramped and unattached log configurations are most conducive to scour and buried logs are most conducive to sediment deposition.

Decay category, ranging from one to four, implies a relative age and residence time for each piece of wood based on condition (Figure 9). Level-one logs are assumed to have the shortest residence time in the channel or have had minimal interaction with flow; they have intact bark, branches, and growths (needles, cones, leaves). These logs are generally channel-spanning or have a large proportion situated in the floodplain. Level-four logs are assumed to have the longest residence time or have been submerged for an extended period of time; they have lost all bark, branches, and growths, and are often saturated to the point of softness and breakage. These logs are generally buried or unattached. Levels two and three make up the intermediate conditions between these endmembers. In certain cases, distribution of decay stages may be used for identification and interpretation of disturbances in beads, given that certain events (floods, wildfires, debris flows) are associated with recruitment and transport of large wood.

Figure 11: Illustration of decay state from one (least decayed) to four (most decayed). All photographed logs in beads on Beaver Creek.

Complexity level, ranging from “none” to “high complexity,” was a non-numerical descriptor intended to provide information about the trapping potential of each piece of wood (Figure 10). Log complexity, including branches, growths, and piece geometry, facilitates entrapment of wood, CPOM, and sediment and can locally slow and divert water. High complexity can also increase habitat diversity. Pieces with no complexity tend to act as rough hydraulic obstacles, initiating both deposition and scour depending on the configuration. Some

channel-spanning low-complexity pieces act as knickpoints and create small hydraulic jumps. Complexity level is also a function of age and exposure – water and time both cause decay and loss of complexity. Low complexity logs tended to be older and more decayed than higher-complexity logs.

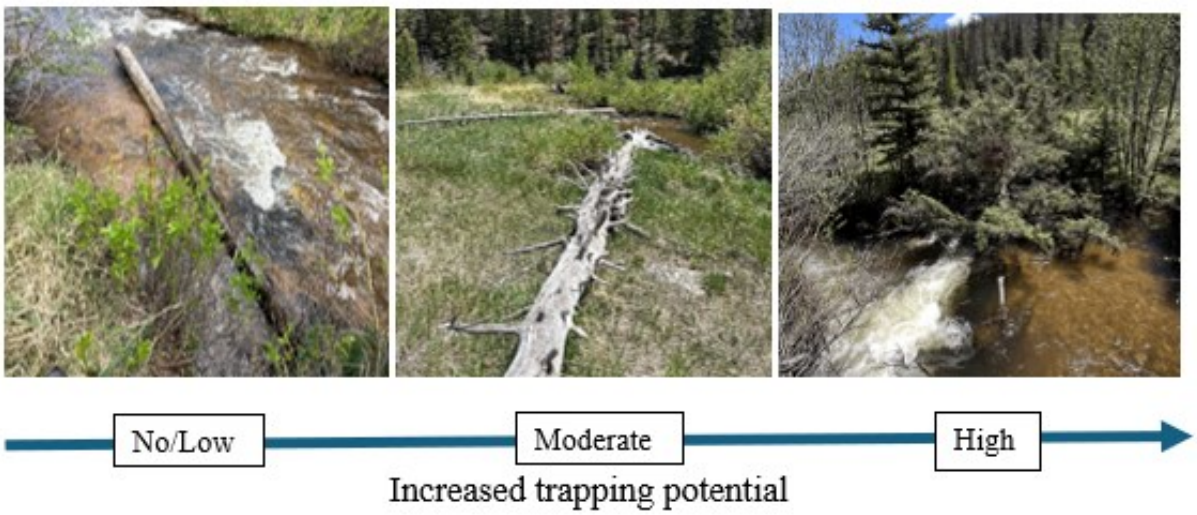

Figure 12: Illustration of piece complexity, from no/low complexity to high complexity. All logs located in fourth bead on Little Beaver Creek.

Characterization of sizeable wood accumulations, particularly large jams (Figure 11) and segments of river with extensive and complex wood configurations (Figure 12), proved to be difficult and time-consuming with the aforementioned methodology. Instead, field measurements of length, width, and height of these features as well as an empirically derived estimated porosity of 0.5 were used to estimate total wood volume at these sites (Livers et al., 2020). At these sites, large jam/complex system wood volume totals were added to the singular piece and smaller jam wood volume totals. Complexity and piece configurations in these zones were not measured, under the assumption that the size and structural complexities of the jams create high levels of complexity and are primarily depositional environments, although more in-depth studies of the jams themselves would be required to further define their roles in river hydraulics. As mentioned

earlier, jams and trapped wood can be ephemeral, and thus it was important to concurrently assess overall channel capacity to store and trap wood while documenting the existing wood features.

Figure 13: Large jam on channel left on the North St. Vrain Creek at Wild Basin, resulting from the 2013 flood (Ellen Wohl, pers. comm., Aug. 2024). Field personnel for scale. Flow direction denoted with yellow arrow. Photo taken August 2024.

Figure 14: Complex wood accumulations and secondary channels on the South Fork Poudre River restoration at Lazy D Ranch. Flow direction denoted with yellow arrow. (Photo credit: Larimer Conservation District). Photo taken September 2024.

5.2.2 Beaver Modifications

Beaver modification was characterized by mapping the locations and spatial extent of beaver berms within each bead (Figure 13). Active and inactive berms were not differentiated in this study, but active berms were observed infrequently. Field berm surveys included walking the length of the bead or a subsection of the bead as explained above. Each berm was counted and assigned a GPS location. GPS points were either collected in-channel or on valley margins, depending on channel accessibility and discharge. In particularly complex beaver meadows, berms were traced on foot across the valley and assigned left and right valley margin GPS points to prevent confusion in later visualization and patch delineation. In some cases, small clusters of

laterally discontinuous berms, or “berm complexes” were found; extracting details of each small structure would be difficult, and these complexes were therefore counted as one berm each.

Figure 15: Field-collected berm points (red dots) for the first bead on Elkhorn Creek. Bead boundaries outlined in green. Vegetation differences can be used to locate berms, but field surveys and GPS points increase the accuracy of minimum berm counts.

Varied berm ages and flow conditions between and within beads resulted in a wide range of appearances and conditions of these structures. Differences in berm prominence and width, particularly in relict beaver meadows or elk grasslands with subtler variations in topography, introduced the possibility of underestimating total number of berms. Therefore, the field counts represent a minimum value. Minimum berm count and primary channel length were used to calculate berm density, or the number of berms per kilometer of valley length. Nearly all berms were valley-spanning, and total channel length was not used to calculate berm density, as it was assumed that berms cross multithread systems more than once, which could result in over-counting for channel presence and artificially lowering berm density. As noted earlier,

incompletely surveyed beads were assessed for homogeneity of berm spacing, and both minimum berm count and berm density were extrapolated to fit the total size of the bead.

5.2.3 Riparian Vegetation

Riparian buffers were characterized using field observation and satellite imagery. Vegetation, specifically dominant class and estimated spatial extent, was used to divide beads into three categories: forested, elk grassland, and beaver meadows (Figure 14), with dominance of conifers, grasses, and willows, respectively. Forested beads, located in conifer forests in the upper elevations of the studied catchments, are ecologically distinct from elk grasslands and beaver meadows due to differences in vegetation density and species. Forested beads support stands of large conifers as well as conifer saplings and varied vegetation species in the understory. Forested bead soils tended to be moist and organic-rich. Small conifer patches were observed in beaver meadows where soil was drier and/or topography was slightly higher, but most vegetation in these beads is hydrophytic and includes willow, herbaceous plants, and rushes or sedges. Conifer patches were more frequently observed in elk grasslands, but these beads generally supported higher surface coverages of grasses and relict willow stands (overbrowsed or dead). Vegetation heights in beaver meadow and elk grassland beads was generally < 2 m.

Beaver Meadow

- Supports multithread channels
- Floodplain inundation, ponding, and/or high soil moisture common
- Willow-dominated, with marshy vegetation and grasses
- Geomorphically and topographically complex
- Act as wildfire refugia

Forested

- Can have multithread channels, typically seasonal
- Soil moisture varied
- Conifer-dominated, varied understory vegetation – mosses, grasses, etc.
- Geomorphically and topographically complex
- At risk of wildfires

Elk Grassland

- Typically single-thread channels, can have inactive relict channels on floodplain
- Soil moisture lower, floodplain dry
- In non-exclosed areas, dominated by grasses with relict willow stands; exclosures support growth of willow stands
- Lower topographic and geomorphic variability
- Wildfire risk varied

Figure 16: Stream corridor at the North St. Vrain Creek at Wild Basin (top; Bead 4), the North St. Vrain Creek uplands (middle; Bead 3), and Big Thompson River at Moraine Park (bottom) reveals key ecological variations contributing to differences in functionality and process domains. Note that a grazing exclosure was present at Moraine Park; the resulting dense vegetation growth is visible in the right of the image; this vegetation should not be considered representative of elk grasslands.

Remote identification of forested beads is difficult - satellite imagery cannot penetrate canopy cover, rendering it nearly impossible to spot the topographic differences and geomorphic features associated with beads. In addition, vegetation differences between beads and strings are subtle or nonexistent due to dominance of conifers in heavily forested stands. Understory vegetation is longitudinally and temporally variable with differences in floodplain width, degree of floodplain-channel connectivity, and seasonal presence of ponded or flowing water in secondary channels (e.g., Peipoch et al., 2023). High-resolution Digital Elevation Models (DEMs) and LiDAR (Light Detection and Ranging) can be used to identify the topographic signature of forested beads; forested beads can also be found on foot, depending on accessibility and forest cover.

Elk grasslands and beaver meadows are considered end-member conditions representative of the degree of human, ungulate, and disturbance-related modifications impacting connectivity, heterogeneity, and flux attenuation potential in the channel and floodplain. Elk grasslands have been heavily impacted and active beaver meadows have been minimally impacted. Most elk grasslands were formerly (according to historical accounts and satellite imagery) wet, complex beaver meadows, and have evolved into the alternate state of single-thread systems with incised, unstable banks and disconnected floodplains following beaver disappearance from the site. However, some elk grasslands have retained signatures of beaver modification or geomorphic complexity, and some relict beaver meadows have begun to show signs of connectivity loss. Thus, the meadow-grassland relationship is a continuum rather than a binary.

5.3 Functionality Drivers – Geomorphic

Geomorphic drivers of importance are catchment-scale water and sediment inputs, which were all estimated using indirect proxy variables that were measured remotely.

Table 4: Geomorphic drivers, methods of characterization, and use in statistical analyses.

Variable	Method	Statistical variable?
Water		
16H100Y (mm)	Measured remotely using StreamStats	Y
STORNHD (%)	Measured remotely using StreamStats	Y
1% AEP (cms)	Measured remotely using StreamStats	Y
50% AEP (cms)	Measured remotely using StreamStats	Y
Precipitation (mm)	Measured remotely using StreamStats	Y
Sediment		
High Severity Burn (%)	dNBR calculated in ENVI 6.0 using 30-meter Landsat 8 Collection-2 Level-2 imagery; ArcGIS Pro used to extract and analyze pixel-scale burn metrics	Y
Total Burn (%)	dNBR calculated in ENVI 6.0 using 30-meter Landsat 8 Collection-2 Level-2 imagery; ArcGIS Pro used to extract and analyze pixel-scale burn metrics	Y
Burn Ratio	High severity burn divided by total burn	Y

5.3.1 Water Inputs

The USGS StreamStats Batch Processing Tool was used to calculate important catchment-scale parameters influencing water and sediment inputs into each bead. This tool calculated drainage area, mean basin elevation, maximum basin elevation, minimum basin elevation, and outlet elevation, percentage of catchment over 2300 m, percentage of forest cover in NLCD class 41-43 (Deciduous, Evergreen, and Mixed Forest), and slope. All elevation data were extracted from a 10-m DEM, and ArcGIS Pro was therefore used to calculate these metrics with 1-meter accuracy. Because all beads were found to be above the 2300 m elevation threshold, this metric was determined to be unimportant to the study. The Batch Processing tool also provided estimated discharges of 2-year (50% AEP) and 100-year floods (1% AEP), average yearly catchment precipitation, 6-hour precipitation amount expected to occur on average once

every 100 years (16H100Y), and percentage of catchment with surface storage of water in wetlands and water bodies (STORNHD).

The flow paths on the second and third beads on Witiak Creek were not recognized by StreamStats; the contributing catchments for these beads were delineated by hand using the catchment for the first Witiak Creek bead and 1-m DEM with visualized hillslopes as a guide. Basin and hydrologic parameters for these two catchments were estimated using ArcGIS Pro.

Many of the beads are located within the same catchment or are proximal to each other, introducing the possibility for interactions, especially if upstream fluxes are insufficiently attenuated. Bead positional aspects such as location, relative abundance, and size were considered but not factored into statistical analyses.

5.3.2 Sediment Inputs

Burn severity can be accurately estimated with dNBR (Δ Normalized Burn Ratio), a band arithmetic function that calculates the difference in a landscape following a fire. dNBR is a metric that estimates and summarizes the effects of fire on a landscape and assigns both a categorical and a numerical value to express the magnitude of burn severity. Loss of vegetation understory in any capacity will impact hillslope erosion and conveyance of runoff, but moderate and high severity burns have strong implications for sediment loading. In addition, mortality of conifer stands in forested uplands can contribute locally to hillslope roughness; burnt hillslope wood can also reach and be transported within fluvial corridors, increasing wood density.

For this study, 30-m Landsat 8 Collection-2 Level-2 satellite pre- and post-fire imagery were extracted via the USGS EarthExplorer web tool. Imagery was selected for minimal cloud cover and collection date during the spring or summer months to capture peak riparian spatial footprint. The Cameron Peak Wildfire achieved 100% containment on December 2, 2020, but residual

smokiness from the burn scar made spring/early summer 2021 imagery suboptimal for dNBR calculations. Pre-fire imagery was collected in early July 2020, and post-fire imagery was collected in early September 2021. Before dNBR can be calculated, NBR must be calculated for pre-fire and post-fire scenarios. ENVI 6.0 was used to create pre-fire NBR and post-fire NBR rasters. NBR itself is calculated with the following equation, where NIR is near-infrared radiation (0.75 – 1.4 μm) and SWIR is short-wave infrared radiation (1.4 - 3μm):

$$NBR = \frac{NIR - SWIR}{NIR + SWIR} \quad (1)$$

dNBR is then calculated as the difference in pre -and post-fire outputs using the following simple equation:

$$dNBR = (prefire\ NBR) - (postfire\ NBR) \quad (2)$$

The dNBR output raster provides differenced values for each pixel which are used to summarize the extent of vegetation mortality. From the dNBR raster, severity classes can be assigned within each drainage based on predetermined thresholds (Table 2). Low to moderate burn is consistent with smaller proportions of total vegetation mortality, and high severity burns are consistent with complete or near-complete mortality of vegetation (Miller & Thode, 2007).

Table 5: Burn severity classes for dNBR assessment (from Rakholia et al., 2020)

Severity Level	**dNBR value range**
Enhanced regrowth, high (post-fire)	-0.500 to -0.251
Enhanced regrowth, low (post-fire)	-0.250 to -0.101
Unburned	-0.100 to +0.099
Low Severity	+0.100 to +0.269
Moderate-Low Severity	+0.270 to +0.439
Moderate-High Severity	+0.440 to +0.639
High Severity	+0.640 to +1.300

ENVI 6.0 was used to create pre-fire NBR and post-fire NBR rasters, as well as differencing the two to create the finalized dNBR product. The dNBR raster was then uploaded to ArcGIS

Pro and assigned a custom color scheme in accordance with the severity thresholds (Figure 15). Green pixels corresponded with areas of low or high regrowth and a yellow-to-dark red ramp corresponded with escalating burn severity. Unburned land was not of interest and was not assigned a color. An attribute split was performed in ArcGIS Pro to clip the burn scar to catchments, and a zonal histogram provided burn metrics for each catchment.

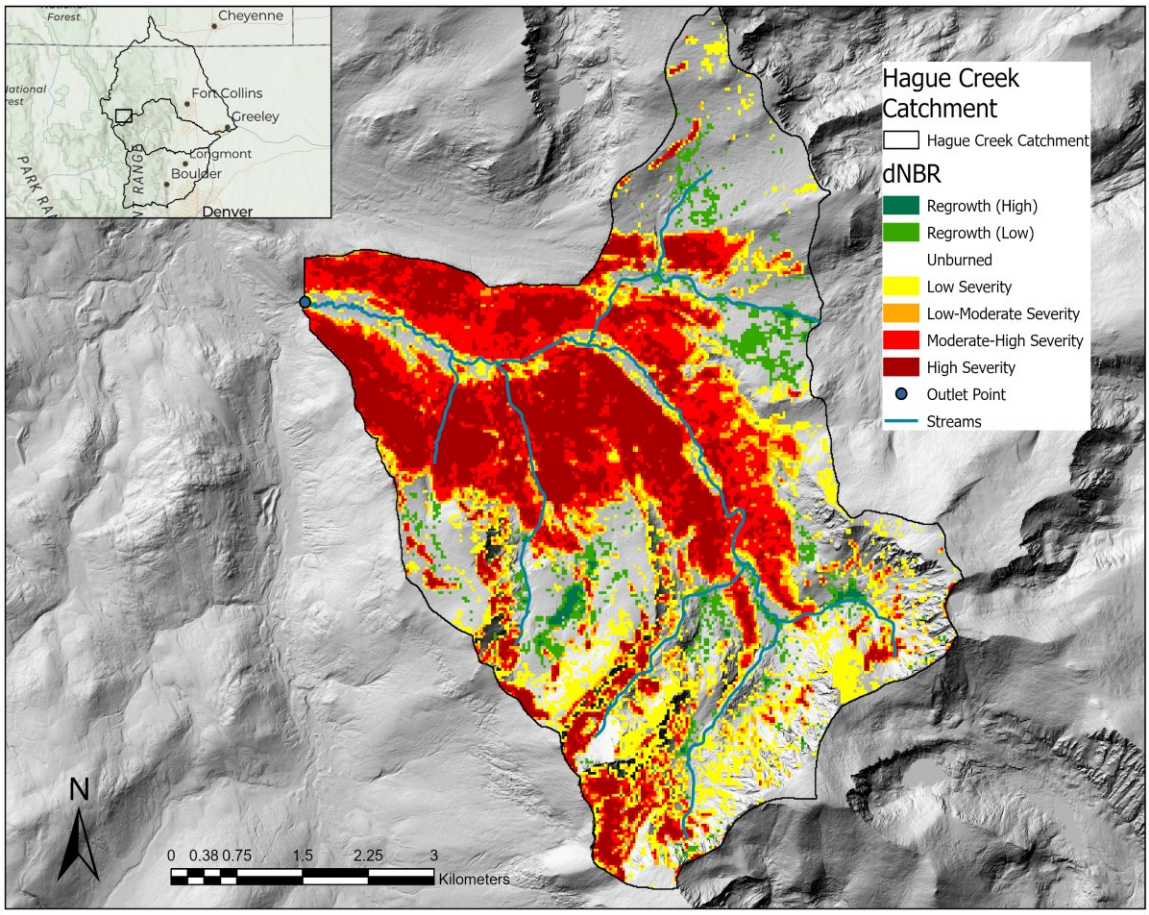

Figure 17: dNBR visualized for the Hague Creek catchment. Bead extent is outlined in purple. Note the lack of burn in the river corridor.

Zonal histograms assigned a burn severity to each pixel in each catchment, including unburnt pixels. Totals from each severity bin were summed to give the total size of each catchment in pixels. Zonal histograms were used to calculate three different burn metrics for

each catchment. High severity burn percent calculated the proportion of the catchment burned at high severity (dNBR >0.66):

$$High\ Severity\ Burn\ \% = \frac{\#\ of\ severely\ burnt\ pixels}{total\ \#\ of\ pixels\ in\ catchment} \quad (3)$$

Total burn percentage calculated the proportion of the total catchment burned to any extent, including high severity:

$$Total\ Burn\ \% = \frac{\#\ of\ burnt\ pixels}{total\ \#\ of\ pixels\ in\ catchment} \quad (4)$$

Lastly, burn ratio calculated the proportion of high severity burn to total burn:

$$Burn\ Ratio = \frac{\#\ of\ severely\ burnt\ pixels}{\#\ of\ burnt\ pixels} \quad (5)$$

Although high severity and total burn are appropriate metrics to capture the nature and extent of burn for each catchment, catchment size was theorized to have a statistically significant effect on burn severity. Burn ratio was calculated to nullify the effects of catchment size on burn severity by calculating the proportion of the total burn that was severe and canceling the effects of total catchment size.

5.4 Functionality Responses

Existing bead functionality was evaluated through the lens of response variables, which are assumed to be indicative of healthy stream corridors capable of attenuating fluxes and absorbing disturbances. Proposed bead functionality responses included Normalized Difference Vegetation Index (NDVI) and/or Normalized Difference Water Index (NDWI), spatial heterogeneity as quantified using patch metrics, and sinuosity.

Table 6: Response variables, methods of characterization, and use in statistical analyses.

	Variable	Method	Statistical variable?
	Total sinuosity	Primary channels, secondary channels, and valley length measured using Google Earth Pro satellite imagery	Y
	Bead NDVI	Measured remotely using 3-m ArcGIS Pro	Y
	Bead NDWI	Measured remotely using 3-m ArcGIS Pro	Y
	Patch count	Patches delineated in Google Earth Pro based on satellite imagery and field verification	Y
	Patch density (patches/ km²)	Patch count divided by bead area	Y

5.4.1 NDVI and NDWI

NDVI and NDWI are remotely sensed metrics that require near-infrared radiation (0.75 – 2.5µm), red light (0.625 – 0.74µm), and green light (0.510 – 0.565µm). For NDWI I opted to use the original methodology proposed by McFeeters (1996), which highlights surface water, as opposed to Gao (1996), which focuses on leaf water content. Although leaf water content differs with climatic conditions and species, among other things, the presence of surface water bodies and/or wetlands was assumed to be more directly indicative of floodplain-channel connectivity and thus functionality. The respective band arithmetic functions for NDVI and NDWI are as follows:

$$NDVI = \frac{NIR - Red}{NIR + Red} \tag{6}$$

and

$$NDWI = \frac{NIR - Green}{NIR + Green} \tag{7}$$

To calculate NDVI and NDWI for this study, I extracted PlanetScope 3-m RGBNIR imagery from Planet taken in July 2021. Imagery timing was selected to attempt to capture peak riparian conditions following the Cameron Peak Fire. Consideration was taken to avoid the months immediately post-fire and to avoid years with climate anomalies, which may have

atypically high greenness or wetness levels. NDVI and NDWI were both calculated in ArcGIS Pro; a raster function provided NDVI and band math was used to calculate NDWI. NDVI and NDWI rasters were clipped to bead polygons and histograms provided minimums, maximums, ranges, and averages for both metrics.

Table 7: Vegetation classes for NDVI assessment (from Akbar et al., 2019)

Vegetation Classes	NDVI value range
Water	-0.28 – 0.015
Built-Up	0.015 – 0.14
Barren Land	0.14 – 0.18
Shrub & Grassland	0.18 – 0.27
Sparse Vegetation	0.27 – 0.36
Dense Vegetation	0.36 – 0.74

Table 8: Water content classes for NDWI assessment (from McFeeters, 1996)

Water Content Classes	NDWI value range
Water surface	0.2 – 1.0
Flooding, humidity	0.0 – 0.2
Moderate drought, non-aqueous surfaces	-0.3 – 0.0
Drought, non-aqueous surfaces	-1.0 – -0.3

NDVI and NDWI thresholds can be used to categorize or classify pixels and land cover statistics (Tables 3 and 4).

5.4.2 Patch Metrics

The distribution and density of floodplain patches can be assessed with numerous metrics developed by landscape ecologists (Iskin and Wohl, 2023); for this study, patch density, or number of patches per unit area, was used. Spatial heterogeneity was evaluated through patch density as an indirect indicator of bead storage capability by identifying distinct habitats and structures, or patches, in the channel and floodplain (Iskin and Wohl, 2023). These patches were identified through field observation (Figure 16), delineated in Google Earth Pro, and

characterized with a remote sensing in ArcGIS Pro. A combination of field verification and high-resolution Google Earth Pro satellite imagery was used to hand-delineate patches of geomorphic and biotic significance (Figure 16). Minimum patch size was 1 square meter, on the assumption that combined satellite imagery and DEMs do not provide the spatial resolution necessary to determine finer details; due to the spatial constraints, most patch sizes greatly exceeded the minimum. Patches in the floodplain were delineated using remote data based on changes in vegetation reflecting substrate grain size, soil moisture, and relative elevation (Table 5).

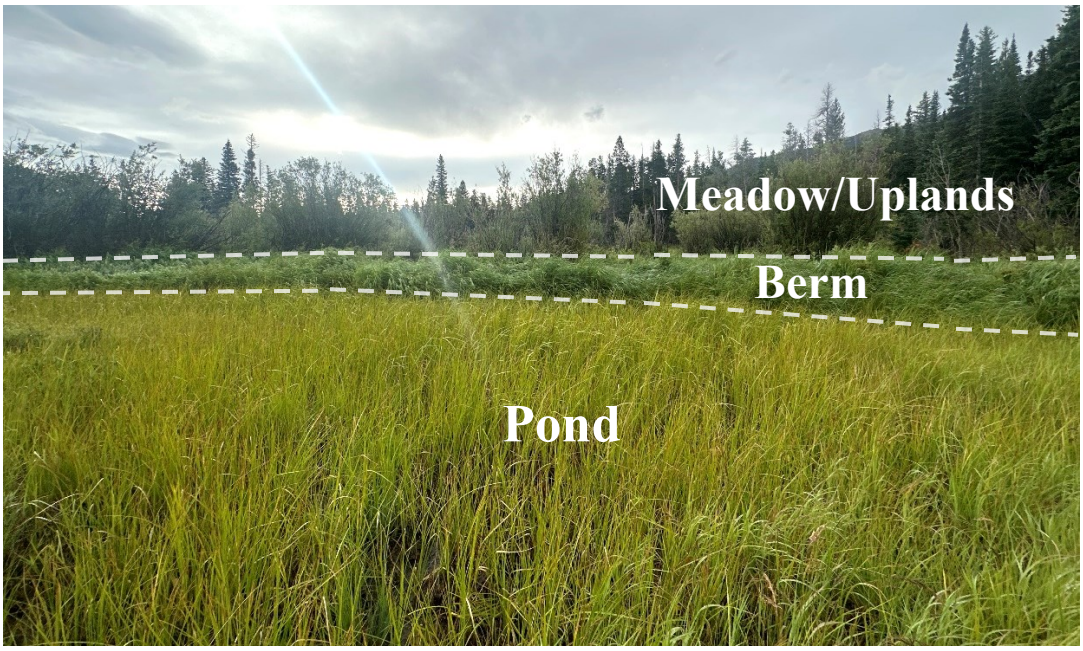

Figure 16: Contrasts between beaver berm, relict beaver pond, and uplands at Glacier Creek illustrated with white dashed lines. Known differences in vegetation, topographic relief, and geomorphic function separate these distinct floodplain patches and contribute to spatial heterogeneity in this bead. Field visits and photographs aided in the remote classification and delineation of landscape patches. Photo taken July 2024.

Patch polygons were then visualized and analyzed in ArcGIS Pro (Figure 17). Patches on incompletely surveyed beads were delineated for the area surveyed in the field; the size of this area was then used to calculate patch density. Patch density for these beads should be considered representative of an average patch density for these beads.

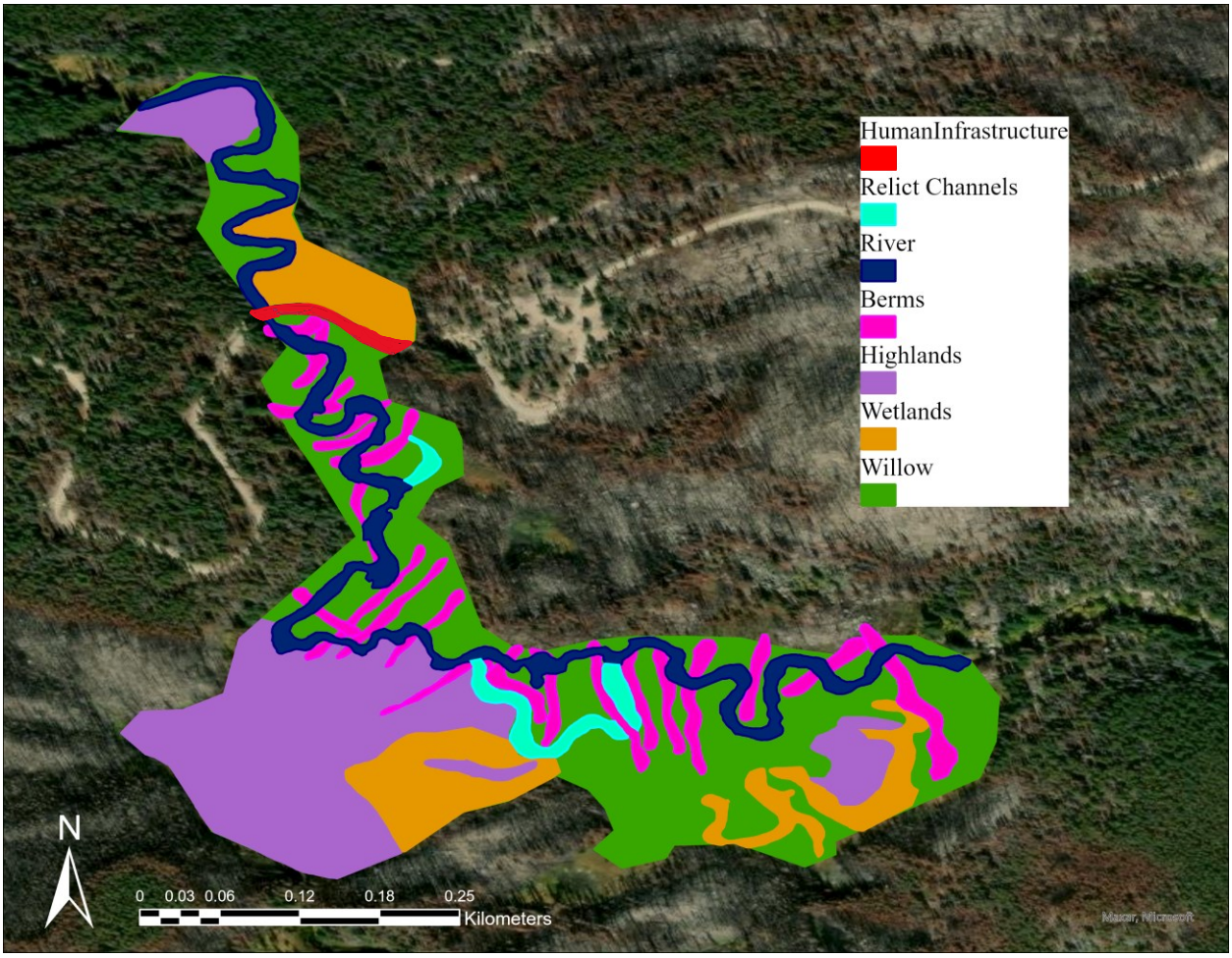

Figure 17: Patch density illustrated for the third bead on Beaver Creek. Beaver modification, human infrastructure, and a large, complex floodplain increased patch density in this bead.

Patch density does not account for smaller logjams and individual pieces of wood. The locations of these features were identified through wood surveys, but their sizes may not meet the patch minimum. Dominant patch types for elk grasslands, beaver meadows, and forested beads (highlands, willow, and forested floodplain, respectively) were drawn to fit the size of the entire bead. Overlying features were drawn and the bead-scale dominant vegetation patch was clipped around these features. This workflow eliminated unassigned ground and made the patch delineation process run far smoother. The target metric, patch density, was calculated as the number of patches per unit area. The number of continuous patches was counted for each bead.

Table 9: Patch types, definitions, and examples as observed in study beads. Patch definitions were established through fieldwork and observation.

Patch Type	Definition	Photo example
Stream Corridor	Primary perennially active flow path. (Picture: stream corridor on Beaver Creek, outlined in dark blue)	
Secondary Channel	Non-primary channels that divert flow from and eventually reconnect back to the primary channel; can be active at high flow or perennially active. (Picture: secondary channels on Pennock Creek, outlined in aqua)	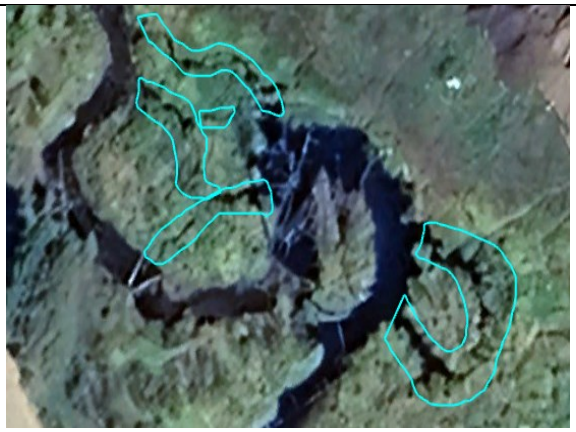
Tributary	Flow that joins and contributes water to the primary channel. (Picture: Little Beaver Creek intersecting the South Fork Poudre River, outlined in lavender)	

Relict Channel	Floodplain channel segment, often discontinuous, that has lost connectivity with main channel; filled in with sediment gradually. (Picture: relict channel on Beaver Creek, outlined in dark orange)	
Willow	Moderate-elevation floodplain associated with willow. (Picture: willow on Jacks Gulch, outlined in green)	
Wetlands	Lower-elevation floodplain with surface groundwater expression; associated with marshy vegetation. (Picture: wetlands on Swamp Creek, outlined in light orange)	
Highlands	Higher-elevation area of floodplain associated with grasses and conifers. (Picture: highlands on Hidden Valley Creek, outlined in lavender)	

Forest Floodplain	Conifer-dominated floodplain found in forested beads. Hard to distinguish from surrounding forest and generally requires fieldwork to delineate accurately. (Picture: stream corridor on Little Beaver Creek, outlined in reddish brown)	
Carr	Inundated colony of willows associated with high flow or beaver modification. (Picture: carr on Glacier Creek, outlined in white)	
Beaver Berm	Active or relict structure created by beaver, local topographic high. Supports willow colonies. Can be breached. (Picture: berms on Elkhorn Creek, outlined in hot pink)	
Beaver Pond	Surface water feature created by beaver dams. Ponds may fluctuate in size with season and cohesive strength of berm. (Picture: beaver ponds on Swamp Creek, outlined in yellow)	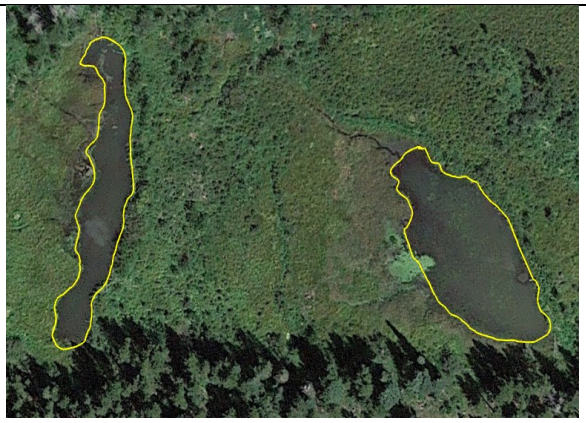

Logjam	Large cluster of logs. (Picture: logjam on the North St. Vrain Creek, outlined in light brown)	
Human Infrastructure	Manmade structures of any variety, including roads, concrete dams, diversion structures, etc. (Picture: human infrastructure (road) on Beaver Creek, outlined in black)	

5.4.3 Sinuosity

Sinuosity measures the ratio of primary channel length, or the length of the dominant or highest-discharge flow paths, to valley length, or the total straight-line distance from valley start to end. Primary channel length was delineated by hand in Google Earth Pro by tracing the channel midline from bead start to end (Figure 16). Primary channels were estimated using satellite imagery and confirmed in the field. Valley length was calculated as the straight-line distance between the bead inlet and outlet points. Sinuosity can be as low as 1 in a perfectly straight channel and increases with the degree of channel meandering in the floodplain. Sinuosity is typically less than 2 apart from some highly sinuous channels.

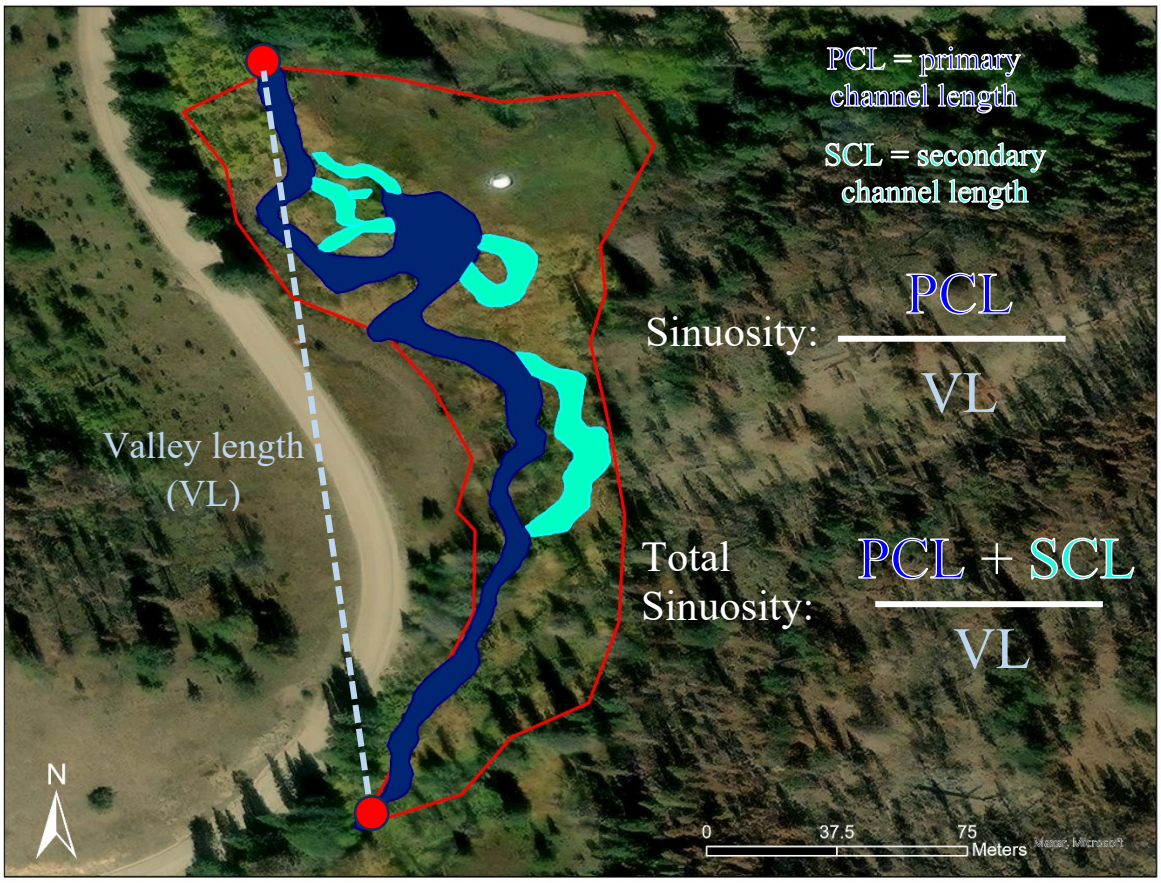

Figure 18: Sinuosity and total sinuosity illustrated for the first bead on Pennock Creek. Bead boundaries outlined in red. Primary channel colored in dark blue and secondary channels colored in aqua.

Beads with secondary channels and/or bifurcations were also assessed for total sinuosity. Total sinuosity accounts for multithread reaches by calculating the ratio of total channel segment length to valley length (Figure 16). Secondary channels were also delineated by hand in Google Earth Pro and added to the primary channel length to create total channel length. Depending on the number and length of secondary channels, total sinuosity can be far larger than sinuosity. Secondary channels were generally narrower and rejoined the main channel at relatively short distances downstream, ranging from 9 m to 48 m. Sinuosity and total sinuosity were both measured, but only total sinuosity was analyzed further.

5.5 Statistical Analyses

All statistical analyses were completed using R version 4.4.3 in R Studio, and all tests were run at a significance level of $\alpha=0.05$. Following processing and analysis of all data, exploratory data analysis (EDA) was used to summarize and present graphical and numerical findings. Means, ranges, minimums, and maximums for each variable were calculated and graphed as boxplots. All variables were assessed for normality of distribution both using Shapiro-Wilk's Tests and transformations were performed where necessary to approximate normal distributions. Variable transformations included logarithmic, square-root, logarithm plus a constant, and inverse. Several variables (Total Burn Percent, Mixed Forest Percent, X16H100Y, 1% AEP, 50% AEP, Berm Density, Minimum Berm Count, Precipitation, STORNHD, Minimum NDVI, Maximum NDVI, and Patch Count) could not be transformed to achieve normality using those methods and were assessed with non-parametric tests.

Categories were assigned under the assumption that each will have different functionalities and geometries based on their different modification levels, vegetation, and spatiotemporal distributions of water and sediment in the channel (timing and nature of geomorphically significant flows). Each bead was grouped three times, by status (natural, impaired, or restored), type (beaver meadow, forest, or elk grassland), and elevation zone (montane or subalpine). Bead status was assigned based on field and historical context. Restored beads have received human attention with the aim of restoring connectivity and promoting the return of natural processes, biota, and geomorphic landforms. Impairment was determined physically in the field (see Section 6.1.3) or was known prior to field visits. Beads with severe catchment burn (e.g., Little Beaver Creek), upstream modifications (e.g., Beaver Creek), or known floodplain modification (e.g., Big Thompson River) were all chosen as candidates for impairment. Bead type was

established using the criteria in Section 5.2.3 and elevation zone was assigned using the elevation stratifications from Veblen and Donnegan (2006).

Categorical analysis tested for the statistical significance of three different categories and attempted to characterize naturally occurring groups within the dataset. Thirty variables, both predictors and responses, were assessed by category. Transformed variables were tested with one-way ANOVA to locate statistically significant differences in catchment- and reach-scale characteristics by category. Tukey Honest Significant Difference (HSD) tests returned metrics for pairwise comparisons between differential categorical groups (i.e., beaver meadow – elk grassland). Variables violating normality assumptions were tested with Kruskal-Wallis Rank Sum Test, a non-parametric test for statistically significant differences in catchment- and reach-scale characteristics by category. Dunn's test (Dunn, 1964) with a Bonferroni-adjusted p-value returned metrics for pairwise comparisons between differential categorical groups. Elevation zone did not meet the criteria for Kruskal-Wallis and Dunn analysis, which requires at least 3 factors for pairwise comparison. Transformed variables in this category were analyzed with two-sample t-tests and non-parametric variables were assessed with Mann-Whitney U Tests.

Correlation matrices were produced for driver variables to identify and quantify the weightedness of relationships between and within reach-scale, catchment-scale, biotic, and geomorphic factors. Some of these relationships were predicted in Figure 2 and found to be present within the dataset; for example, increases in catchment elevation correlate negatively with percentage of forest cover in the catchment, which corresponds to changes in vegetation classes with ecoregion. Highly correlated predictor variables, otherwise known as confounding variables, can interact with predictor-response relationships and are therefore not appropriate to

include together in MLRs. Correlation matrices also do not account for the presence of nonlinear relationships, which could be studied later.

Lastly, multiple linear regressions (MLRs) were used to define the relative impacts of select driver variables on each response variable, with the goal of producing a model or series of models able to explain and/or predict functionality with some reliability. These models can also help identify certain factors to be dismissed through lack of correlation with bead functionality. Given that MLR models only have the capacity for one response variable, each response variable was considered individually. Although individual effects of controls are of primary interest, logical interactions with significant high-magnitude correlation between variables were taken into account during the model selection process by experimenting with variable interactions and/or removal. Beads were considered as individual units and signal propagation between them was not accounted for.

Backward and forward stepwise linear regression was used to choose variables for the model selection process. Backward regressions started with all 23 predictor variables and eliminated variables until the model with the lowest AIC, or Akaike's Information Criterion, is found. AIC calculates a metric of model fittedness that is commonly used for model selection (Akaike, 1973). Conversely, forward regressions start with an empty model and add variables until the model with the lowest AIC is found.

Corrected Akaike's Information Criterion, or AICc, was developed later and is appropriate for relatively small dataset sample size and large number of parameters (Hurvich & Tsai, 1989), both of which are true for this dataset. AICc also penalizes model overfitting. Thus, to reduce tradeoff between accuracy and complexity, model selection was performed with AICc using the "AICc" function from the MuMIn package in R. Different combinations of variables from the

stepwise linear regressions were tried, and models with the smallest AICc were selected as the best-fitting. All selected models were assessed for statistical significance and checked for acceptable use via the Assumptions of Homogeneity, Linearity, and Normality.

6. RESULTS

Tables 11 through 17 in Appendix 2 contain all supporting field and remote data collected and analyzed for this research. Appendix 3 contains field photos and detailed descriptions of beaver modifications, field indicators of connectivity, and field indicators of impairment.

6.1 Exploratory Data Analysis

6.1.1 Categorical Analysis

Categorical analysis was performed successfully for all three groupings of variables. Tables 29, 30, and 31 in the Appendix provide comparison results for type, status, and elevation zone, respectively. Testing for statistical significance revealed significant relationships at the $\alpha = 0.05$ level for individual variables as well as between categorical levels as pairwise comparisons for all three categories, although these categories had varied success in capturing and explaining the spread of differences in the magnitudes of inputs and responses found in the dataset. Categorizing beads by type was statistically significant for 23 of the 30 predictor and response variables investigated. Pairwise comparisons between beaver meadows and elk grasslands, beaver meadows and forested beads, and forested beads and elk grasslands were statistically significant for 10, 14, and 12 predictor and response variables, respectively. Categorizing beads by status was statistically significant for 13 of the 30 predictor and response variables investigated. Pairwise comparisons between natural and impaired, restored and impaired, and natural and restored were statistically significant 12, 0, and 0 times, respectively. Categorizing

beads by elevation zone was statistically significant for 10 of the 30 predictor and response variables investigated.

6.1.2 Bead and Catchment Dimension Patterns

Elevation difference between the highest and lowest sites is approximately 827 m, from the bead inlet of Phantom Creek at 3192 m and the bead outlet of Cow Creek at 2365 m. In the field, bead width appeared to be controlled locally by the presence or absence of bedrock outcrops; additionally, impaired beads, many with a history of incision and loss of floodplain-channel connectivity, had lower floodplain-channel width ratios ($p<0.001$). Site visits upheld the expectation that bead conditions are varied as a function of natural conditions and human influence. A statistically significant positive linear relationship between catchment area and bead size was found, wherein larger catchments tend to have beads with greater surface area ($p<0.001$). A size ratio, referred to as "bead ratio," was calculated to offset this effect and was used in place of drainage area and bead size in the model selection process.

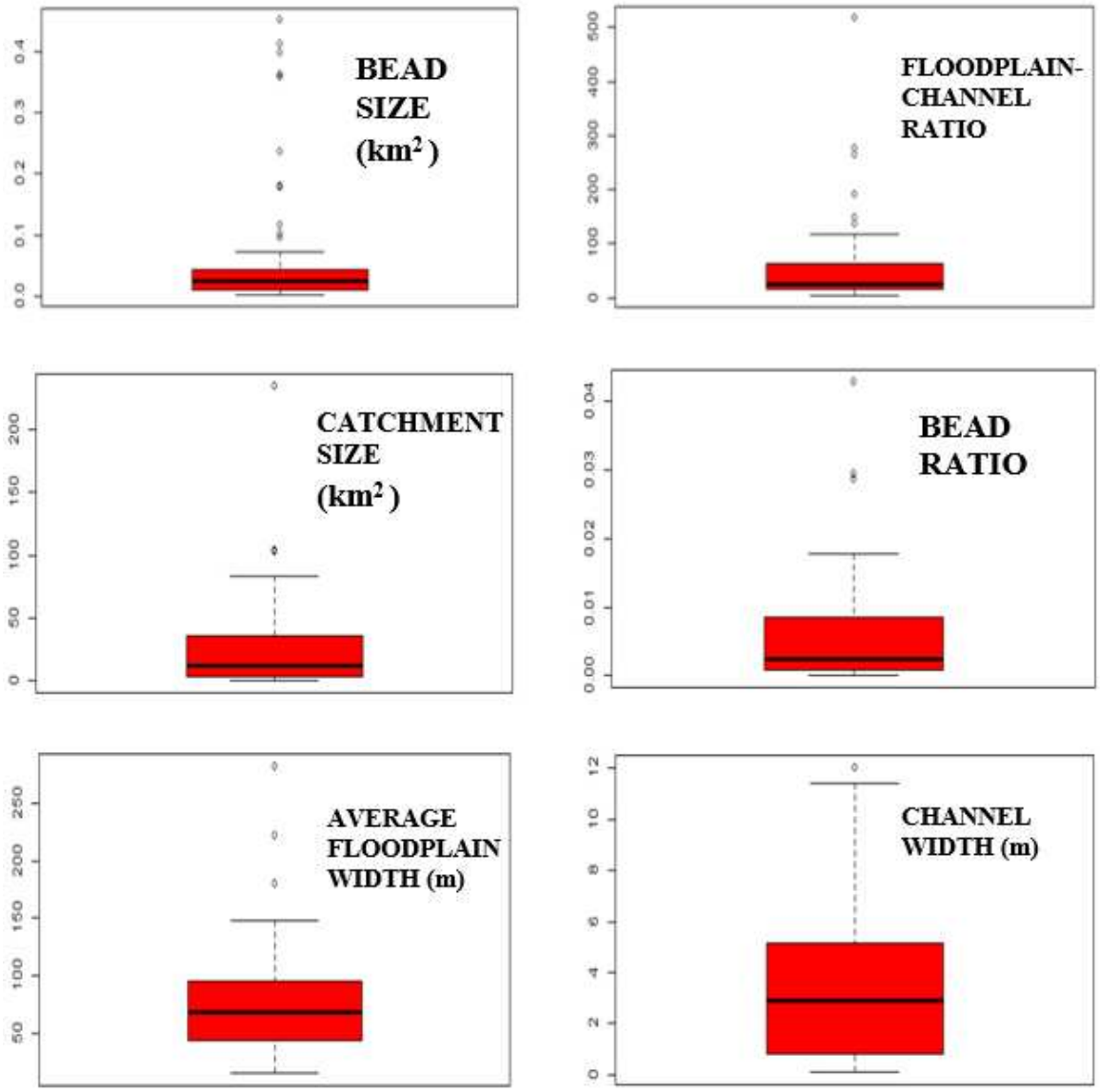

Figure 17: Distributions of bead- and catchment-scale dimensions.

Bead size ranged from 0.00133 km^2 to 0.452 km^2, with 1st and 3rd quartile means of 0.01 km^2 and 0.04 km^2. Mean bead size was 0.072 km^2. Bead size varied significantly by type ($p<0.001$); elk grasslands had significantly larger bead sizes than beaver meadows and forested beads ($p<0.001$, $p<0.001$).

Bead slope ranged from 0.0036 to 0.109, with 1st and 3rd quartile means of 0.019 and 0.04. Mean bead slope was 0.034. Bead slope varied significantly by type ($p=0.045$) and status ($p<0.001$). Elk grasslands had lower slopes than forested beads ($p=0.035$) and impaired beads had lower slopes than natural beads ($p<0.001$).

Floodplain-channel ratio (FP-C ratio) ranged from 3.84 to 517.1, with 1st and 3rd quartile means of 16.6 and 61.4. Mean ratio was 59.8. FP-C ratio varied significantly by type ($p=0.00133$), status ($p<0.001$), and elevation zone ($p=0.014$). Forested beads had lower FP-C ratios than beaver meadows ($p<0.001$), impaired beads had lower FP-C ratios than natural beads ($p<0.001$), and subalpine beads have lower FP-C ratios than montane beads.

Bead ratio ranged from 4.25E-05 to 0.043, with 1st and 3rd quartile means of 0.00082 to 0.0085. Mean bead ratio was 0.006. Bead ratio varied significantly by type ($p=0.014$) and status ($p=0.017$). Forested beads had lower ratios than elk grasslands, or smaller beads relative to catchment size ($p=0.013$) and natural beads had larger ratios than impaired beads ($p=0.012$).

Catchment size ranged from 0.363 km^2 to 233.9 km^2, with 1st and 3rd quartile means of 3.35 km^2 and 35.7 km^2. Mean size was 24.86 km^2. Catchment size varied significantly by type ($p=0.014$) and status ($p>0.001$). Elk grasslands have larger catchments than beaver meadows ($p=0.015$) and impaired beads have larger catchments than natural beads ($p<0.001$).

Average catchment slope ranged from 0.0586 to 0.292, with 1st and 3rd quartile means of 0.115 and 0.206. Mean catchment slope was 0.163. Average catchment slope varied by type ($p<0.001$) and elevation zone ($p<0.001$). Forested beads had higher slopes than beaver meadows ($p<0.001$), and subalpine beads had higher slopes than montane beads.

Average catchment elevation ranged from 2547.8 m to 3543.6 m, with 1st and 3rd quartile means of 2817.4 m and 3287.3 m. Mean elevation was 3069.6 m. Average catchment elevation

varied by type and elevation zone. Forested beads had higher average catchment elevations ($p<0.001$); subalpine beads had higher average catchment elevations ($p<0.001$), reflecting the ecoregion stratifications used to delineate these zones.

Mixed forest percent (MF) ranged from 13.6% to 98.4%, with 1st and 3rd quartile means of 48.7% and 89.4%. Mean MF was 67.3%. MFP varied significantly with type ($p=0.002$) and elevation zone ($p<0.001$). Beaver meadows had higher proportions of forest coverage in catchments than forested beads ($p=0.0035$), and montane beads had higher proportions of forest coverage in catchments. Between subalpine and montane beads with origins above timberline, subalpine beads naturally have lower forest cover due to the larger proportion of their catchments in more sparsely vegetated zones.

6.1.3 Functionality Driver Patterns – Biotic

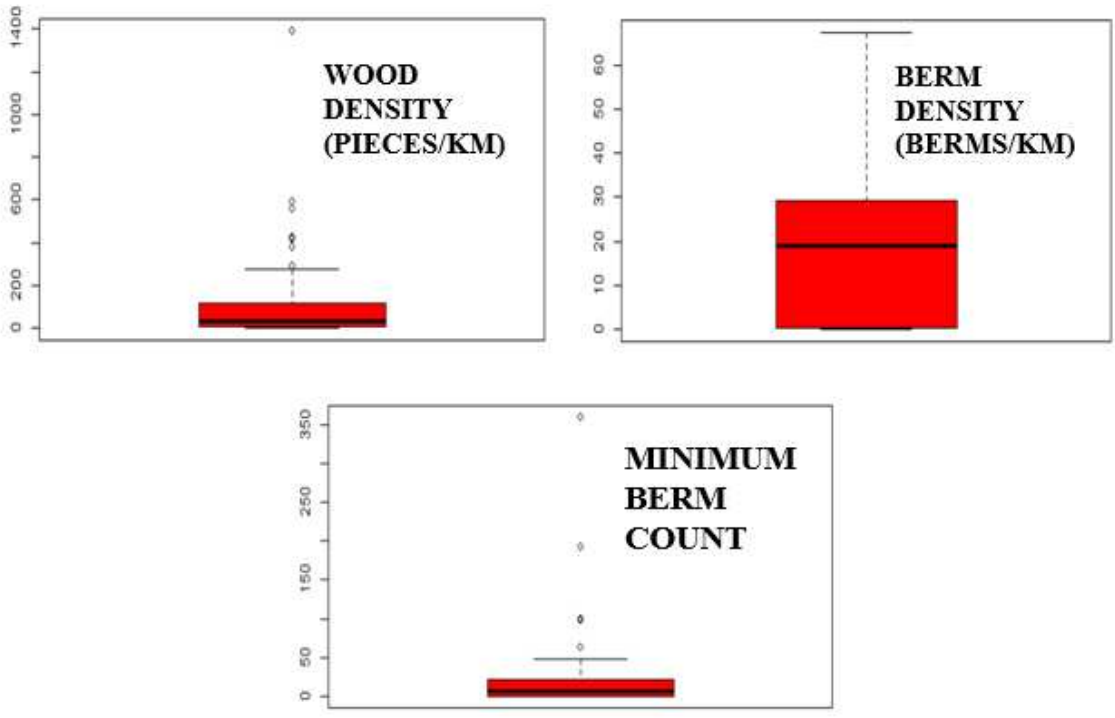

Figure 18: Distributions of biotic variables.

Berm density ranged from 0 to 67.3, with 1st and 3rd quartile means of 0.38 berms/km and 29.1 berms/km. Mean density was 19.8 berms/km. Berm density varied significantly by type ($p=0.0061$); beaver meadows were found to have higher berm densities than forested beads ($p=0.0059$).

Minimum berm count ranged from 0 to 359, with 1st and 3rd quartile means of 0.75 and 22.3. Mean berm count was 24.058. Minimum berm count varied by status; impaired beads had higher minimum berm counts than natural beads ($p=0.012$).

Wood density ranged from 0 to 1389.7 pieces/km with 1st and 3rd quartile means of 9.6 pieces/km and 115.3 pieces/km. Mean density was 120.072 pieces/km. Wood density varied significantly by type ($p<0.001$); elk grasslands had lower wood densities than beaver meadows ($p=0.018$), forested beads had higher wood densities than both elk grasslands and beaver meadows ($p<0.001$, $p<0.001$), and beaver meadows had higher wood densities than elk grasslands ($p=0.018$).

6.1.4 Functionality Driver Patterns – Geomorphic

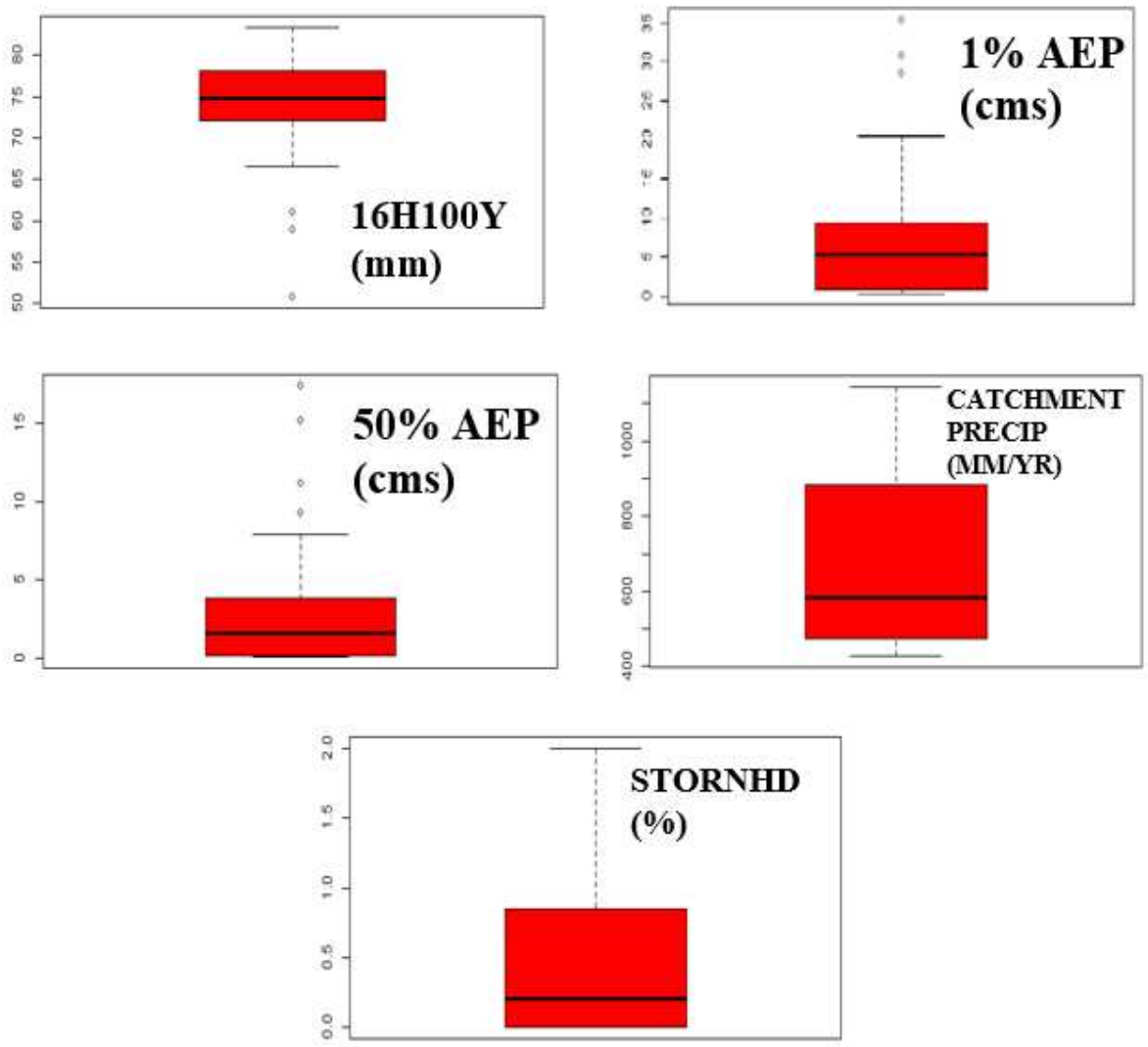

Figure 19: Distributions of hydrologic variables.

16H100Y (6-hour precipitation that occurs every 100 years on average) ranged from 50.8 mm to 83.3 mm, with 1st and 3rd quartile means of 73.3 mm and 78 mm. Mean 16H100Y was 73.1 mm. 16H100Y varied significantly by type (p=0.026); elk grassland catchments receive lower 6-hour 100-year-recurrence precipitation intensities than forested beads (p=0.022).

1% Annual Exceedance Probability (AEP) ranged from 0.34 cms to 35.4 cms, with 1st and 3rd quartile means of 0.84 cms and 9.33 cms. Mean 1% AEP was 7.0 cms. 1% AEP varied

significantly by type (p=0.0021), status (p=0.0014), and elevation zone (p=0.027). Beaver meadow beads had lower 1% AEPs than elk grasslands (p=0.0076), impaired beads had higher 1% AEPs than natural beads (p<0.001), and montane beads had lower 1% AEPs than subalpine beads.

50% Annual Exceedance Probability (AEP) ranged from 0.077 cms to 17.4 cms, with 1st and 3rd quartile means of 0.21 cms and 3.81 cms. Mean AEP was 2.85 cms. 1% AEP varied significantly by type (p<0.001), status (p=0.0067), and elevation zone (p=0.0083). Beaver meadows had lower 50% AEPs than both forested beads and elk grasslands (p=0.016, p=0.011), impaired beads had higher 50% AEPs than natural beads (p=0.005), and montane beads had lower 50% AEPs than subalpine beads.

Catchment precipitation ranged from 427.5 mm/yr to 1144.3 mm/yr, with 1st and 3rd quartile means of 475.2 mm and 883.9 mm. Mean precipitation was 670.9 mm/yr. Catchment precipitation varied by type (p<0.001) and elevation zone (p<0.001). Forested bead catchments receive higher yearly catchment precipitation than beaver meadow bead catchments (p=0.0038), and subalpine bead catchments receive more precipitation than montane bead catchments.

STORNHD (total percent of catchment surface water storage) ranged from 0% to 2%, with 1st and 3rd quartile means of 0% and 0.83%. Mean STORNHD was 0.479%. STORNHD did not vary significantly by category.

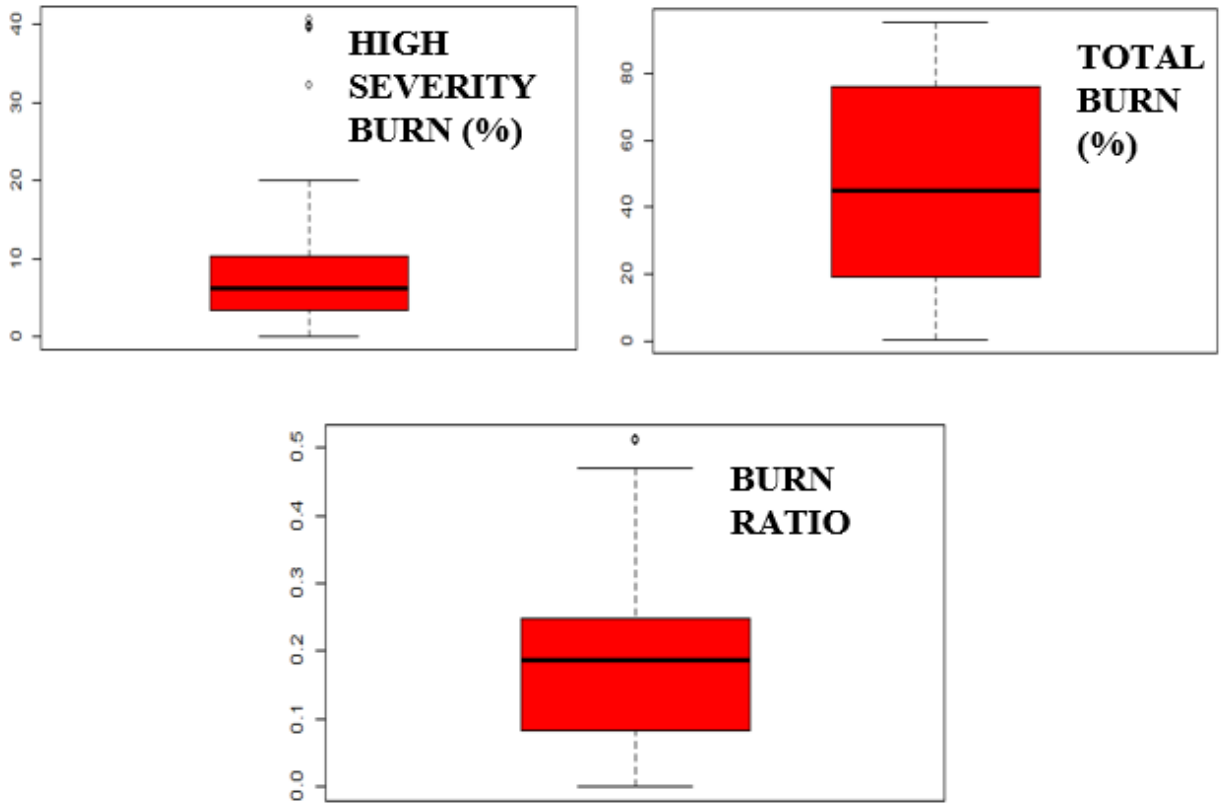

Figure 20: Distribution of sediment proxy variables.

High severity burn percent (HSB) ranged from 0% to 40.6%, with 1st and 3rd quartile means of 3.39% and 9.89%. Mean HSB was 9.26%. HSB did not vary significantly by category.

Total burn percent (TB) ranged from 0.27% to 95.3%, with 1st and 3rd quartile means of 19.4% and 75.2%. Mean TB was 46.2%. TB varied significantly by elevation zone (p=0.011). Subalpine beads had lower catchment burn coverage than montane beads.

Burn ratio (BR) ranged from 0 to 0.513, with 1st and 3rd quartile means of 0.08 and 0.25. Mean BR was 0.182. Burn ratio varied significantly by type (p=0.026) and status (p=0.017). Beaver meadows had lower burn ratios, or reduced coverage of high-severity burn, compared to forested beads (p=0.021), and impaired beads had lower burn ratios than natural beads (p=0.041).

6.1.5 Response Patterns

NDVI ranged from 0.051 to 0.569, with 1st and 3rd quartile means of 0.371 and 0.429. Mean NDVI was 0.402. Minimum NDVI varied significantly by type ($p<0.001$) and status ($p=0.011$), mean NDVI varied significantly by status ($p=0.034$), and NDVI range varied significantly by type ($p<0.001$). Elk grasslands had lower minimum NDVIs than beaver meadows ($p=0.012$) and forested beads (pp<0.001), impaired beads had lower minimum NDVIs than natural beads ($p=0.018$), and elk grasslands had higher NDVI ranges than beaver meadows ($p<0.001$) and forested beads ($p<0.001$).

NDWI ranged from -0.954 to -0.393, with 1st and 3rd quartile means of -0.725 and -0.676. Mean NDWI was -0.705. Minimum NDWI varied significantly by type ($p=0.021$) and elevation zone ($p=0.0062$), maximum NDWI varied significantly by type ($p<0.001$) and status ($p=0.0012$), mean NDWI varied significantly by type ($p<0.001$) and status ($p=0.012$), and NDWI range varied significantly by type ($p<0.001$). Forested beads have lower minimum NDWI than beaver meadows ($p=0.026$), subalpine beads have lower minimum NDWI than montane beads. Forested beads have lower maximum NDWIs than elk grasslands ($p<0.001$) and beaver meadows ($p=0.0021$), elk grasslands have higher maximum NDWIs than beaver meadows ($p=0.0032$), and natural beads had lower maximum NDWIs than impaired beads ($p=0.001$). Forested beads had higher mean NDWIs than beaver meadows ($p<0.001$) and elk grasslands ($p<0.001$), and natural beads had higher mean NDWIs than impaired beads ($p=0.025$). Elk grasslands have higher ranges than beaver meadows ($p<0.001$) and forested beads ($p<0.001$).

Patch count ranged from 3 to 131, with 1st and 3rd quartile means of 11 and 56.5. Mean patch count was 38.058. Patch count varied significantly by type ($p=0.013$) and status

(p=0.0088). Forested beads had lower patch counts than beaver meadows and elk grasslands (p=0.030, p=0.023), and impaired beads had higher patch counts than natural beads (p=0.0066).

Patch density ranged from 19.3 patches/km to 41469.4 patches/km, with 1st and 3rd quartile means of 343.3 patches/km and 3640.9 patches/km. Mean density was 3806 patches/km. Patch density varied significantly by type ($p<0.001$) and elevation zone (p=0.017). Elk grasslands had lower patch densities than beaver meadows (p=0.0017) and forested beads ($p<0.001$), and subalpine beads had lower patch densities than montane beads.

Total sinuosity ranged from 1.009 to 3.04, with 1st and 3rd quartile means of 1.26 and 1.67. Mean total sinuosity was 1.508. Total sinuosity did not vary significantly by category.

Table 10: Summary of significant relationships between predictor/response variables and categories. An "X" signifies the presence of a significant ($p<0.05$) relationship. EG = elk grassland, BM = beaver meadow, F = forested, Nat = natural, Imp = impaired, Mont = montane, and Sub = subalpine.

	Type	Status	Elevation Zone	Relationships
Bead Size	X			EG > F & BM
Bead Slope	X	X		F > EG, Nat > Imp
Floodplain-Channel Width Ratio	X	X	X	BM > F, Nat > Imp, Mont > Sub
Bead Ratio	X	X		EG > F, Nat > Imp
Catchment Size	X	X		EG > BM, Imp > Nat
Average Catchment Slope	X		X	F > BM & EG, Sub > Mont
Average Catchment Elevation	X		X	F > BM & EG, Sub > Mont
Mixed Forest	X		X	BM > F, Mont > Sub
Berm Density	X			BM > F
Minimum Berm Count		X		Imp > Nat

Wood Density	X			F > BM > EG
16H100Y	X			F > EG
1% AEP	X	X	X	EG > BM, Imp > Nat, Sub > Mont
50% AEP	X	X	X	EG & F > BM, Imp > Nat, Sub > Mont
Precipitation	X		X	F > BM, Sub > Mont
STORNHD				N/A
High Severity Burn				N/A
Total Burn			X	Mont > Sub
Burn Ratio	X	X		F > BM, Nat > Imp
Minimum NDVI	X	X		F & BM > EG, Nat > Imp
Maximum NDVI				N/A
Average NDVI		X		No significant pairwise relationships
NDVI Range	X			EG > F & BM
Minimum NDWI	X		X	BM > F, Mont > Sub
Maximum NDWI	X	X		EG > BM > F, Imp > Nat
Average NDWI	X	X		F > EG & BM, Nat > Imp
NDWI Range	X			EG > F & BM
Patch Count	X	X		BM > EG > F, Imp > Nat
Patch Density	X		X	BM > EG, Mont > Sub
Total Sinuosity				N/A

6.1.6 Predictor Variable Correlation

In addition to examining the strength of association between categorical variables, strength of association between predictor variables was examined prior to the model selection process. Tables 18 and 19 in the Appendix contain correlation matrix data, color-coded for strength of association, as well as the associated p-values. Aside from two perfectly uncorrelated relationships (mixed forest percent – bead slope; 16H100Y – burn ratio), all variables in the dataset showed varying levels of negative or positive correlation. Many correlation indices were low-magnitude with low p-values; these were not mentioned due to the relative insignificance of minimally correlated variables.

Moderate to high statistically significant positive correlation (>0.6) was found between bead size and 1% AEP (0.67), 50% AEP (0.63), and minimum berm count (0.67); average catchment slope and 50% AEP (0.63), average catchment elevation (0.82), and precipitation (0.81); drainage area and 1% AEP (0.8) and 50% AEP (0.66), STORNHD and average catchment elevation (0.64); 1% AEP and 50% AEP (0.97); and precipitation and 50% AEP (0.61) and average catchment elevation (0.81). All correlations were statistically significant with $p<0.05$.

Moderate to high statistically significant negative correlation (<-0.6) was found between average catchment slope and total burn (-0.66) and mixed forest percent (-0.77); total burn and average catchment elevation (-0.64) and precipitation (-0.65); and mixed forest percent and STORNHD (-0.63), average catchment elevation (-0.82), and precipitation (-0.77). All correlations were statistically significant with $p<0.05$.

6.2 Model Selections

Checks for linearity, homogeneity, and normality revealed no violations among any of the six selected models. Given the number of statistically significant correlations between

predictors, models were also assessed for multicollinearity via Variable Inflation Factor (VIF). A VIF of over 5 is generally considered large and necessitates adjustment or removal of predictor variables in the model.

Table 11: Model statistics and AICc for functionality drivers and NDVI range.

Response Variable	Model Terms	F-statistic	p-value	AICc
log(NDVIRange)	**BeadRatio + BeadSlope + MixedForestPct + 16H100Y + factor(Type)**	**9.543**	**9.2e-07**	**30.45247**
log(NDVIRange)	BeadRatio + MixedForestPct + X16H100Y + factor(Type) + TotalBurnPct	8.329	4.324e-06	34.29413
log(NDVIRange)	BeadRatio + factor(Type) + BermDensity	4.888	0.002228	49.56552
log(NDVIRange)	factor(Type) + BeadRatio + MixedForestPct	9.947	6.48e-06	35.76088
log(NDVIRange)	BeadSlope + MixedForestPct + X16H100Y + factor(Type) + FPCR	8.539	3.286e-06	33.61001

The NDVI range model with the lowest AICc contains bead ratio, bead slope, mixed forest percent, 16H100Y and type. This model is statistically significant (F-statistic = 9.543, p = 9.2e-07) and has an AICc of 30.45247.

Table 12: Summary statistics for the best-fitting model for NDVI range.

Term	Estimate [95% CI]	p-value
Intercept	-1.78 [-2.61, -0.94]	***<0.001***
BeadRatio	8.98 [-1.68, 19.63]	0.097
BeadSlope	-4.45 [-8.95, 0.045]	0.052
MixedForestPct	-0.0088 [-0.013, -0.0047]	***<0.001***
16H100Y	0.014 [0.0028, 0.026]	**0.015**
factor(Type)EG	0.434 [0.152, 0.716]	**0.0033**
factor(Type)FC	-0.447 [-0.745, -0.149]	**0.0042**
Adjusted R-squared = 0.5013		

This model implies a positive relationship with bead ratio, a negative relationship with bead slope, a slight negative relationship with mixed forest percent, and a slight positive relationship with 16H100Y, with the highest NDVI ranges in elk grasslands, and the lowest in forested beads. Bead ratio and bead slope are not statistically significant in the model.

Table 13: Model statistics and AICc for functionality drivers and mean NDVI.

Response Variable	Model Terms	F-statistic	p-value	AICc
NDVIMean	BeadRatio + AvgCatchSlope + TotalBurnPct + MixedForestPct + X16H100Y + X1pctAEP + X50pctAEP + AvgBasinElev + MinBermCount + factor(ElevationZone)	3.224	0.003812	-184.351
NDVIMean	BeadRatio + MixedForestPct + X50pctAEP + MinBermCount + WoodDensity + factor(ElevationZone)	3.062	0.01343	-184.6327
NDVIMean	BeadRatio + MixedForestPct + MinBermCount + WoodDensity + factor(ElevationZone)	2.7	0.032	-183.0164
NDVIMean	factor(Status) + HighSevBurnPct + X16H100Y + BeadRatio + FPCR	3.095	0.01268	-184.7958
NDVIMean	**factor(Status) + HighSevBurnPct + 16H100Y +BeadRatio**	**3.717**	**0.00657**	**-187.2794**

The NDVI average model with the lowest AICc contains status, high severity burn percent, 16H100Y, and bead ratio. This model is statistically significant (F-statistic = 3.717, p = 0.00657) and has an AICc of -187.2794.

Table 14: Summary statistics for the best-fitting model for mean NDVI.

Term	Estimate [95% CI]	p-value
Intercept	0.259 [0.156, 0.362]	***<0.001***
factor(Status)Natural	0.028 [0.0058, 0.051]	**0.015**
factor(Status)Restored	-0.014 [-0.050, 0.023]	0.45
HighSevBurnPct	0.0012 [2.0e-04, 0.0023]	**0.021**
16H100Y	0.0015 [1.8e-04, 0.0029]	**0.027**
BeadRatio	1.22 [-0.120, 2.558]	0.073
Adjusted R-squared = 0.2103		

This model implies a strong positive relationship with bead ratio, slight positive relationships with 16H100Y and high severity burn percent, highest mean NDVI in natural beads, and lowest mean NDVI in restored beads. The coefficient of difference between impaired and restored beads is not statistically significant in the model.

Table 15: Model statistics and AICc for functionality drivers and NDWI range.

Response Variable	**Model Terms**	**F-statistic**	**p-value**	**AICc**
sqrt(NDWIRange)	**BeadRatio + BeadSlope + BurnRatio + MixedForestPct + 16H100Y + factor(Type)**	**10.88**	**7.069-08**	**-130.1376**
sqrt(NDWIRange)	1pctAEP + BeadRatio + BeadSlope + AvgCatchSlope + factor(Type) + TotalBurnPct + Precip	8.699	5.697-07	-124.8629
sqrt(NDWIRange)	BeadSlope + Precip + factor(Type) + BermDensity + 1pctAEP + BeadRatio	8.689	1.165e-06	-123.03
sqrt(NDWIRange)	BeadRatio + BeadSlope + MixedForestPct + X16H100Y + factor(Type)	11.32	1.13e-07	-128.6606
sqrt(NDWIRange)	BeadRatio + BeadSlope + MixedForestPct + X16H100Y + factor(Type) + WoodDensity	9.637	3.329e-07	-126.2213

The NDWI range model with the lowest AICc contains bead ratio, bead slope, burn ratio, mixed forest percent, 16H100Y, and type. This model is statistically significant (F-statistic = 10.88, p = 7.069e-08) and has an AICc of -130.1376.

Table 16: Summary statistics for the best-fitting model for NDWI range.

Term	**Estimate [95% CI]**	**p-value**
Intercept	0.289 [0.101, 0.478]	**0.0034**
BeadRatio	4.38 [2.00, 6.76]	***<0.001***
BeadSlope	-1.04 [-2.03, -0.043]	**0.041**
BurnRatio	0.168 [-0.0035, 0.34]	0.054

MixedForestPct	-0.0021 [-0.0030, 0.34]	***<0.001***
16H100Y	0.0041 [0.0017, 0.0066]	**0.0015**
factor(Type)EG	0.095 [0.035, 0.154]	**0.0024**
factor(Type)FC	-0.110 [-0.181, -0.038]	**0.0036**
Adjusted R-squared = 0.5756		

This model implies a positive relationship with bead ratio, a slight positive relationship with burn ratio and 16H100Y, a negative relationship with bead slope, a slight negative relationship with mixed forest percent, highest NDWI ranges in elk grasslands, and lowest in forested beads. Burn ratio is not statistically significant in the model.

Table 17: Model statistics and AICc for functionality drivers and mean NDWI.

Response Variable	Model Terms	F-statistic	p-value	AICc
1/NDWIMean	BeadRatio + AvgCatchSlope + TotalBurnPct + MixedForestPct + 16H100Y + 1pctAEP + 50pctAEP + AvgBasinElev + MinBermCount + factor(Type) + factor(ElevationZone)	10.59	7.198e-09	-134.8591
1/NDWIMean	BeadRatio + TotalBurnPct + MixedForestPct + AvgCatchSlope + MinBermCount + factor(Type) + factor(ElevationZone) + 50pctAEP	9.422	1.152e-07	-127.7123
1/NDWIMean	**BeadRatio + TotalBurnPct + MixedForestPct + MinBermCount + factor(Type) + factor(ElevationZone) + 50pctAEP**	**10.54**	**4.912e-08**	**-129.9373**
1/NDWIMean	BeadRatio + MixedForestPct + MinBermCount + factor(Type) + factor(ElevationZone) + 50pctAEP	9.669	3.194e-07	-125.0072
1/NDWIMean	factor(Type) + TotalBurnPct + Precip + MixedForestPct + factor(Status) + BurnRatio + MinBermCount + 50pctAEP + 1pctAEP + factor(ElevationZone) + BeadRatio + AvgCatchSlope + 16H100Y + FPCR	8.002	1.697e-07	-122.1345

The selected NDWI average model contains bead ratio, total burn percent, mixed forest percent, minimum berm count, type, elevation zone, and 50% AEP. This model is statistically significant

(F-statistic = 10.54, p = 4.912e-08) and has an AICc of -129.9373. One other model has a lower AICc, but this model had significant multicollinearity and was eliminated as the best-fitting model.

Table 18: Summary statistics for the best-fitting model for mean NDWI.

Term	Estimate [95% CI]	p-value
Intercept	-1.68 [-1.78, -1.57]	***<0.001***
BeadRatio	2.83 [0.56, 5.10]	**0.016**
TotalBurnPct	9.3e-04 [2.3e-04, 1.6e-03]	**0.01**
MixedForestPct	-0.0019 [5.9e-04, -0.0031]	**0.005**
MinBermCount	-3.8e-04 [-7.4e-04, -2.1e-05]	**0.038**
factor(Type)EG	-0.071 [-0.141, -0.002]	**0.044**
factor(Type)FC	0.161 [0.097, 0.225]	***<0.001***
factor(ElevationZone)	0.083 [0.016, 0.15]	**0.017**
50% AEP	0.014 [0.0068, 0.022]	***<0.001***
Adjusted R-squared = 0.5994		

The selected model implies a positive relationship with bead ratio, a slight positive relationship with total burn percent, mixed forest percent, and 50% AEP, a slight negative relationship with minimum berm count, highest mean NDWI in forested beads, lowest mean NDWI in elk grasslands, and slightly higher mean NDWI in subalpine beads.

Table 19: Model statistics and AICc for functionality drivers and patch density.

Response Variable	Model Terms	F-statistic	p-value	AICc
log(PatchDensity)	**BermDensity + BeadRatio + X1pctAEP + MinBermCount**	**29.05**	**3.492e-12**	**115.1127**
log(PatchDensity)	BermDensity + Precip + BeadRatio + X1pctAEP + MinBermCount + factor(Status)	17.91	5.377e-11	118.1877
log(PatchDensity)	BermDensity + Precip + BeadRatio + X1pctAEP + MinBermCount	23.65	1.089e-11	116.3474
log(PatchDensity)	factor(Type) + BermDensity + Precip + BeadRatio + 1pctAEP + MinBermCount + factor(Status)	14.99	1.625e-10	119.8084

log(PatchDensity)	BermDensity + Precip + BeadRatio + X1pctAEP + MinBermCount + factor(Type)	18.02	4.862e-11	117.9405

The patch density model with the lowest AICc contains type, berm density, bead ratio, 1% AEP, and minimum berm count. This model is statistically significant (F-statistic = 29.05, p = 3.492e-12) and has an AICc of 115.1127.

Table 20: Summary statistics for the best-fitting model for patch density.

Term	Estimate [95% CI]	p-value
Intercept	7.1 [6.7, 7.5]	***<0.001***
BermDensity	0.037 [0.025, 0.048]	***<0.001***
BeadRatio	-56.6 [-81.8, -31.4]	***<0.001***
1% AEP	-0.069 [-0.096, -0.042]	***<0.001***
MinBermCount	-0.005 [-0.009,-0.001]	**0.014**
Adjusted R-squared = 0.6875		

This model implies a strong negative relationship with bead ratio, slight negative relationships with 1% AEP and minimum berm count, and a slight positive relationship with berm density.

Table 21: Model statistics and AICc for functionality drivers and total sinuosity.

Response Variable	Model Terms	F-statistic	p-value	AICc
log(TotalSinuosity)	**AvgCatchSlope + AvgBasinElev + factor(ElevationZone)**	**5.982**	**0.001505**	**-15.21085**
log(TotalSinuosity)	BeadRatio + AvgCatchSlope + AvgBasinElev + factor(ElevationZone)	4.404	0.004179	-12.68307
log(TotalSinuosity)	AvgCatchSlope + TotalBurnPct + AvgBasinElev + factor(ElevationZone)	5.149	0.001595	-15.02961

log(TotalSinuosity)	AvgBasinElev + factor(ElevationZone) + MixedForestPct + AvgCatchSlope	4.517	0.003601	-13.04766
log(TotalSinuosity)	BeadSlope	4.491	0.03907	-7.970658

The total sinuosity model with the lowest AICc contains average catchment slope, average catchment elevation, and elevation zone. This model is statistically significant (F-statistic = 5.982, p = 0.001505) and has an AICc of -15.21085.

Table 22: Summary statistics for the best-fitting model for total sinuosity.

Term	Estimate [95% CI]	p-value
Intercept	-1.55 [-2.55, 0.56]	***≤0.001***
AvgCatchSlope	-0.015 [-0.032, 0.0015]	0.074
AvgCatchElev	7.3e-04 [3.4e-04, 1.1e-03]	***≤0.001***
Factor(ElevationZone)	-0.291 [-0.466, -0.115]	**0.0017**
Adjusted R-squared = 0.2266		

This model implies a slight negative relationship with average catchment slope, a slight positive relationship with average catchment elevation, and lower total sinuosity in subalpine beads. Average catchment slope is not statistically significant in the model.

6.3 Results summary

Bead type was the most statistically successful category used to group beads. Bead types most often differ significantly in relation to wood density and maximum NDWI; all three pairwise comparisons were significant for these two metrics, indicating that all three bead types are statistically distinct in their magnitudes of these variables. Two of the three pairwise comparisons, or partial statistical distinctness, were observed for bead size, 50% AEP, minimum NDVI, NDVI range, mean NDWI, NDWI range, patch count, and patch density. All other

variables were either insignificant when examined by type or had one significant pairwise comparison.

Selected predictive model outputs differed in their size, selected variables, and strength of variable influence. Bead ratio, the ratio of bead size to catchment size, appeared in five of the six selected predictive models – the most of any variable - suggesting that the catchment-bead size relationship is of primary importance in determining functionality. Coefficients for two of these five instances (mean NDVI and NDVI range) were not statistically significant, but the significance of the entire model fails to discount the possibility that bead ratio does exercise control on NDVI. Additionally, both p-values were less than 0.1, so these results are significant with a slightly larger margin of error. Bead ratio did not appear in the predictive model for total sinuosity. Certain variables were deemed insignificant or were detrimental to model performance. Wood density, STORNHD, floodplain-channel width ratio, and precipitation did not appear in any of the models. In particular, wood density tended to decrease model performance.

In addition to bead ratio, NDVI and NDWI were slightly negatively influenced by 16H100Y (6-hour precipitation occurring on average once every 100 years) and slightly positively influenced by catchment forest coverage. All four NDVI/NDWI metrics contained one or both of these variables; the selected models otherwise contained different combinations of variables.

Patch density was influenced primarily by bead ratio, wherein lower bead ratios, or smaller beads relative to catchment size, are strongly associated with high patch densities. Also influential were l00-year flood magnitudes and beaver modifications. Smaller beaver-modified beads tended to favor higher berm densities, as opposed to larger beads, which typically had

higher berm counts but with greater spacing between them. Total sinuosity was influenced primarily by catchment position and geometry; slope, elevation, and elevation zone were selected as the most influential variables in determining total sinuosity.

6.4 Alternative Models

Models were also run a second time without categories as driver variables for all functionality proxy variables to assess patterns within the entire dataset. Five of the six models changed. The model for patch density remained the same; the most significant driver variables explaining variations in patch density, regardless of category, are bead ratio, berm density, 100-year flood (X1pctAEP), and minimum berm count.

For the functionality indicators of wetness (mean and range for NDVI and NDWI), the potential driver of bead ratio remained important, though it was dropped from the mean NDWI model. The coefficient for bead ratio was significant in all three cases and was strongly positively correlated with NDVI mean/range and NDWI range. Wood density appeared in all four NDVI/NDWI models; previously, wood density was found to be insignificant or detrimental to model performance. In all four cases, higher wood density was very slightly correlated with increases in NDVI/NDWI means and decreases in NDVI/NDWI ranges. However, the coefficient for wood density was significant in only one of those four models, NDWI mean. Additional drivers present in more than one NDVI/NDWI model were bead slope, some measure of burn severity, 100-year precipitation (16H100Y), 100-year flood (X1pctAEP), forest coverage, minimum berm count, and precipitation. The model for total sinuosity became univariate, explained only by bead slope. In this model, bead slope is strongly negatively correlated with total sinuosity. Overall, bead ratio remains the most important control on bead functionality.

Table 23: Summary of differences between selected functionality models run with and without categories.

Variable	Model with categories	Model without categories
log(NDVIRange)	BeadRatio + BeadSlope + MixedForestPct + 16H100Y + factor(Type)	X1pctAEP + BeadRatio + BeadSlope + MixedForestPct + WoodDensity
NDVIMean	factor(Status) + HighSevBurnPct + 16H100Y +BeadRatio	TotalBurnPct + Precip + MixedForestPct + MinBermCount + BeadRatio + WoodDensity
sqrt(NDWIRange)	BeadRatio + BeadSlope + BurnRatio + MixedForestPct + 16H100Y + factor(Type)	X1pctAEP + BeadRatio + BeadSlope + AvgCatchSlope + WoodDensity
(1/NDWIMean)	BeadRatio + TotalBurnPct + MixedForestPct + MinBermCount + factor(Type) + factor(ElevationZone) + 50pctAEP	WoodDensity + TotalBurnPct + Precip + MinBermCount + MixedForestPct
log(PatchDensity)	BermDensity + BeadRatio + X1pctAEP + MinBermCount	NO CHANGE
log(TotalSinuosity)	AvgCatchSlope + AvgBasinElev + factor(ElevationZone)	BeadSlope

7. DISCUSSION

Hypothesis one stated that bead functionality will be strongly correlated with bead categories. Parametric tests, non-parametric tests, and pairwise comparisons found varied category success in capturing dataset variations, with type being most successful. Bead type found significant differences between elk grasslands, beaver meadows, and forested beads in their catchment/bead geometry, magnitude of inputs, and magnitude of responses. Status captured significant differences between natural and impaired beads but failed to differentiate restored beads from either of those groups. Elevation zone primarily captured inherent differences in geometry and hydrology between montane and subalpine beads but did identify a relationship between elevation and level of channel confinement, which alters bead geometry as well as patch density. The categorization process did reveal significant differences in

bead/catchment geometry, system inputs, and perceived functionality by dominant vegetation, extent of disturbance influence, and elevation. However, differences in beads are most likely the manifestation of a more complex combination of variables, and correlation between type and elevation zone complicates the interpretation of these results; thus, this hypothesis is only partially supported.

Hypothesis two stated that bead functionality cannot be reliably defined by one metric and instead correlates with multiple driver variables. For all six evaluated functionality proxy variables, stepwise linear regression and subsequent AICc values showed a greater statistical validity of multivariate models over univariate models, supporting this hypothesis. All six models had at least two statistically significant variables of interest; although the coefficients (and relative impacts) of these variables differed greatly, it is clear that functionality is extremely complex. For the functionality indicators of wetness (mean and range for NDVI and NDWI), the potential driver of bead ratio was consistently selected in every model although not significant in every model. Additional drivers present in more than one model were bead slope, some measure of burn severity, 100-year precipitation (16H100Y), and bead type. For patchiness, the most significant driver variables are bead ratio, berm density, 100-year flood (X1pctAEP), and minimum berm count. For total sinuosity, the most significant driver variables are average basin elevation and bead elevation. Overall, bead ratio appears to be an important control on bead functionality as reflected in the indicators analyzed here.

Hypothesis three stated that there is a progressive relationship between bead functionality and bead size. Five of the six selected functionality models included bead ratio, or the ratio of bead size to catchment size, although this variable was only significant for three of those five instances. Bead ratio has a moderate significant positive influence on both NDWI range (4.38,

p<0.001) and NDWI mean (2.83, p=0.016) and a very strong significant negative influence on patch density (-56.6, p<0.001). Bead ratio had a moderate insignificant positive influence on NDVI mean (1.22, =0.073) and a strong insignificant positive influence on NDVI range (8.98, p=0.097). Bead ratio had no measurable or significant influence on total sinuosity. No relationship between bead ratio and other predictor variables was identified. Based on this evidence, bead ratio appears to exercise varying degrees of control on the magnitudes of functionality proxy variables, partially supporting this hypothesis. Functionality models were assessed as linear regressions, which estimate the linear relationships between predictors and outcomes. The presence of well-fitted, statistically significant linear regressions containing bead ratio and explaining bead functionality suggests that bead ratio and bead functionality are related linearly.

Strong positive relationships were found between catchment size and bead size (p<0.001) as well as catchment size and average floodplain width (p=0.0046); increasing catchment size correlates with increasing fluvial power, which is conducive to expansion and erosion in stream corridors. However, there is a strong negative relationship between catchment size and floodplain-channel width ratio (p<0.001), suggesting that smaller first-order streams might have the highest proportion of accessible floodplain relative to their discharge.

7.1 Differences Among Beads in Relation to Category

Success in defining natural and artificial variance in inputs, bead and drainage geometry, and functionality differed between and within categories. Type, status, and elevation zone were all also found to be statistically significant identifiers for predicting functionality response magnitude during the model selection process. The “type” category had a 77% success rate in

capturing variance in individual driver and response variables, the highest of the three tested categories. Status had the second highest rate, and elevation zone was the least successful.

Prior to categorical analysis, Chi-square Tests of Independence were used to evaluate the strength of association between categories. Chi-square tests found no significant correlation between type and status and between status and elevation zone, but type and elevation zone were significantly correlated ($p<0.001$). While this observation does indicate a strong association between these variables, it also suggests that climate, ecoregion, and elevation play a role in bead morphology and functionality.

Despite statistical tests suggesting only low to moderate degrees of correlation between type and status, inferred overlap between impaired beads and elk grasslands may warrant further investigation. Impaired beads, which are known to or observed to have undergone modification and thus loss of complexity and/or functionality, is a larger umbrella category containing but not limited to elk grasslands. Impairment status was observed in both beaver meadows and elk grasslands, but elk grasslands are generally considered to be an endmember condition suggestive of a sustained loss in floodplain-channel connectivity and an adaptation of vegetation and geomorphic structure as a result. Relict beaver meadows did show field signs of impairment, including incision and bank collapse, but still retained structural complexities thought to increase flux attenuation – highly sinuous channels and floodplains with varied topography, vegetation diversity, and water retention.

Comparisons among beads categorized by type found statistically significant differences between all three pairwise groups for both driver and response variables, suggesting that measurable differences are present between elk grasslands, forested beads, and beaver meadows at the catchment- and reach-scale. Most variables only had one or two significant pairwise

comparisons; pairwise comparisons for wood density were the only instance of all three relationships showing significant differences. Forested beads had higher wood densities than both elk grasslands and beaver meadows, and beaver meadows had higher wood densities than elk grasslands. Given the abundance of conifers in forested beads and catchments, this observation makes sense. Regardless, in-channel wood load is known to strongly control localized storage and uptake, so this observation suggests strong links between functionality and forested beads.

Pairwise comparisons between restored and impaired beads found no statistically significant differences between the two groups, providing no evidence to discount similarity between them. This result was also observed for pairwise comparisons between natural and restored beads. Natural and impaired beads were found to be somewhat distinct, differing at statistically significant levels for 12 of the 30 variables. I infer that this is suggestive of weak sample size in the restored category; natural and impaired bead sample sizes were four to five times larger than the restored sample size, making these comparisons uneven in terms of dataset richness. In addition to the dataset size limitations, restored beads varied in time of implementation, scope of restoration, and restoration strategies, increasing heterogeneity within this group and making comparisons more difficult. Some restored beads might be more reflective of poor antecedent conditions than actual improvement in conditions post-restoration. For example, fieldwork at Elkhorn Creek 1 revealed a high wood load, lots of logjams (artificially emplaced but have received further fluvial deposits of large wood), and well-developed beaver meadows, but an entrenched channel and signs of low connectivity, creating conflicting signals. In general, timing of the change in signal from impaired to restored (or a quasi-natural state) is

unknown and likely varies from case to case. Status may be a useful metric for field practitioners and observation-based science, but did not appear to withstand statistical testing.

Certain driver variables displayed statistically significant relationships which I predicted would be observed prior to analysis due to the implications of the category and/or variable. For example, a strong relationship ($p<0.001$) between average catchment elevation and elevation zone was observed; categorization of beads as montane or subalpine was contingent on their elevation, strongly biasing this result. The elevation stratifications and resultant ecological differences between montane and subalpine beads appeared to most strongly control the results of comparisons between these groups; variations at the reach-scale were either not accurately captured or were simply not statistically significant. However, beads in the subalpine region had lower floodplain-channel widths. Given the relationships between catchment geometry and bead geometry, subalpine beads were expected to have smaller catchment sizes. However, catchment size was not found to differ significantly by elevation zone, suggesting that floodplain structure may vary in other ways independent of the scaling relationships inherent to catchment-stream systems. In addition, lower values of total sinuosity and patch density in subalpine beads suggest that elevation zone plays a role in determining the degree of lateral confinement observed in beads and may act as a control on bead functionality by reducing lateral mobility. Although higher average catchment slopes are also inherent to the higher-elevation, more mountainous subalpine zones, higher catchment and bead slopes were associated with lower NDVI ranges (catchment), NDWI ranges (bead), and total sinuosity (catchment), providing additional evidence for ecoregion-related functionality limitations.

7.2 Model Implications for Bead Functionality

Bead functionality is the product of an array of inputs and conditions, as reflected in the strongest statistical relationships for models with multiple variables as opposed to a single predictor variable, supporting hypothesis one. Selected models mostly contained mixtures of geomorphic and biotic variables but tended to favor geomorphic factors. Patch density was the only response variable that favored biotic factors, particularly beaver modification. Geomorphic variables were both catchment- and reach-scaled and biotic variables were typically only measured on the reach scale. Within the scaled groupings of geomorphic inputs, catchment geometry and inputs tended to have stronger correlations, suggesting that the influence of catchment-scale or even regional-scale factors tends to be more influential in determining functionality on the reach-scale.

Some coefficients appeared to be slightly contradictory; higher elevations were associated with small increases in total sinuosity, despite montane beads having higher total sinuosity; however, this might be independent of these elevation zones. In addition, the positive relationship between patch density and negative relationship between minimum berm count and patch density appears contradictory, however, higher minimum berm count was associated with larger beads ($p<0.001$), which were associated with far lower patch densities ($p<0.001$). Patch density favors smaller beads with more densely packed berms, as opposed to larger beads with a greater number of berms.

Models including and excluding categories as driver variables differed for five of the six functionality proxy variables. Bead ratio remains the most significant control on bead functionality and once again appeared in five of the six models; however, the coefficient for bead ratio was significant all five times as opposed to only three times in the category-included models. Retention of all variables in the patch density model between both scenarios suggests

that, while patch density does differ significantly by type, it is most strongly controlled by hydrologic inputs, the catchment-reach geometrical relationship, and beaver modification. Total sinuosity changed from a multivariate model (with categories) to a univariate model (without categories), and differences in total sinuosity within the entire dataset are most strongly controlled by reach-scale geometry as opposed to catchment-scale geometry and elevation. Changes in models seemed to increasingly favor biotic inputs, which were reach-scaled; this may imply that the inclusion of categories highlighted catchment-scale differences in functionality, but analyzing the bead dataset as a cohesive whole was more effective at identifying reach-scale variations and inputs. For example, the inclusion of wood density in all four NDVI/NDWI category-excluded models (coupled with insignificant p-values in three of the four cases and small coefficients in all four cases) introduces the possibility that including bead categories in the model selection process broadened the focus of the models, reducing the signal emitted by variations in wood density between beads. It seems that wood density exercises a very small control on functionality, which is difficult to identify and analyze. Narrowing of resolution may help to more strongly parse out the reach-scale effects of wood density on functionality. In-channel wood is known to influence both deposition and scour, as previously mentioned, which may complicate the bead-scale attempts at understanding functionality dynamics. In particular, some large wood pieces or jams were associated with increases in pool volume and magnitude of sediment retention, whereas others facilitated the emplacement or migration of knickpoints and/or localized incision and shearing. Large wood hydraulic effects were sometimes varied within jams themselves, resulting in complex bathymetry and geomorphic signals. Thus, it is difficult to study large wood presence in beads as a monolith, and smaller-scale methods of

characterizing their geomorphic effects may provide clearer insights into their relationship with functionality.

7.3 Study Challenges

Adding complexity to this study were human interferences, which created unique instances of floodplain and channel modification. On Beaver Creek, the presence of Comanche Reservoir directly upstream of all four beads directly impacts hydrologic and ecologic conditions in these beads. Observed modifications included presence of concrete diversion structures and known periodic releases of water and sediment (Scot Barker, pers. comm., July 2024), the latter resulting in stagnation and algae overgrowth in Beaver Creek Bead 1, just below the reservoir. Characterization of these impacts in this study was difficult; it is unknown whether StreamStats took the reservoir and diversion structures into account when calculating peak discharge metrics. Colorado catchments can be assessed for the presence of upstream regulation in StreamStats, although there is no mention of resultant hydrologic alterations and thus this metric may only be used to calculate total area of regulation interference in the catchment. However, reservoir impacts in this study appeared to be limited to the channel and had not propagated into the floodplain and did not appear to significantly alter the magnitude of functionality response variables here. Additional smaller engineering structures, usually road crossings and weirs, were present in other beads and were accounted for as patches when calculating patch density.

In some cases, human interference was associated with localized increases in patchiness and geomorphic complexity. A culvert and channel-spanning bridge over Beaver Creek at the third bead narrowed flow width and trapped wood; the subsequently raised water level propagated far upstream, creating a large, geomorphically and hydrologically complex wetland with a high wood load and abundant secondary channels. In Rocky Mountain National Park,

increases in ungulate (elk, moose) populations and loss of native predator species have created overpopulation, threatening riparian vegetation communities. Ungulate over-browsing discourages aspen and willow growth, contributing to homogeneity, stream corridor destabilization, and loss of floodplain-channel connectivity, among other ecosystem impacts (Wolf et al., 2007; Baker et al., 2012). The implementation of exclosures has become a common management strategy to promote regeneration of riparian vegetation and encourage channel restabilization and connectivity. Exclosures were observed to support greater ecological diversity and higher patch density; exclosed areas also had higher wood loads than non-exclosed areas (see Figure 14), although this assessment was purely visual and cannot be supported with statistics at present. Exclosures have been implemented on many streams in Rocky Mountain National Park, but the only exclosure incorporated into study data was on the Big Thompson River at Moraine Park. Broadly, most restoration efforts on Colorado Front Range streams inherently increase bead patchiness by artificially emplacing in-channel or floodplain structures to enhance connectivity and improve functionality, among other goals.

Measurement of catchment-scale variables introduces the possibility of data oversimplification. Slope was averaged for the entire catchment, potentially muddling the signals of high-gradient or low-gradient zones with significant geomorphic implications. Expansion of this metric could include setting an elevation threshold and evaluating percent threshold exceedance for each catchment, providing a more accurate picture of basin conditions and sediment transport capacity. Consolidation also impacts supply and transport of sediment; a geologic base map could be used to determine proportions of catchments with loosely consolidated alluvial/colluvial material and solid bedrock. Averaging basin-scale metrics was

appropriate for this study given the size and extent of the dataset, but a smaller, more intensive project might benefit from taking these factors into account.

Remote data were sourced from satellite imagery with varying spatial resolutions. dNBR was calculated for images with 30-m spatial resolution, NDWI/NDVI were calculated with 3-m imagery, and all topographic data were provided from 1-m DEMs. Given the small-scale complexities inherent to beads and the abundance of smaller catchments in the study, higher-resolution imagery may improve study results by better representing actual topographic conditions relevant to the variables analyzed here. Temporal resolution also plays a role in data accuracy - this project was a snapshot of conditions immediately after the Cameron Peak wildfire and does not consider revegetation or restoration that has occurred in the years following the fire. It could be beneficial to reassess dNBR to check on the more recent progress of burn scar healing and forest regrowth. Fire recovery requires immediate action and commitment, especially in the first 5 years following the event, and therefore consistent updates on basin conditions can ensure the health of both the upland areas and distant downstream in local catchments.

Improvement of spatial resolution may additionally refine selected predictive models. Patch density did not account for large wood pieces and smaller jams – only the large jams with measured dimensions were included. Wood density may become a factor of statistical significance if the spatial resolution of the functionality proxy variables were improved. The insignificance of wood density in models may imply that large wood is functional on a more localized scale or is simply too ephemeral to result in the manifestation of structural differences in the channel and floodplain, but the latter seems unlikely given the known links between large wood and improvements in connectivity. NDVI, NDWI, and total sinuosity generally do not directly account for wood presence and would not necessarily need to be changed.

7.4 Implications for River Restoration

Generally, bead conditions were highly variable, making it difficult to provide universal recommendations for restoration techniques. Prior to restoration, however, practitioners should take care in the site selection process to assess existing conditions and potential for restoration. In particular, consideration for unchangeable variables, such as slope, elevation, and floodplain-channel width ratio may provide the best chances for a high return on investment. For example, beads with lower floodplain-channel width ratio or channel confinement may not allow for increases in sinuosity and may not possess necessary space to support optimal levels of floodplain diversity. Techniques for restoration will vary with each project depending on the physical template provided by the bead as well as the goals of restoration practitioners and shareholders. However, improvement of channel-floodplain connectivity will provide widespread benefits by activating secondary channels, increasing the active floodplain width, encouraging storage and retention of water, sediment, and nutrients in the floodplain, addressing all four studied aspects of functionality.

The inclusion of four different methods of assessing bead functionality (patch metrics, sinuosity, NDVI, and NDWI) supports the assumption that functionality is a complex, multifaceted concept, but model results suggest a degree of connectivity between these methods and may be used for site interpretation. In particular, patchiness and NDVI/NDWI may be concurrently used to roughly measure and mark the transition from hydrologically connected beaver meadows to hydrologically disconnected elk grasslands. As part of a continuum, beaver meadows and elk grasslands shared high levels of patchiness (Figure 19), typically the result of active or relict beaver activity and channel migration. However, NDVI and NDWI reveal

differences in biology and subsurface hydrology that highlight the degree of connectivity and, likely, accessibility of floodplain heterogeneity units.

Figure 19 illustrates these differences in connectivity state. Patchiness of beaver meadows was coupled with a low NDVI/NDWI range, indicating that, despite variations in surface topography and vegetation, conditions were less variable. Patches in beaver meadows, with the exclusion of highlands, are all associated with high soil moisture levels and retention of water. In contrast, patchiness of elk grasslands was coupled with a high NDVI/NDWI range, illustrating systemic disconnectivity that manifests most clearly through variations in surface topography and vegetation. Grass and highland patches typically contain lower soil moisture, whereas low-lying abandoned channels and organic-and-fines-rich beaver berms are associated with greater water retention and higher moisture levels. Beaver meadows and elk grasslands were not found to have statistically significant differences in average NDVI and NDWI, but NDVI/NDWI ranges and visual cues from satellite imagery and fieldwork supported increased wetness and ponding in beaver meadows. Combined patch metrics and NDVI/NDWI may be used as pre-selection to assess conditions prior to emplacement of restoration strategies, or as a monitoring tool to examine spatiotemporal changes in hydrologic connectivity.

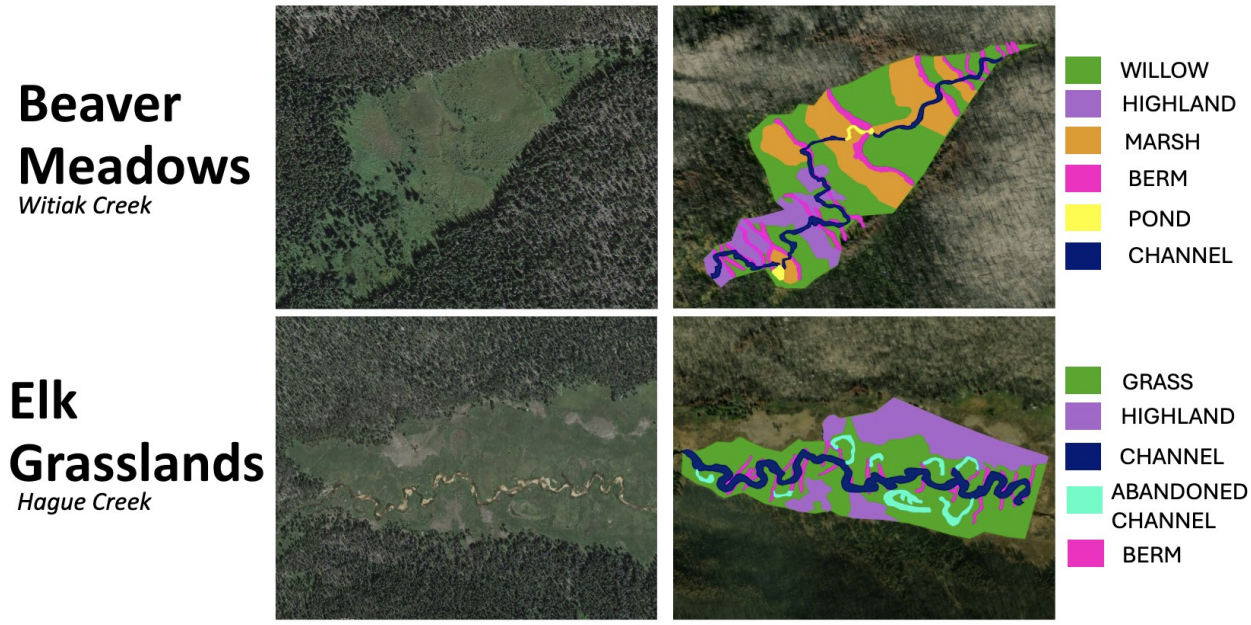

Figure 19: Variations in bead patch types between beaver meadows and elk grasslands, as seen for Witiak Creek and Hague Creek.

8. CONCLUSION

Study results imply that beads, while influenced by certain regionally scaled relationships and patterns (discharge, elevation zone), are generally the unique products of their physical settings, the inputs they receive, and (to some extent) the extent of alterations to the stream corridors and uplands from human and natural disturbances. Therefore, it would be unwise and difficult to try to develop a simple framework for restoration and management of beads. Instead, a holistic approach would be the wisest way to account for the complexities of flux attenuation.

Certain factors controlling bead functionality cannot be modified – for example, while lower floodplain-channel ratios are associated with lower patch density, widening a floodplain is destructive and not feasible. These aspects must be worked with to find a solution. However, the positive relationship between berm density and patch density suggests that reintroduction of

beaver could lead to an improvement in functionality. Total sinuosity appears to be a difficult measure to improve, as it is the product of elevation and slope, both of which are unchanging variables. Although statistics did not directly imply this, restoration of channel-floodplain connectivity is known to reactivate secondary channels, making this a feasible option to increase total sinuosity.

Statistical analyses did not suggest a clear or immediate route for addressing functionality in a restoration context. However, the importance of bead ratio to nearly all measures of functionality suggests that recapturing natural floodplain extent and restoration of connectivity would have a positive impact. Strategies that will improve water retention and lead to floodplain inundation and reversal of incised, single-thread channel behavior will create the most measurable improvements. Certain functionality proxy variables, particularly patch density, would respond well to reintroduction of beaver, or to a lesser extent construction of structures to simulate their presence.

9. FUTURE DIRECTIONS

In order to study beads as individual units, I assumed them to be independent systems bounded up- and downstream by strings and did not account for interactions between beads within the same catchment or small study catchments contained within the footprint of larger ones. In practice, the exchanges of energy and physical materials (sediment, water, solutes) occurring in all directions, particularly longitudinally, in stream corridors invalidates the above assumptions. The propagation of signals facilitated by regional-scale controls such as drainage geometry, geology, and hydroclimatology remains poorly understood for mountain stream corridors. In the subsurface, bedrock properties and fracture density/geometry influence stream corridor geometry; erodible and highly fractured bedrock encourages valley widening and

storage of water, supporting wetland vegetation, allowing room for channel complexity and meandering, and facilitating further storage. Drainage geometry, a function of bedrock and regional structure, determines catchment-scale channel network morphology and, in turn, long-term flux attenuation potential. Periglacial environments, which have current or historic proximity to glaciers, experience freeze-thaw dynamics, which can enhance weathering and erosion and associated wide valleys and water storage. Hydroclimate, or regional trends in the seasonal distribution of water, dictates the timing and magnitude of high-flow events and controls the spatial and temporal distribution of shear stress within the channel.

Regional-scale factors are the proposed foundational qualities that define a catchment's base spatial and temporal patterns of fluvial storage and transport. Dynamic system inputs such as biologic activity, natural disturbances (wildfires, mass movements), and human influence (deforestation, agriculture, development) interact constantly with this 'blueprint', altering flux attenuation on shorter timescales. Aside from regional-scale factors, such as slope and lithology, which are either unchanging or change over very long periods of time, most aspects of and inputs into stream corridors are extremely variable, making functionality an inherently dynamic concept. In particular, improvement of spatial resolution for remote sensing aspects of analyses and implementation of long-term recurring assessments of functionality predictors and responses might shed more light on the reach-scale (and smaller) and temporal complexities that are likely to exist within and between beads. Future work could thus incorporate solutions to some of the data complications addressed in the Discussion above.

10. REFERENCES

Akaike, H. (1998). Information theory and an extension of the maximum likelihood principle. In E. Parzen, K. Tanabe, & G. Kitagawa (Eds.), *Selected Papers of Hirotugu Akaike* (pp. 199–213). Springer. https://doi.org/10.1007/978-1-4612-1694-0_15

Akbar, T. A., Hassan, Q. K., Ishaq, S., Batool, M., Butt, H. J., & Jabbar, H. (2019). Investigative spatial distribution and modelling of existing and future urban land changes and its impact on urbanization and economy. *Remote Sensing*, *11*(2), 105. https://doi.org/10.3390/rs11020105

Anderson, R. S., Riihimaki, C. A., Safran, E. B., & MacGregor, K. R. (2006). Facing reality: Late Cenozoic evolution of smooth peaks, glacially ornamented valleys, and deep river gorges of Colorado's Front Range. In S. D. Willett, N. Hovius, M. T. Brandon, & D.M. Fisher, *Tectonics, Climate, and Landscape Evolution*. Geological Society of America. https://doi.org/10.1130/2006.2398(25)

Arp, C. D., Schmidt, J. C., Baker, M. A., & Myers, A. K. (2007). Stream geomorphology in a mountain lake district: Hydraulic geometry, sediment sources and sinks, and downstream lake effects. Earth Surface Processes and Landforms, 32(4), 525–543. https://doi.org/10.1002/esp.1421

Baker, B.W., Peinetti, H.R., Coughenour, M.B., & Johnson, T.L. (2012). Competition favors elk over beaver in a riparian willow ecosystem. *Ecosphere, 3*, 1-15. https://doi.org/10.1890/ES12-00058.1

Barinas, G., Good, S.P., & Tullos, D. (2024). Continental scale assessment of variation in floodplain roughness with vegetation and flow characteristics. *Geophysical Research Letters, 51*,1 e2023GL105588. https://doi.org/10.1029/2023GL105588

Beechie, T. J., Sear, D. A., Olden, J. D., Pess, G. R., Buffington, J. M., Moir, H., Roni, P., & Pollock, M. M. (2010). Process-based principles for restoring river ecosystems. *BioScience*, 60(3), 209–222. https://doi.org/10.1525/bio.2010.60.3.7

Benson, L., Madole, R., Landis, G., & Gosse, J. (2005). New data for Late Pleistocene Pinedale alpine glaciation from southwestern Colorado. *Quaternary Science Reviews*, *24*(1–2), 49–65. https://doi.org/10.1016/j.quascirev.2004.07.018

Biron, P.M., Buffin-Bélanger, T., Larocque, M., Choné, G., Cloutier, C.A., Ouellet, M.A., Demers, S., Olsen, T., Desjarlais, C., & Eyquem, J. (2014). Freedom space for rivers: a sustainable management approach to enhance river resilience. *Environmental Management, 54*, 1056-1073. https://doi.org/10.1007/s00267-014-0366-z

Chapman, S.S., Griffith, G.E., Omernik, J.M., Price, A.B., Freeouf, J., and Schrupp, D.L., 2006, Ecoregions of Colorado (color poster with map, descriptive text, summary tables, and photographs): Reston, Virginia, U.S. Geological Survey (map scale 1:1,200,000).

Coe, J. A., Kean, J. W., Godt, J. W., Baum, R. L., Jones, E. S., Gochis, D. J., & Anderson, G. S. (2014). New insights into debris-flow hazards from an extraordinary event in the Colorado Front Range. GSA Today, 24(10), 4-10.

Costa, J. E., & Jarrett, R. D. (1981). Debris flows in small mountain stream channels of colorado and their hydrologic implications. Environmental & Engineering Geoscience, xviii(3), 309–322. https://doi.org/10.2113/gseegeosci.xviii.3.30

Dahms, D. E. (2004). Glacial limits in the middle and southern Rocky mountains, U.S.A., south of the Yellowstone ice cap. In *Developments in Quaternary Sciences* (Vol. 2, pp. 275–288). Elsevier. https://doi.org/10.1016/S1571-0866(04)80203-3

Dunn, O. J. (1964). Multiple comparisons using rank sums. *Technometrics*, *6*(3), 241–252. https://doi.org/10.1080/00401706.1964.10490181

Fairfax, E., & Whittle, A. (2020). Smokey the Beaver: Beaver-dammed riparian corridors stay green during wildfire throughout the western United States. *Ecological Applications, 30*(8), e02225. https://doi.org/10.1002/eap.2225

Ferreira, C. S. S., Kašanin-Grubin, M., Solomun, M. K., Sushkova, S., Minkina, T., Zhao, W., & Kalantari, Z. (2023). Wetlands as nature-based solutions for water management in different environments. *Current Opinion in Environmental Science & Health*, *33*, 100476. https://doi.org/10.1016/j.coesh.2023.100476

Fitzpatrick, F.A., Knox, J.C., & Schubauer-Berigan, J.P. (2009). Channel, floodplain, and wetland responses to floods and overbank sedimentation, 1846-2006, Halfway Creek Marsh, Upper Mississippi Valley, Wisconsin. In, *Management and Restoration of Fluvial Systems with Broad Historical Changes and Human Impacts*, L.A. James, S.L. Rathburn, & G.R. Whittecar, eds. Geological Society of America, Boulder, CO. https://doi.org/10.1130/2009.2451(02)

Furniss, M. J. (2011). Water, climate change, and forests: Watershed stewardship for a changing climate. DIANE Publishing.

Griffin, E. R., Kean, J. W., Vincent, K. R., Smith, J. D., & Friedman, J. M. (2005). Modeling effects of bank friction and woody bank vegetation on channel flow and boundary shear stress in the Rio Puerco, New Mexico. *Journal of Geophysical Research: Earth Surface, 110*(F4), 2005JF000322. https://doi.org/10.1029/2005JF000322

Guo, L., Wu, Z., Li, S., & Xie, G. (2024). The relative impacts of vegetation, topography and weather on landscape patterns of burn severity in subtropical forests of southern China. Journal of Environmental Management, 351, 119733. https://doi.org/10.1016/j.jenvman.2023.119733

Gurnell, A. M., Piégay, H., Swanson, F. J., & Gregory, S. V. (2002). Large wood and fluvial processes. Freshwater Biology, 47(4), 601–619. https://doi.org/10.1046/j.1365-2427.2002.00916.x

Hallock, D., N. Lederer, and M. Figgs. 1986. Ecology, status and avifauna of willow carrs in Boulder County. Boulder County Nature Association Publication No. 4. Boulder, CO. 38 pp.

Hurvich, C. M., & Tsai, C.-L. (1989). Regression and time series model selection in small samples. *Biometrika*, *76*(2), 297–307. https://doi.org/10.1093/biomet/76.2.297

Iskin, E. P., & Wohl, E. (2023). Quantifying floodplain heterogeneity with field observation, remote sensing, and landscape ecology: Methods and metrics. R*iver Research and Applications, 39*(5), 911–929. https://doi.org/10.1002/rra.4109

Jarrett, R. D. (1990). Hydrologic and hydraulic research in mountain rivers. *Journal of the American Water Resources Association, 26*(3), 419–429. https://doi.org/10.1111/j.1752-1688.1990.tb01381.x

Jarrett, R. D. (1990). Paleohydrologic techniques used to define the spatial occurrence of floods. *Geomorphology, 3*(2), 181–195. https://doi.org/10.1016/0169-555X(90)90044-Q

Kean, J. K., Robert G. Schmitt, Francis K. Rengers, Jason W. (2022, February 24). Cameron peak fire: Flooding and debris flows. ArcGIS StoryMaps. https://storymaps.arcgis.com/stories/af3cd28cad6040e9a3a3d608f58292a7

Kornse, Z., & Wohl, E. (2020). Assessing restoration potential for beaver (castor canadensis) in the semiarid foothills of the Southern Rockies, USA. *River Research and Applications, 36*(9), 1932–1943. https://doi.org/10.1002/rra.3719

Larsen, A., Larsen, J. R., & Lane, S. N. (2021). Dam builders and their works: Beaver influences on the structure and function of river corridor hydrology, geomorphology, biogeochemistry and ecosystems. *Earth-Science Reviews, 218*, 103623. https://doi.org/10.1016/j.earscirev.2021.103623

Lazarus, E.D., & Constantine, J.A. (2013). Generic theory for channel sinuosity. *Proceedings National Academy of Sciences, 110*, 8447-8452. https://doi.org/10.1073/pnas.1214074110

Lee, S.-W., Lee, M.-B., Lee, Y.-G., Won, M.-S., Kim, J.-J., & Hong, S. (2009). Relationship between landscape structure and burn severity at the landscape and class levels in Samchuck, South Korea. *Forest Ecology and Management, 258*(7), 1594–1604. https://doi.org/10.1016/j.foreco.2009.07.017

Leonard, J. M., Magaña, H. A., Bangert, R. K., Neary, D. G., & Montgomery, W. L. (2017). Fire and floods: The recovery of headwater stream systems following high-severity wildfire. *Fire Ecology, 13*(3), 62–84. https://doi.org/10.4996/fireecology.130306284

Livers, B., Lininger, K. B., Kramer, N., & Sendrowski, A. (2020). Porosity problems: Comparing and reviewing methods for estimating porosity and volume of wood jams in the field. *Earth Surface Processes and Landforms, 45*(13), 3336–3353. https://doi.org/10.1002/esp.4969

Livers, B., & Wohl, E. (2015). An evaluation of stream characteristics in glacial versus fluvial process domains in the Colorado Front Range. Geomorphology, 231, 72–82. https://doi.org/10.1016/j.geomorph.2014.12.003

Livers, B., & Wohl, E. (2016). Sources and interpretation of channel complexity in forested subalpine streams of the Southern Rocky Mountains. *Water Resources Research*, *52*(5), 3910–3929. https://doi.org/10.1002/2015WR018306

Madole, R. F., 1976, Glacial geology of the Front Range, Colorado, *in* Quaternary Stratigraphy of North America. Dowden Hutchinson & Ross, Stroudsburg PA. p. 297–318.

Manners, R. B., Doyle, M. W., & Small, M. J. (2007). Structure and hydraulics of natural woody debris jams. Water Resources Research, 43(6), 2006WR004910. https://doi.org/10.1029/2006WR004910

McArthur, A.G. 1968. *Fire Behaviour in Eucalypt Forests*. Leaflet No. 107. Ninth Commonwealth Forestry Conference, India, 1968.

McCain, J. F., & Shroba, R. R. (1979). Storm and flood of July 31-August 1, 1976, in the Big Thompson River and Cache la Poudre River basins, Larimer and Weld Counties, Colorado (Vol. 1115). US Government Printing Office.

McFeeters, S. K. (1996). The use of the Normalized Difference Water Index (NDWI) in the delineation of open water features. *International Journal of Remote Sensing, 17*(7), 1425–1432. https://doi.org/10.1080/01431169608948714

Miller, J. D., & Thode, A. E. (2007). Quantifying burn severity in a heterogeneous landscape with a relative version of the delta Normalized Burn Ratio (Dnbr). *Remote Sensing of Environment, 109*(1), 66–80. https://doi.org/10.1016/j.rse.2006.12.006

Miranda, L. E., & Bettoli, P. W. (2010). Large reservoirs. *Inland fisheries management in North America*, *3*, 545-586.

Moody, J. A., & Martin, D. A. (2001). Initial hydrologic and geomorphic response following a wildfire in the Colorado front range. *Earth Surface Processes and Landforms, 26*(10), 1049–1070. https://doi.org/10.1002/esp.253

Montgomery, D., Collins, B., Buffington, J., & Abbe, T. (2003). Geomorphic effects of wood in rivers. In, *The Ecology and Management of Wood in World Rivers*, S.V. Gregory, K.L. Boyer, & A.M. Gurnell, eds. American Fisheries Society, Bethesda, MD, 21-38. https://www.semanticscholar.org/paper/Geomorphic-effects-of-wood-in-rivers-Montgomery-Collins/a0d0ea864a166e5dbd27b1243f0ef2c22a71852f

Morgan, P., G. H. Aplet, J. B. Haufler, H. C. Humphries, M. M. Moore, and W. D. Wilson (1994), Historical range of variability: A useful tool for evaluating ecosystem change, J. Sustainable For., 2, 87–111.

Paul, M. J., LeDuc, S. D., Lassiter, M. G., Moorhead, L. C., Noyes, P. D., & Leibowitz, S. G. (2022). Wildfire induces changes in receiving waters: A review with considerations for water quality management. *Water Resources Research, 58*(9), e2021WR030699. https://doi.org/10.1029/2021WR030699

Pausas, J. G., & Keeley, J. E. (2019). Wildfires as an ecosystem service. Frontiers in Ecology and the Environment, 17(5), 289–295. https://doi.org/10.1002/fee.2044

Peipoch, M., Brauns, M., Hauer, F. R., Weitere, M., & Valett, H. M. (2015). Ecological simplification: Human influences on riverscape complexity. *BioScience*, *65*(11), 1057–1065. https://doi.org/10.1093/biosci/biv120

Peipoch, M., Davis, P.B., & Valett, H.M. (2023). Biophysical heterogeneity, hydrologic connectivity, and productivity of a montane floodplain forest. *Ecosystems, 26*, 510-526. https://doi.org/10.1007/s10021-022-00769-2

Pelletier, J. D., & Orem, C. A. (2014). How do sediment yields from post-wildfire debris-laden flows depend on terrain slope, soil burn severity class, and drainage basin area? Insights from airborne-LiDAR change detection. *Earth Surface Processes and Landforms, 39*(13), 1822–1832. https://doi.org/10.1002/esp.3570

Polvi, L. E., & Wohl, E. (2012). The beaver meadow complex revisited – the role of beavers in post-glacial floodplain development. *Earth Surface Processes and Landforms, 37*(3), 332–346. https://doi.org/10.1002/esp.2261

Rak, G., Kozelj, D., & Steinman, F. (2016). The impact of floodplain land use on flood wave propagation. *Natural Hazards, 83*, 425-443. https://doi.org/10.1007/s11069-016-2322-0

Rakholia, S., Mehta, A., & Suthar, B. (2020). Forest fire monitoring of Shoolpaneshwar Wildlife Sanctuary, Gujarat, India using geospatial techniques. *Current Science, 119*(12), 1974. https://doi.org/10.18520/cs/v119/i12/1974-1981

Rood, S. B., Pan, J., Gill, K. M., Franks, C. G., Samuelson, G. M., & Shepherd, A. (2008). Declining summer flows of Rocky Mountain rivers: Changing seasonal hydrology and probable impacts on floodplain forests. *Journal of Hydrology*, *349*(3), 397–410. https://doi.org/10.1016/j.jhydrol.2007.11.012

Rosell, F., Bozsér, O., Collen, P., & Parker, H. (2005). Ecological impact of beavers Castor fiber and Castor canadensis and their ability to modify ecosystems. *Mammal Review, 35*(3–4), 248–276. https://doi.org/10.1111/j.1365-2907.2005.00067.x

Ryan, S. E., Shobe, C. M., Rathburn, S. L., & Dixon, M. K. (2024). Suspended-sediment response to wildfire and a major post-fire flood on the Colorado Front Range. *River Research and Applications, 40*(7), 1256–1272. https://doi.org/10.1002/rra.4286

Shakesby, R.A., & Doerr, S.H. (2006). Wildfire as a hydrological and geomorphological agent. *Earth-Science Reviews, 74*, 269-307. https://doi.org/10.1016/j.earscirev.2005.10.006

Solander, K. C., Bennett, K. E., Fleming, S. W., Gutzler, D. S., Hopkins, E. M., & Middleton, R. S. (2018). Interactions between climate change and complex topography drive observed streamflow changes in the Colorado river basin. Journal of Hydrometeorology, 19(10), 1637–1650. https://doi.org/10.1175/JHM-D-18-0012.1

Stanford, J. A., & Ward, J. V. (1993). An ecosystem perspective of alluvial rivers: Connectivity and the hyporheic corridor. J*ournal of the North American Benthological Society, 12*(1), 48–60. https://doi.org/10.2307/1467685

Stewart, H., Mascarenas, R., Kuehr, S., & Lafferty, E. (2018). Innovative use of soil mixing for US-34, Big Thompson Canyon flood recovery. Rocky Mountain Geo-Conference 2018, 181–191. https://doi.org/10.1061/9780784481936.014

Swayze, N., Choi, C. T. H., Knowlton, G., & Klisauskaite, J. (2021). Colorado Front Range disasters: Understanding the impact of forest management on the Cameron Peak and Calwood fire. https://ntrs.nasa.gov/citations/20210014944

Tank, J.L., Rosi-Marshall, E.J., Griffiths, N.A., Entrekin, S.A., & Stephen, M.L. (2010). A review of allochthonous organic matter dynamics and metabolism in streams. *Journal North American Benthological Society, 29*, 118-146. https://doi.org/10.1899/08-170.1

Thomas, R. F., Kingsford, R. T., Lu, Y., Cox, S. J., Sims, N. C., & Hunter, S. J. (2015). Mapping inundation in the heterogeneous floodplain wetlands of the Macquarie Marshes, using Landsat Thematic Mapper. *Journal of Hydrology, 524*, 194–213. https://doi.org/10.1016/j.jhydrol.2015.02.029

Thurman, E. M., Ferrer, I., Bowden, M., Mansfeldt, C., Fegel, T. S., Rhoades, C. C., & Rosario-Ortiz, F. (2023). Occurrence of benzene polycarboxylic acids in ash and streamwater after the cameron peak fire. *ACS ES&T Water, 3*(12), 3848–3857. https://doi.org/10.1021/acsestwater.3c00246

Tweto, Ogden. Geologic map of Colorado. 1:500,000. US Geological Survey, 1979. https://ngmdb.usgs.gov/Prodesc/proddesc_68589.htm

VanSistine, P., Madole, R. F., & Michael, J. A. (2022). *Data release—Pleistocene glaciation in the upper platte river drainage basin, colorado* [Dataset]. U.S. Geological Survey. https://doi.org/10.5066/P9ROZWAZ

Veblen, Thomas & Donnegan, Joseph. (2006). Historical Range of Variability of Forest Vegetation of the National Forests of the Colorado Front Range. USDA Forest Service, Rocky Mountain Region and the Colorado Forest Restoration Institute, Fort Collins. 151 pages.

Wohl, E. (2001). Virtual rivers: Lessons from the mountain rivers of the Colorado Front Range. Yale University Press.

Wohl, E. (2011). What should these rivers look like? Historical range of variability and human impacts in the Colorado Front Range, USA. Earth Surface Processes and Landforms, 36(10), 1378–1390. https://doi.org/10.1002/esp.2180

Wohl, E. (2013). Floodplains and wood. *Earth-Science Reviews, 123*, 194-212. https://doi.org/10.1016/j.earscirev.2013.04.009

Wohl, E. (2017). Bridging the gaps: An overview of wood across time and space in diverse rivers. *Geomorphology, 279*, 3–26. https://doi.org/10.1016/j.geomorph.2016.04.014

Wohl, E. (2021). Legacy effects of loss of beavers in the continental United States. *Environmental Research Letters, 16*(2), 025010. https://doi.org/10.1088/1748-9326/abd34e

Wohl, E. (2024). *Landscapes on Fire: Impacts on Uplands, Rivers, and Communities*. Wiley.

Wohl, E., & Cenderelli, D.A. (2000). Sediment deposition and transport patterns following a reservoir sediment release. *Water Resources Research, 36*, 319-333. https://doi.org/10.1029/1999WR900272

Wohl, E., Cenderelli, D. A., Dwire, K. A., Ryan-Burkett, S. E., Young, M. K., & Fausch, K. D. (2010). Large in-stream wood studies: A call for common metrics. *Earth Surface Processes and Landforms, 35*(5), 618–625. https://doi.org/10.1002/esp.1966

Wohl, E., & Iskin, E. P. (2022). The transience of channel-spanning logjams in mountain streams. W*ater Resources Research, 58*(5), e2021WR031556. https://doi.org/10.1029/2021WR031556

Wohl, E., Lininger, K. B., & Scott, D. N. (2018). River beads as a conceptual framework for building carbon storage and resilience to extreme climate events into river management. *Biogeochemistry, 141*(3), 365–383. https://doi.org/10.1007/s10533-017-0397-7

Wohl, E., Marshall, A. E., Scamardo, J., White, D., & Morrison, R. R. (2022). Biogeomorphic influences on river corridor resilience to wildfire disturbances in a mountain stream of the Southern Rockies, USA. *Science of The Total Environment, 820*, 153321. https://doi.org/10.1016/j.scitotenv.2022.153321

Wolf, E.C., Cooper, D.J., & Hobbs, N.T. (2007). Hydrologic regime and herbivory stabilize an alternative state in Yellowstone National Park. *Ecological Applications, 17*, 1572-1587. https://doi.org/10.1890/06-2042.1

Wright, J. P., Jones, C. G., & Flecker, A. S. (2002). An ecosystem engineer, the beaver, increases species richness at the landscape scale. *Oecologia, 132*(1), 96–101. https://doi.org/10.1007/s00442-002-0929-1

11. APPENDIX 1 - VARIABLE DIRECTORY

Average Catchment Elevation – Average elevation over entire catchment
Average Catchment Slope – Average slope over entire catchment and bead
Bead Size – Total area of flat, wide, floodplain associated with bead
Bead Ratio – Ratio of bead size to drainage area
Bead Slope – Elevation change from bead inlet to bead outlet
Berm Density – Approximate number of berms per unit length
Burn Ratio – Ratio of high severity catchment burn to total burn
Channel Length – Length of primary channel from bead start to end
Channel Substrate – Grain size fractions observed in-channel
Drainage Area – Size of catchment - total contributing area
Forest Cover – Percent of drainage area covered with NLCD 2021 classes 41-43 (Deciduous, Evergreen, and Mixed Forest)
High Severity Burn – Percent coverage of high severity burn in each catchment
Minimum Berm Count – Total number of observed beaver berms in each bead**
NDWI – Remotely sensed indicator of water content and soil moisture
NDVI – Remotely sensed indicator of vegetation health and stress
Precipitation – Mean annual precipitation
Patch Count - Total number of observed patches in each bead**
Patch Density – Approximate number of patches per unit area
Status – Observed level of modification in bead
STORNHD - Percent storage (wetlands and waterbodies) determined from 1:24K NHD
Total Burn – Percent coverage of burn of any severity in each catchment
Total Channel Length – Length of primary and secondary channels from bead start to end
Total Sinuosity – Sum of primary and secondary channel length, divided by valley length
Total Wood Load – Total number of observed large wood pieces in each bead**
Type – Bead ecology as determined by dominant vegetation & floodplain-channel connectivity
Valley length – Raw distance from valley start to valley end
Wood Density - Approximate number of large wood pieces per unit length
1% AEP - Maximum instantaneous flow that occurs with a 1% annual exceedance probability
50% AEP - Maximum instantaneous flow that occurs with a 50% annual exceedance probability
16H100Y - 6-hour precipitation that is expected to occur on average once in 100 years

12. APPENDIX 2 - DATA

Table 24: Field Data – Bead Locations and Descriptions

Bead Name	Start Latitude	Start Longitude	End Latitude	End Longitude	Description	Type	Climatic Zone
Beaver Brook	40.37299	-105.61439	40.36939*	-105.597*	Bead end not field verified - approximated using Google Earth	EG	Montane
Beaver Creek 1	40.58408	-105.64207	40.58462	-105.639	Heavily impacted by Comanche Reservoir releases. Stinky, full of algae, evidence of high flow everywhere	BM	Subalpine
Beaver Creek 2	40.58208	-105.62848	40.58054	-105.625		BM	Subalpine
Beaver Creek 3	40.58053811	-105.6213438	40.57687	-105.615		BM	Subalpine
Beaver Creek 4	40.57728	-105.60165	40.57716	-105.599		BM	Subalpine
Big Thompson River	40.35497	-105.61462	40.35392*	-105.585*	Bead end not field verified - approximated using Google Earth	EG	Montane
Boulder Brook	40.31797	-105.61017	40.32039	-105.608		BM	Montane
Cony Creek**	40.18018	-105.59913	40.1831	-105.5965		FC	Subalpine
Corral Creek	40.526422	-105.804967	40.51901*	-105.776*	Bead start and end not field verified - approximated using Google Earth	EG	Subalpine
Cow Creek	40.43126	-105.50042	40.43351	-105.494	Series of BDAs placed; culvert at head of bead	BM	Montane
Elkhorn 1	40.75857	-105.63818	40.75811	-105.636	Lots of PALS	BM	Montane
Elkhorn 2	40.756	-105.61132	40.75695	-105.609		BM	Montane
Fall Creek	40.54965	-105.63147	40.55138	-105.628	Extensive beaver activity but has begun to degrade due to inactivity	BM	Subalpine
Glacier Creek	40.31925	-105.62183	40.31881	-105.619		BM	Montane
Hague Creek	40.512123*	-105.714774*	40.5174	-105.734	Bead start not field verified - approximated using Google Earth	EG	Subalpine
Hidden Valley Creek	40.39894	-105.64732	40.39912	-105.64		BM	Subalpine
Hunters Creek**	40.22147	-105.59065	40.21871	-105.5877		FC	Subalpine

Jacks Gulch 1	40.64225	-105.57448	40.64067	-105.572	Start of Jacks Gulch here!	BM	Montane
Jacks Gulch 2	40.63882626	-105.5649418	40.637	-105.56		BM	Montane
Jacks Gulch 3	40.6364917	-105.5602285	40.63488	-105.559		BM	Montane
Jacks Gulch 4	40.6341	-105.55865	40.63357	-105.558		BM	Montane
Jacks Gulch 5	40.63217974	-105.5533803	40.62986	-105.552		BM	Montane
Jacks Gulch 6	40.62558426	-105.5344789	40.62531	-105.532	History of cattle ranching nearby	BM	Montane
Little Beaver Creek 1	40.63823	-105.61275	40.6372	-105.609		BM	Montane
Little Beaver Creek 2	40.63623	-105.6089	40.62531	-105.532		FC	Montane
Little Beaver Creek 3	40.62303	-105.56678	40.63554	-105.609		FC	Montane
Little Beaver Creek 4	40.62175306	-105.5369549	40.62307	-105.566	History of cattle ranching nearby	BM	Montane
Mill Creek	40.33685	-105.611	40.34041*	-105.606*	Active beaver berm found	BM	Montane
Monument Gulch	40.59252	-105.49715	40.59816	-105.498		BM	Montane
North St Vrain 1**	40.2156	-105.6386	40.2140	-105.6372		FC	Subalpine
North St Vrain 2**	40.21026	-105.63235	40.21019	-105.624		FC	Subalpine
North St Vrain 3	40.20654	-105.61508	40.20682	-105.613		FC	Subalpine
North St Vrain 4	40.21205	-105.55041	40.21797*	-105.536*	Bead end not field verified - approximated using Google Earth	BM	Montane
Ouzel Creek**	40.20267	-105.61883	40.20245	-105.6140		FC	Subalpine
Pennock Creek 1	40.57703	-105.54414	40.57899	-105.544	Part of Lazy D Ranch Property	BM	Montane
Pennock Creek 2	40.57944	-105.54434	40.58516	-105.544	Part of Lazy D Ranch Property	BM	Montane
Phantom Creek	40.40902	-105.82343	40.40767	-105.824		BM	Subalpine
Poudre River	40.43147	-105.80077	40.47566*	-105.733*	Bead end not field verified - approximated using Google Earth	EG	Subalpine
South Fork Poudre 1	40.550191*	-105.607923*	40.5686	-105.591	At CSU Mountain Campus; Bead start not field verified - approximated using Google Earth	BM	Subalpine

South Fork Poudre 2	40.58297	-105.5581	40.58776*	-105.549*	Part of Lazy D Ranch Property; 3 wood regimes (single-thread restored, multi-thread restored, single-thread unrestored); possible history of cattle ranching nearby; end approximated with Google Earth	BM	Montane
South Fork Poudre 3	40.618252	-105.525344	40.6302	-105.506	Log survey completed Sept 2023	EG	Montane
South Fork Poudre Tributary 1	40.63263954	-105.5457334	40.6298	-105.541		BM	Montane
South Fork Poudre Tributary 2	40.62812707	-105.5359181	40.62625	-105.535	23 small BDAs counted along the channel (more before start of bead); history of cattle ranching nearby	BM	Montane
Stumble Creek 1	40.569046*	-105.612594*	40.5718	-105.605	Tributary of Beaver Creek; Bead start not field verified - approximated using Google Earth	BM	Subalpine
Stumble Creek 2	40.57173	-105.60437	40.57182	-105.604		BM	Subalpine
Stumble Creek 3	40.574934	-105.602066	40.57676	-105.602		BM	Subalpine
Swamp Creek 1	40.74	-105.62801	40.74163	-105.625		BM	Montane
Swamp Creek 2	40.74257	-105.62454	40.74536	-105.622		BM	Montane
Swamp Creek 3	40.7458	-105.62187	40.74656	-105.62		BM	Montane
Witiak Creek 1	40.57122	-105.62064	40.57371	-105.617	Tributary of Beaver Creek	BM	Subalpine
Witiak Creek 2	40.57495	-105.61189	40.57576	-105.61	Tributary of Beaver Creek	BM	Subalpine
Witiak Creek 3	40.57594	-105.60983	40.57649	-105.608	Tributary of Beaver Creek	BM	Subalpine

* = coordinates were estimated using Google Earth Pro
** = site was not visited during the Summer 2024 field season; data provided from Bridget Livers
EG = elk grassland
BM = beaver meadow
FC = forest cover

Table 25: Field Data – Bead Characteristics

Bead Name	Avg Flow Depth (cm)	Avg Flow Width (cm)	Channel Substrate	Status
Beaver Brook	13	190	Sand, gravel, fines	Restored
Beaver Creek 1	23	400	Cobbles, gravel, sand	Impaired
Beaver Creek 2	7-25	600	Cobbles, gravel, sand	Impaired
Beaver Creek 3	38-70	1100	Sand, gravel, swampy fine sed (dark, organic-rich)	Impaired
Beaver Creek 4	10-50	1140	Cobbles, gravel, sand	Impaired
Big Thompson River	43	1100	Gravel, cobbles, sand, fines, occasional boulders	Impaired
Boulder Brook	24	200	Sand, some gravel and boulders (mostly at start)	Impaired
Cony Creek**	NA	NA	NA	Natural
Corral Creek	3-18	290	Angular cobbles, some gravel, minimal fines and sand	Impaired
Cow Creek	13	210	Sand and fines, some gravel stringers	Restored
Elkhorn 1	20	200	Sand, gravel, cobbles, some fine sediment	Restored
Elkhorn 2	13	200	Some cobbles at start, but changes quickly to almost entirely sand and fines	Impaired
Fall Creek	3-15	530	Cobbles and gravel at start -> sand and fines -> heavy fines and organics	Impaired
Glacier Creek	68	500	Cobbles and gravel, some fines and sand	Impaired
Hague Creek	3-35	800	Cobbles, some gravel, minimal fines and sand	Impaired
Hidden Valley Creek	20	260	Fine seds, gravel, some cobbles; plane-bed sand and gravel system near end	Impaired
Hunters Creek**	NA	NA	NA	Natural
Jacks Gulch 1	1	10	Fines and sand	Natural
Jacks Gulch 2	5-8.5	81.5	Fine sed (some sand and gravel, angular granite from surrounding hillslopes)	Natural
Jacks Gulch 3	5-16	102	Fine sed (some sand stringers and boulders from surrounding hillslopes)	Natural
Jacks Gulch 4	4-10	80	Sand and gravel, some fines	Natural
Jacks Gulch 5	7	95	Sand, gravel, and fines	Natural
Jacks Gulch 6	7-15	120	Organic-rich fines, sand, gravel	Impaired
Little Beaver Creek 1	15	370	Sand, gravel, cobbles, some boulders	Impaired
Little Beaver Creek 2	12	330	Cobbles and gravel, some sand, few boulders	Impaired
Little Beaver Creek 3	18	410	Sand, gravel, cobbles, some boulders	Impaired

Little Beaver Creek 4	20-40	400	Sand, gravel	Impaired
Mill Creek	26	420	Gravel, cobbles, sand	Natural
Monument Gulch	5	15	Fine organic-rich sed, some sand in channelized reaches	Natural
North St Vrain 1**	NA	NA	NA	Natural
North St Vrain 2**	NA	NA	NA	Natural
North St Vrain 3	10-40	1000	Cobbles, boulders, and gravel. Sand and fines in backwater deposits	Natural
North St Vrain 4	32	930	Cobbles and gravel, some sand; ample organics and fines in heavily beaver-modified areas	Natural
Ouzel Creek**	NA	NA	NA	Natural
Pennock Creek 1	14-49	290	Sand, gravel, cobbles, abundant fine seds in lower velocity zones (thick coatings observed)	Impaired
Pennock Creek 2	14-24	360	Sand, cobbles, abundant fine seds, more boulders/larger clasts than previous bead	Impaired
Phantom Creek	4	55	Gravel, fine seds, larger boulders in strings	Natural
Poudre River	30	125	Gravel, fine seds, sand, cobbles	Impaired
South Fork Poudre 1	10-68	730	Gravel-bed, some sand and fines	Impaired
South Fork Poudre 2	10-80	540	Sand, gravel, cobbles, boulders	Restored
South Fork Poudre 3	10-35	1200	Cobbles, gravel, sand	Impaired
South Fork Poudre Tributary 1	4.5	15	Fine sed upstream, sand and gravel after spring	Natural
South Fork Poudre Tributary 2	6	60	Sand, gravel, and fine sed	Restored
Stumble Creek 1	15	50	Fine sediment and sand	Natural
Stumble Creek 2	20	65	Fine sediment and sand	Natural
Stumble Creek 3	15	50	Fine sediment and sand	Natural
Swamp Creek 1	15	45	Sand, gravel	Natural
Swamp Creek 2	12-25	120	Sand, gravel	Natural
Swamp Creek 3	30	40	Sand, gravel, some clay	Natural
Witiak Creek 1	9-20	64	Sand, gravel, few granite cobbles; fine sediment in shallower-sloped beaver meadows	Natural
Witiak Creek 2	4-17	80	Sand, some gravel & fine seds	Natural
Witiak Creek 3	2-13	70	Sand, some gravel & fine seds	Natural

** = site was not visited during the Summer 2024 field season; data provided from Bridget Livers
NA = data not collected

Table 26: Field Data – Large Wood & Beaver Modification

Bead Name	Total Wood Load (# pieces)	Wood Density (by VL) (pieces/km)	Wood Density (by CL) (pieces/km)	Min Berm Count	Berm Density (by VL) (berms/km)	Berm Density (by CL) (berms/km)
Beaver Brook*	15	9.7	7.7	1	0.6	0.5
Beaver Creek 1	25	105.5	57.5	9	38.0	20.7
Beaver Creek 2	35	101.9	94.8	10	29.1	27.1
Beaver Creek 3	139	216.3	93.9	22	34.2	14.9
Beaver Creek 4	55	217.0	130.5	6	23.7	14.2
Big Thompson River*	37	14.7	8.8	0	NA	NA
Boulder Brook	33	96.4	47.8	25	73.0	36.2
Cony Creek**	305	726.2	592.2	0	NA	NA
Corral Creek*	0	NA	NA	99	36.9	23.6
Cow Creek	9	14.5	11.5	48	77.3	61.2
Elkhorn 1	60	344.9	245.1	5	28.7	20.4
Elkhorn 2	20	89.3	74.3	12	53.6	44.6
Fall Creek	12	31.7	23.3	15	39.6	29.1
Glacier Creek	0	NA	NA	24	86.4	63.1
Hague Creek*	3	1.7	1.2	46	26.5	18.0
Hidden Valley Creek	3	4.6	3.0	23	35.4	22.6
Hunters Creek**	160	397.0	290.9	0	NA	NA
Jacks Gulch 1	8	32.2	20.3	2	8.1	5.1
Jacks Gulch 2	30	64.6	47.5	8	17.2	12.7
Jacks Gulch 3	9	44.4	38.6	0	NA	NA
Jacks Gulch 4	1	11.5	9.9	1	11.5	9.9
Jacks Gulch 5	45	167.3	116.3	2	7.4	5.2
Jacks Gulch 6	11	61.6	49.9	0	NA	NA
Little Beaver Creek 1	152	484.0	274.6	11	35.0	19.9
Little Beaver Creek 2	15	190.3	144.1	6	76.1	57.6
Little Beaver Creek 3	24	261.6	154.5	0	NA	NA
Little Beaver Creek 4	25	45.3	34.2	25	45.3	34.2
Mill Creek	2	3.4	1.1	63	108.6	35.7
Monument Gulch	1	1.6	1.5	0	NA	NA
North St Vrain 1**	595	2587.0	377.8	0	NA	NA

North St Vrain 2**	966	2077.4	414.6	0	NA	NA
North St Vrain 3	489	2746.4	2257.7	0	NA	NA
North St Vrain 4*	52	37.1	18.2	192	137.1	67.3
Ouzel Creek**	417	937.1	558.2	0	NA	NA
Pennock Creek 1	53	242.7	114.9	10	45.8	21.7
Pennock Creek 2	22	34.5	25.6	25	39.2	29.1
Phantom Creek	8	48.8	46.1	2	12.2	11.5
Poudre River*	1	0.1	0.1	359	47.3	33.6
South Fork Poudre 1*	90	36.0	20.1	97	38.8	21.6
South Fork Poudre 2	216	233.5	140.1	24	25.9	15.6
South Fork Poudre 3	36	17.3	11.4	0	NA	NA
South Fork Poudre Tributary 1	17	74.4	30.6	0	NA	NA
South Fork Poudre Tributary 2	0	NA	NA	2	3.8	6.9
Stumble Creek 1*	20	28.8	21.3	5	7.2	5.3
Stumble Creek 2	4	87.6	62.2	3	65.7	46.7
Stumble Creek 3	4	19.6	12.1	7	34.3	21.2
Swamp Creek 1	0	NA	NA	10	31.5	20.5
Swamp Creek 2	0	NA	NA	7	19.2	11.3
Swamp Creek 3	0	NA	NA	5	29.0	21.6
Witiak Creek 1	26	64.1	30.0	18	44.3	20.8
Witiak Creek 2	7	37.5	27.0	15	80.4	57.9
Witiak Creek 3	6	45.3	34.6	7	52.8	40.3

* = wood load calculated through extrapolation

** = site was not visited during the Summer 2024 field season; data provided from Bridget Livers

Table 27: Remote Data – Bead Dimensions

Bead Name	Bead Size (ha)	Start Elevation (m)	End Elevation (m)	Channel Length (m)	Total Channel Length (m)	Valley length (km)	Bead Slope	Average Catchment Slope	Sinuosity	Total Sinuosity	FP/Channel Width Ratio
Beaver Brook	17.80	2571	2527	1955	1955	1.55	0.029	0.18	1.26	1.26	73
Beaver Creek 1	1.85	2854	2852	435	435	0.24	0.007	0.16	1.84	1.84	17
Beaver Creek 2	2.31	2843	2841	369	369	0.34	0.006	0.16	1.07	1.07	9
Beaver Creek 3	10.05	2838	2831	1480	1480	0.64	0.010	0.16	2.30	2.30	13
Beaver Creek 4	2.00	2755	2750	496	411	0.25	0.020	0.15	1.62	1.96	6
Big Thompson River	45.23	2462	2438	4206	4206	2.53	0.009	0.24	1.67	1.67	20
Boulder Brook	1.91	2661	2649	691	494	0.34	0.035	0.19	1.44	2.02	31
Cony Creek**	2.88	3031	3022	515	515	0.42	0.022	0.22	1.23	1.23	10
Corral Creek	39.92	3119	3072	4196	4196	2.68	0.018	0.14	1.56	1.56	48
Cow Creek	1.97	2379	2365	784	784	0.62	0.024	0.21	1.26	1.26	17
Elkhorn 1	1.03	2710	2705	245	245	0.17	0.033	0.12	1.41	1.41	35
Elkhorn 2	0.88	2623	2616	269	269	0.22	0.029	0.10	1.20	1.20	20
Fall Creek	4.45	2992	2990	516	516	0.38	0.004	0.24	1.36	1.36	25
Glacier Creek	2.53	2688	2683	380	380	0.28	0.018	0.29	1.37	1.37	16

Hague Creek	17.94	3028	3003	2562	2562	1.74	0.014	0.20	1.48	1.48	17
Hidden Valley Creek	9.43	2802	2791	1016	1016	0.65	0.017	0.21	1.56	1.56	31
Hunters Creek**	2.76	3013	2992	550	550	0.40	0.051	0.24	1.37	1.37	17
Jacks Gulch 1	1.17	2674	2657	395	395	0.25	0.071	0.11	1.59	1.59	517
Jacks Gulch 2	3.52	2622	2604	632	632	0.46	0.039	0.11	1.36	1.36	108
Jacks Gulch 3	0.72	2601	2591	233	233	0.20	0.050	0.11	1.15	1.15	39
Jacks Gulch 4	0.17	2585	2583	101	101	0.09	0.031	0.12	1.16	1.16	25
Jacks Gulch 5	2.41	2560	2549	387	387	0.27	0.039	0.12	1.44	1.44	99
Jacks Gulch 6	0.65	2436	2425	220	220	0.18	0.062	0.12	1.24	1.24	28
Little Beaver Creek 1	2.56	2735	2722	554	554	0.31	0.041	0.14	1.76	1.76	22
Little Beaver Creek 2	0.22	2718	2714	104	104	0.08	0.045	0.14	1.32	1.32	9
Little Beaver Creek 3	0.13	2553	2551	155	155	0.09	0.018	0.15	1.69	1.69	4
Little Beaver Creek 4	2.90	2439	2425	730	730	0.55	0.027	0.15	1.32	1.32	15
Mill Creek	11.50	2567	2548	1763	679	0.58	0.033	0.15	1.17	3.04	43

Monument Gulch	3.43	2686	2659	656	656	0.63	0.044	0.09	1.03	1.03	264
North St Vrain 1**	2.07	3088	3067	232	232	0.23	0.089	0.26	1.01	1.01	23
North St Vrain 2**	3.82	3043	2992	731	731	0.47	0.109	0.26	1.57	1.57	14
North St Vrain 3	1.08	2915	2909	207	207	0.18	0.038	0.25	1.17	1.17	6
North St Vrain 4	35.89	2546	2530	2689	1931	1.40	0.012	0.22	1.38	1.92	30
Ouzel Creek**	2.22	2994	2980	747	747	0.45	0.031	0.27	1.68	1.68	10
Pennock Creek 1	1.01	2536	2530	461	274	0.22	0.028	0.18	1.26	2.11	13
Pennock Creek 2	3.25	2529	2512	860	860	0.64	0.026	0.18	1.35	1.35	17
Phantom Creek	0.51	3192	3185	174	174	0.16	0.040	0.23	1.06	1.06	77
Poudre River	41.31	3247	3073	10692	10692	7.58	0.023	0.19	1.41	1.41	20
South Fork Poudre 1	36.33	2769	2743	4488	4488	2.50	0.010	0.21	1.79	1.79	19
South Fork Poudre 2	7.24	2520	2502	1542	1107	0.93	0.020	0.17	1.20	1.67	18
South Fork Poudre 3	23.59	2408	2375	3164	3164	2.08	0.016	0.16	1.52	1.52	10
South Fork Poudre Tributary 1	1.89	2521	2490	556	556	0.53	0.060	0.11	1.06	1.06	275

South Fork Poudre Tributary 2	0.71	2456	2441	288	288	0.23	0.066	0.11	1.26	1.26	56
Stumble Creek 1	4.21	2854	2812	941	941	0.70	0.062	0.11	1.35	1.35	117
Stumble Creek 2	0.16	2807	2804	64	64	0.05	0.051	0.11	1.41	1.41	56
Stumble Creek 3	1.48	2762	2755	331	331	0.20	0.037	0.11	1.62	1.62	137
Swamp Creek 1	2.84	2710	2702	488	488	0.32	0.025	0.06	1.54	1.54	192
Swamp Creek 2	2.54	2696	2683	622	622	0.36	0.037	0.06	1.71	1.71	59
Swamp Creek 3	0.69	2680	2674	231	231	0.17	0.036	0.06	1.34	1.34	112
Witiak Creek 1	3.45	2856	2840	867	867	0.41	0.040	0.15	2.14	2.14	149
Witiak Creek 2	0.71	2781	2774	259	259	0.19	0.037	0.15	1.39	1.39	53
Witiak Creek 3	0.72	2773	2769	174	174	0.13	0.033	0.15	1.31	1.31	67

** = site was not visited during the Summer 2024 field season; data provided from Bridget Livers
Channel Length = length of primary channel only
Total Channel Length = length of primary and secondary channels

Table 28: Remote Data - StreamStats

Bead Name	DrainageArea (km^2)	Mixed Forest (%)	16H100Y (mm)	Mean Basin Elevation (m)	Precip. (mm)	STORNHD (%)	1% AEP (cms)	50% AEP (cms)
Beaver Brook	12.6	73.2	75	2818	692	0	4.5	1.6
Beaver Creek 1	42.2	55.8	70	3281	605	2	9.1	3.0
Beaver Creek 2	44.0	57.5	70	3268	599	1.9	9.3	3.1
Beaver Creek 3	46.1	59.3	70	3252	592	1.8	9.5	3.1
Beaver Creek 4	53.4	62	70	3210	573	1.6	10.1	3.2
Big Thompson River	102.6	44.6	72	3235	958	0.8	35.4	17.4
Boulder Brook	10.2	49	78	3400	1130	0	7.5	3.9
Cony Creek**	13.1	43.2	77	3406	1006	0.1	8.0	3.8
Corral Creek	13.5	65.3	61	3247	1040	0	8.0	1.4
Cow Creek	23.5	81.2	82	2817	584	0	5.8	1.9
Elkhorn 1	4.7	95.3	73	2979	606	0.1	1.7	0.5
Elkhorn 2	16.2	90.8	74	2824	528	0.4	3.4	1.0
Fall Creek	9.3	39.1	72	3362	635	1.3	3.4	1.1
Glacier Creek	33.9	34.4	79	3332	1144	0.2	20.5	11.2
Hague Creek	35.0	36.2	51	3445	883	0	13.8	6.1
Hidden Valley Creek	8.7	63.5	74	3171	888	0	4.9	2.1
Hunters Creek**	10.8	28.5	78	3544	1090	0	7.9	4.0
Jacks Gulch 1	1.4	98.4	76	2772	446	0	0.4	0.1
Jacks Gulch 2	3.7	95.9	78	2741	442	0	0.9	0.2
Jacks Gulch 3	3.9	95.8	78	2737	442	0	0.9	0.2
Jacks Gulch 4	4.3	95.9	78	2731	441	0	1.0	0.2
Jacks Gulch 5	5.0	94.1	78	2714	439	0	1.1	0.3
Jacks Gulch 6	6.0	94	78	2687	437	0	1.3	0.3
Little Beaver Creek 1	18.1	81	72	3105	546	0	4.2	1.2
Little Beaver Creek 2	18.2	81.1	72	3103	546	0	4.2	1.2
Little Beaver Creek 3	31.3	88.5	74	3003	512	0.4	5.8	1.7
Little Beaver Creek 4	43.5	90.6	75	2907	490	1.4	6.9	2.0

Mill Creek	13.2	80	75	2989	873	0.9	6.2	2.6
Monument Gulch	0.8	91	76	2714	521	0	0.4	0.1
North St Vrain 1**	14.0	13.6	80	3513	1124	0	10.1	5.2
North St Vrain 2**	15.3	20.4	80	3481	1108	1.4	10.5	5.5
North St Vrain 3	18.6	28.9	80	3438	1078	0.2	11.7	5.9
North St Vrain 4	83.4	47.9	77	3306	978	0.3	30.9	15.1
Ouzel Creek**	11.3	14.2	79	3463	1084	1	8.1	4.1
Pennock Creek 1	38.1	87.8	83	3032	593	0.4	8.4	2.8
Pennock Creek 2	43.3	89	83	3003	583	0	9.0	2.9
Phantom Creek	0.4	55	59	3280	856	0	0.4	0.2
Poudre River	38.8	52.9	67	3392	971	0	16.6	7.9
South Fork Poudre 1	38.8	39.4	75	3317	638	0	9.6	3.3
South Fork Poudre 2	103.6	56.1	73	3198	583	0	17.2	5.7
South Fork Poudre 3	233.9	75.4	77	3018	543	0.2	28.6	9.3
South Fork Poudre Tributary 1	1.1	81.2	81	2572	427	0.3	0.3	0.1
South Fork Poudre Tributary 2	1.6	80.2	76	2548	427	0.3	0.5	0.1
Stumble Creek 1	1.5	53.7	51	2941	451	0	0.5	0.1
Stumble Creek 2	1.5	53.2	51	2937	450	0.3	0.5	0.1
Stumble Creek 3	2.0	47.3	74	2912	447	0.3	0.6	0.1
Swamp Creek 1	2.0	87.4	75	2768	475	0.3	0.6	0.1
Swamp Creek 2	3.2	85.8	75	2754	475	1.5	0.8	0.2
Swamp Creek 3	3.4	85.1	51	2751	475	0.5	0.9	0.2
Witiak Creek 1	2.4	93.2	73	3088	477	1.8	0.8	0.2
Witiak Creek 2	2.7	93.2	73	3059	477	1.7	0.8	0.2
Witiak Creek 3	2.8	93.2	73	3053	477	1.5	0.8	0.2

** = site was not visited during the Summer 2024 field season; data provided from Bridget Livers

Table 29: Remote Data – Functionality Indicators

Bead Name	Min. NDVI	Max. NDVI	NDVI Mean	NDVI Range	Min. NDWI	Max. NDWI	NDWI Mean	NDWI Range	# of Patches	Patch Density (per km^2)
Beaver Brook	0.169	0.569	0.429	0.400	-0.882	-0.532	-0.700	0.350	7	39
Beaver Creek 1	0.271	0.529	0.436	0.259	-0.821	-0.609	-0.727	0.213	42	2265
Beaver Creek 2	0.294	0.529	0.430	0.235	-0.796	-0.609	-0.689	0.187	29	1254
Beaver Creek 3	0.075	0.553	0.380	0.478	-0.815	-0.421	-0.684	0.394	78	776
Beaver Creek 4	0.020	0.443	0.349	0.424	-0.729	-0.393	-0.654	0.335	31	1547
Big Thompson River	0.059	0.569	0.422	0.510	-0.841	-0.405	-0.695	0.436	58	128
Boulder Brook	0.161	0.451	0.354	0.290	-0.771	-0.513	-0.676	0.257	87	4561
Cony Creek**	0.373	0.569	0.484	0.196	-0.896	-0.706	-0.817	0.190	6	208
Corral Creek	0.051	0.506	0.372	0.455	-0.821	-0.425	-0.660	0.397	61	153
Cow Creek	0.106	0.435	0.357	0.329	-0.747	-0.500	-0.629	0.247	131	6642
Elkhorn 1	0.271	0.451	0.405	0.180	-0.796	-0.624	-0.717	0.172	19	1843
Elkhorn 2	0.318	0.490	0.422	0.173	-0.855	-0.640	-0.711	0.215	42	4762
Fall Creek	0.216	0.569	0.371	0.353	-0.875	-0.545	-0.658	0.330	48	1078
Glacier Creek	0.263	0.522	0.410	0.259	-0.925	-0.645	-0.740	0.279	52	2056
Hague Creek	0.114	0.490	0.386	0.376	-0.875	-0.522	-0.690	0.353	69	385
Hidden Valley Creek	0.208	0.529	0.400	0.322	-0.759	-0.536	-0.664	0.222	56	594
Hunters Creek**	0.349	0.514	0.453	0.165	-0.882	-0.723	-0.806	0.159	5	181
Jacks Gulch 1	0.318	0.467	0.411	0.149	-0.771	-0.635	-0.689	0.136	6	512
Jacks Gulch 2	0.278	0.506	0.425	0.227	-0.815	-0.584	-0.705	0.231	46	1307
Jacks Gulch 3	0.169	0.569	0.429	0.400	-0.882	-0.532	-0.700	0.350	5	693
Jacks Gulch 4	0.271	0.529	0.436	0.259	-0.821	-0.609	-0.727	0.213	3	1803
Jacks Gulch 5	0.294	0.529	0.430	0.235	-0.796	-0.609	-0.689	0.187	10	457
Jacks Gulch 6	0.075	0.553	0.380	0.478	-0.815	-0.421	-0.684	0.394	5	772
Little Beaver Creek 1	0.020	0.443	0.349	0.424	-0.729	-0.393	-0.654	0.335	33	1290
Little Beaver Creek 2	0.059	0.569	0.422	0.510	-0.841	-0.405	-0.695	0.436	17	7687
Little Beaver Creek 3	0.161	0.451	0.354	0.290	-0.771	-0.513	-0.676	0.257	7	5257

Little Beaver Creek 4	0.271	0.522	0.442	0.251	-0.841	-0.594	-0.703	0.247	59	2033
Mill Creek	0.255	0.569	0.436	0.314	-0.917	-0.589	-0.684	0.329	72	626
Monument Gulch	0.357	0.553	0.498	0.196	-0.954	-0.656	-0.771	0.298	5	146
North St Vrain 1**	0.278	0.506	0.417	0.227	-0.861	-0.650	-0.783	0.211	14	677
North St Vrain 2**	0.302	0.498	0.418	0.196	-0.875	-0.683	-0.789	0.192	18	471
North St Vrain 3	0.373	0.553	0.477	0.180	-0.910	-0.771	-0.838	0.139	11	1022
North St Vrain 4	0.184	0.522	0.403	0.337	-0.910	-0.574	-0.720	0.336	116	323
Ouzel Creek**	0.145	0.490	0.333	0.345	-0.848	-0.522	-0.685	0.325	13	585
Pennock Creek 1	0.208	0.388	0.322	0.180	-0.689	-0.564	-0.627	0.124	45	4434
Pennock Creek 2	0.153	0.396	0.327	0.243	-0.723	-0.513	-0.643	0.210	84	2585
Phantom Creek	0.333	0.451	0.389	0.118	-0.783	-0.614	-0.676	0.169	8	1570
Poudre River	0.059	0.506	0.355	0.447	-0.783	-0.483	-0.650	0.301	83	201
South Fork Poudre 1	0.114	0.537	0.362	0.424	-0.777	-0.461	-0.629	0.316	83	228
South Fork Poudre 2	0.208	0.404	0.326	0.196	-0.729	-0.550	-0.655	0.179	38	525
South Fork Poudre 3	0.208	0.529	0.389	0.322	-0.848	-0.555	-0.688	0.293	37	157
South Fork Poudre Tributary 1	0.216	0.522	0.411	0.306	-0.815	-0.555	-0.718	0.260	11	581
South Fork Poudre Tributary 2	0.263	0.459	0.371	0.196	-0.735	-0.614	-0.683	0.121	9	1263
Stumble Creek 1	0.153	0.451	0.366	0.298	-0.783	-0.550	-0.670	0.233	19	451
Stumble Creek 2	0.255	0.396	0.354	0.141	-0.689	-0.594	-0.638	0.095	10	6282
Stumble Creek 3	0.247	0.435	0.388	0.188	-0.753	-0.619	-0.678	0.134	29	1963
Swamp Creek 1	0.247	0.490	0.433	0.243	-0.802	-0.619	-0.715	0.183	49	1725
Swamp Creek 2	0.247	0.490	0.407	0.243	-0.821	-0.645	-0.713	0.176	41	1613
Swamp Creek 3	0.302	0.459	0.385	0.157	-0.771	-0.650	-0.698	0.120	21	3040
Witiak Creek 1	0.318	0.498	0.430	0.180	-0.828	-0.650	-0.724	0.177	84	2432
Witiak Creek 2	0.263	0.522	0.420	0.259	-0.789	-0.640	-0.703	0.150	48	6746
Witiak Creek 3	0.325	0.475	0.412	0.149	-0.765	-0.661	-0.712	0.103	18	2498

** = site was not visited during the Summer 2024 field season; data provided from Bridget Livers

Table 30: Remote Data - dNBR

Bead Name	Percentage of Catchment Severely Burnt	Percentage of Catchment Burnt (Low-Severe)	Ratio of Severe to Total Burn
Beaver Brook	0.27	11.60	0.023
Beaver Creek 1	12.74	45.21	0.282
Beaver Creek 2	12.33	45.09	0.274
Beaver Creek 3	12.24	45.74	0.268
Beaver Creek 4	11.32	46.12	0.246
Big Thompson River	4.08	23.48	0.174
Boulder Brook	0.27	2.98	0.089
Cony Creek**	3.91	19.76	0.198
Corral Creek	3.06	22.61	0.135
Cow Creek	0	0.27	NA
Elkhorn 1	39.52	92.53	0.427
Elkhorn 2	15.46	74.44	0.208
Fall Creek	3.84	18.34	0.210
Glacier Creek	3.64	18.23	0.200
Hague Creek	19.98	55.89	0.357
Hidden Valley Creek	0.17	3.60	0.046
Hunters Creek**	2.32	9.57	0.242
Jacks Gulch 1	15.27	95.27	0.160
Jacks Gulch 2	8.70	93.28	0.093
Jacks Gulch 3	8.51	93.36	0.091
Jacks Gulch 4	8.43	93.04	0.091
Jacks Gulch 5	7.83	92.03	0.085
Jacks Gulch 6	9.41	92.60	0.102
Little Beaver Creek 1	39.80	77.61	0.513
Little Beaver Creek 2	39.71	77.76	0.511
Little Beaver Creek 3	40.60	86.12	0.471
Little Beaver Creek 4	32.12	87.89	0.365
Mill Creek	1.16	25.96	0.045
Monument Gulch	5.52	67.91	0.081
North St Vrain 1**	7.89	36.40	0.217
North St Vrain 2**	7.22	33.45	0.216
North St Vrain 3	5.94	27.66	0.215
North St Vrain 4	3.42	15.15	0.226
Ouzel Creek**	8.04	29.80	0.270
Pennock Creek 1	0.82	7.74	0.105
Pennock Creek 2	4.11	18.29	0.225
Phantom Creek	0	0.73	NA

Poudre River	0.31	8.23	0.037
South Fork Poudre 1	2.46	16.39	0.150
South Fork Poudre 2	7.37	35.99	0.205
South Fork Poudre 3	12.08	47.68	0.253
South Fork Poudre Tributary 1	3.29	87.84	0.038
South Fork Poudre Tributary 2	2.43	87.40	0.028
Stumble Creek 1	4.96	63.56	0.078
Stumble Creek 2	6.39	63.99	0.100
Stumble Creek 3	5.51	58.42	0.094
Swamp Creek 1	3.63	45.91	0.079
Swamp Creek 2	4.14	51.28	0.081
Swamp Creek 3	3.89	51.19	0.076
Witiak Creek 1	7.01	28.67	0.244
Witiak Creek 2	9.38	35.26	0.266
Witiak Creek 3	9.13	35.03	0.261

** = site was not visited during the Summer 2024 field season; data provided from Bridget Livers

Table 31: One-way ANOVA/Kruskal-Wallis Tests and pairwise comparisons for type category, with escalating levels of statistical significance shown in bolding, bolding and underline, and bolding, underline, and italics.

Variable	Transformation	p-value	EG-BM	BM-FC	FC-EG
Bead Size (sq km)	log	***<u>≤0.001</u>***	***<u>≤0.001</u>***	0.442	***<u>≤0.001</u>***
Bead Slope	log	**0.045**	0.214	0.237	**0.035**
Bead Ratio	log	**0.014**	0.296	0.054	**0.013**
Floodplain-Channel Width Ratio	log	**<u>0.00133</u>**	0.439	***<u>≤0.001</u>***	0.192
Total Sinuosity	log	0.563	0.994	0.533	0.771
Average Catchment Slope	none (normal)	***<u>≤0.001</u>***	0.183	***<u>≤0.001</u>***	0.320
High Severity Burn (%)	log + 1	0.278	0.683	0.433	0.265
Total Burn (%)	*none (NP)*	0.264	0.389	1.00	1.00
Burn Ratio	log + 0.1	**0.026**	0.999	**0.021**	0.118
Drainage Area (sq km)	log	**0.014**	**0.015**	0.356	0.369
Mixed Forest (%)	*none (NP)*	**<u>0.002</u>**	0.189	**<u>0.0035</u>**	1.00
16H100Y (mm)	*none (NP)*	**0.026**	0.305	0.180	**0.022**
1% AEP (cms)	*none (NP)*	**<u>0.0021</u>**	**<u>0.0076</u>**	0.077	1.00
50% AEP (cms)	*none (NP)*	***<u>≤0.001</u>***	**0.011**	**0.016**	1.00
Average Catchment Elevation (m)	none (normal)	***<u>≤0.001</u>***	0.130	***<u>≤0.001</u>***	0.361
Berm Density (berms/km VL)	*none (NP)*	**<u>0.0061</u>**	0.637	**<u>0.0059</u>**	0.672
Minimum Berm Count	*none (NP)*	0.845	1.00	1.00	1.00
Wood Density (wood/km VL)	log + 5	***<u>≤0.001</u>***	**0.018**	***<u>≤0.001</u>***	***<u>≤0.001</u>***
Yearly Precipitation (mm)	*none (NP)*	***<u>≤0.001</u>***	0.054	**<u>0.0038</u>**	1.00
STORNHD (%)	*none (NP)*	0.081	1.00	0.076	0.722

Minimum Bead NDVI	*none (NP)*	***<0.001***	**0.012**	0.097	***<0.001***
Maximum Bead NDVI	*none (NP)*	0.1711	0.211	1.00	1.00
Average Bead NDVI	none (normal)	0.236	0.19	0.255	0.314
Bead NDVI Range	log	***<0.001***	***<0.001***	0.321	***<0.001***
Minimum Bead NDWI	none (normal)	**0.021**	0.296	**0.026**	0.757
Maximum Bead NDWI	none (normal)	***<0.001***	**0.0032**	**0.0021**	***<0.001***
Average Bead NDWI	1/x	***<0.001***	0.742	***<0.001***	***<0.001***
Bead NDWI Range	sqrt	***<0.001***	***<0.001***	0.502	***<0.001***
Patch Density (patches/sq km)	log	***<0.001***	**0.0017**	0.417	***<0.001***
Patch Count	*none (NP)*	**0.013**	0.967	**0.030**	**0.023**

Table 32: One-way ANOVA/Kruskal-Wallis Tests and pairwise comparisons for status category, with escalating levels of statistical significance shown in bolding, bolding and underline, and bolding, underline, and italics.

Variable	Transformation	p-value	Imp-Nat	Imp-Rest	Nat-Rest
Bead Size (sq km)	log	0.188	0.163	0.901	0.784
Bead Slope	log	***<u>≤0.001</u>***	***<u>≤0.001</u>***	0.126	0.604
Bead Ratio	log	**0.017**	**0.012**	0.657	0.652
Floodplain-Channel Width Ratio	log	***<u>≤0.001</u>***	***<u>≤0.001</u>***	0.238	0.471
Total Sinuosity	log	0.260	0.320	0.448	0.930
Average Catchment Slope	none (normal)	0.412	0.386	0.815	0.983
High Severity Burn (%)	log + 1	0.361	0.618	0.383	0.712
Total Burn (%)	*none (NP)*	0.474	0.708	1.00	1.00
Burn Ratio	log + 0.1	**0.017**	**0.041**	0.064	0.678
Drainage Area (sq km)	log	***<u>≤0.001</u>***	***<u>≤0.001</u>***	0.234	0.133
Mixed Forest (%)	*none (NP)*	0.582	1.00	1.00	1.00
16H100Y (mm)	*none (NP)*	0.259	0.363	0.948	1.00
1% AEP (cms)	*none (NP)*	**<u>0.0014</u>**	***<u>≤0.001</u>***	0.551	1.00
50% AEP (cms)	*none (NP)*	**<u>0.0067</u>**	**<u>0.005</u>**	0.584	1.00
Average Catchment Elevation (m)	none (normal)	0.052	0.187	0.075	0.459
Berm Density (berms/km VL)	*none (NP)*	0.118	0.117	1.00	1.00
Minimum Berm Count	*none (NP)*	**0.015**	0.912	1.00	1.00
Wood Density (wood/km VL)	log + 5	0.783	0.765	0.986	0.965
Yearly Precipitation (mm)	*none (NP)*	0.175	0.192	1.00	1.00
STORNHD (%)	*none (NP)*	0.363	1.00	0.591	0.48

Minimum Bead NDVI	*none (NP)*	**0.011**	**0.018**	1.00	0.155
Maximum Bead NDVI	*none (NP)*	0.287	1.00	0.356	0.763
Average Bead NDVI	none (normal)	**0.034**	0.073	0.765	0.111
Bead NDVI Range	log	0.17	0.145	0.835	0.840
Minimum Bead NDWI	none (normal)	0.178	0.481	0.548	0.194
Maximum Bead NDWI	none (normal)	**0.0012**	**0.001**	0.932	0.142
Average Bead NDWI	1/x	**0.012**	**0.025**	0.826	0.079
Bead NDWI Range	sqrt	0.06	**0.048**	0.571	0.906
Patch Density (patches/sq km)	log	0.851	0.907	0.874	0.966
Patch Count	*none (NP)*	**0.0088**	**0.0066**	0.612	1.00

Table 33: Two-sample t-tests/Mann-Whitney U Tests for elevation zone category, with escalating levels of statistical significance shown in bolding, bolding and underline, and bolding, underline, and italics.

Variable	**Transformation**	**p-value**
Bead Size (sq km)	log	0.249
Bead Slope	log	0.724
Bead Ratio	log	0.897
Floodplain-Channel Width Ratio	log	**0.014**
Total Sinuosity	log	0.181
Average Catchment Slope	none (normal)	***<u>≤0.001</u>***
High Severity Burn (%)	log + 1	0.338
Total Burn (%)	*none (NP)*	**0.011**
Burn Ratio	log + 0.1	0.47
Drainage Area (sq km)	log	0.547
Mixed Forest (%)	*none (NP)*	***<u>≤0.001</u>***
16H100Y (mm)	*none (NP)*	0.736
1% AEP (cms)	*none (NP)*	**0.027**
50% AEP (cms)	*none (NP)*	**<u>0.0083</u>**
Average Catchment Elevation (m)	none (normal)	***<u>≤0.001</u>***
Berm Density (berms/km VL)	*none (NP)*	0.078
Minimum Berm Count	*none (NP)*	0.562
Wood Density (wood/km VL)	log + 5	0.134
Yearly Precipitation (mm)	*none (NP)*	***<u>≤0.001</u>***
STORNHD (%)	*none (NP)*	0.180
Minimum Bead NDVI	*none (NP)*	0.672
Maximum Bead NDVI	*none (NP)*	0.167
Average Bead NDVI	none (normal)	0.645
Bead NDVI Range	log	0.487
Minimum Bead NDWI	none (normal)	**<u>0.0062</u>**
Maximum Bead NDWI	none (normal)	0.638
Average Bead NDWI	1/x	0.7786
Bead NDWI Range	sqrt	0.157
Patch Density (patches/sq km)	log	**0.017**
Patch Count	*none (NP)*	0.480

Table 34: Correlation matrix for all predictor variables, color coded for strength of association.

	BSi	BeR	BSlo	FPCR	TSin	ACS	HSB	TB	BuR	DrA	MFP	16H	SN	1pct	50pct	ACE	BD	MBC	WD	CP
BSi																				
BeR																				
BSlo																				
FPCR																				
TSin																				
ACS																				
HSB																				
TB																				
BuR																				
DrA																				
MFP																				
16H																				
SN																				
1pct																				
50pct																				
ACE																				
BD																				
MBC																				
WD																				
CP																				

**BSi = Bead Size, BeR = Bead Ratio, BSlo = Bead Slope, FPCR = Floodplain-Channel Width Ratio, Tsin = Total Sinuosity, ACS/E = Avg Catchment Slope/Elev, HBS = High Sev Burn %, TB = Total Burn %, BuR = Burn Ratio, DrA = Drainage Area, MFP = Mixed Forest %, 16H = 16H100Y, SN = STORNHD, 1pct = 1% AEP, 50pct = 50% AEP, BD = Berm Density, MBC = Min Berm Count, WD = Wood Density, CP = Catchment Precipitation

Color code: 0.01 – 0.1, Light pink; 0.11 – 0.6, Salmon; 0.61 – 0.99, Bright red; -0.1 – -0.01, Light blue; -0.6 – -0.11, Medium blue; -0.99 – -0.61; Bright blue; White = 0, Burgundy = 1

Table 35: Correlation matrix p-values, bolded and/or underlined for statistical significance at α=0.05.

	BSi	BeR	BSlo	FPCR	Tsin	ACS	HSB	TB	BuR	DrA	MFP	16H	SN	1pct	50pct	ACE	BD	MBC	WD	CP
BSi		0.08	**0.00**	0.27	0.12	0.07	0.11	**0.01**	0.50	**0.00**	0.06	0.25	0.96	**0.00**	**0.00**	**0.03**	0.66	**0.00**	0.18	**0.01**
BeR	0.08		0.44	**0.00**	0.50	0.06	**0.04**	0.89	**0.00**	0.08	0.45	0.08	0.06	0.09	0.10	0.12	0.12	0.37	0.06	0.71
Bslo	**0.00**	0.44		**0.01**	0.07	0.43	0.92	**0.02**	0.25	**0.00**	0.99	0.40	0.56	**0.00**	**0.03**	0.14	**0.02**	0.06	0.24	0.85
FPCR	0.27	**0.00**	**0.01**		0.48	**0.00**	0.48	**0.01**	**0.03**	**0.03**	**0.01**	0.93	**0.03**	**0.01**	**0.01**	**0.00**	0.14	0.34	0.10	**0.01**
TSin	0.12	0.50	0.07	0.48		0.85	0.86	0.07	0.53	0.20	0.89	0.84	0.55	0.13	0.21	0.18	0.26	0.21	0.41	0.43
ACS	0.07	0.06	0.43	**0.00**	0.85		0.18	**0.00**	0.24	0.09	**0.00**	0.12	**0.00**	**0.00**	**0.00**	**0.00**	0.72	0.27	**0.00**	**0.00**
HSB	0.11	**0.04**	0.92	0.48	0.86	0.18		**0.00**	**0.00**	0.68	**0.05**	0.68	0.37	0.54	0.32	0.72	0.74	0.19	0.53	**0.05**
TB	**0.01**	0.89	**0.02**	**0.01**	0.07	**0.00**	**0.00**		0.11	0.22	**0.00**	0.86	0.01	**0.00**	**0.00**	**0.00**	0.06	0.02	0.44	**0.00**
BuR	0.50	**0.00**	0.25	**0.03**	0.53	0.24	**0.00**	0.11		0.10	0.69	0.99	0.19	0.16	0.30	**0.01**	0.37	0.34	0.06	0.85
DrA	**0.00**	0.08	**0.00**	**0.03**	0.20	0.09	0.68	0.22	0.10		0.33	0.57	0.12	**0.00**	**0.00**	0.11	0.95	0.29	0.95	0.52
MFP	0.06	0.45	0.99	**0.01**	0.89	**0.00**	**0.05**	**0.00**	0.69	0.33		0.42	**0.00**	**0.00**	**0.00**	**0.00**	0.52	0.30	**0.00**	**0.00**
16H	0.25	0.08	0.40	0.93	0.84	0.12	0.68	0.86	0.99	0.57	0.42		0.87	0.48	0.41	0.57	0.52	0.40	0.11	0.53
SN	0.96	0.06	0.56	**0.03**	0.55	**0.00**	0.37	0.01	0.19	0.12	**0.00**	0.87		**0.00**	**0.00**	**0.00**	0.39	0.68	**0.00**	**0.00**
1	**0.00**	0.09	**0.00**	**0.01**	0.13	**0.00**	0.54	**0.00**	0.16	**0.00**	**0.00**	0.48	**0.00**		**0.00**	**0.00**	0.45	**0.01**	0.37	**0.00**
50	**0.00**	0.10	**0.03**	**0.01**	0.21	**0.00**	0.32	**0.00**	0.30	**0.00**	**0.00**	0.41	**0.00**	**0.00**		**0.00**	0.39	**0.01**	0.24	**0.00**
ACE	**0.03**	0.12	0.14	**0.00**	0.18	**0.00**	0.72	**0.00**	**0.01**	0.11	**0.00**	0.57	**0.00**	**0.00**	**0.00**		0.56	0.06	**0.00**	**0.00**
BD	0.66	0.12	**0.02**	0.14	0.26	0.72	0.74	0.06	0.37	0.95	0.52	0.52	0.39	0.45	0.39	0.56		**0.01**	**0.03**	0.93
MBC	**0.00**	0.37	0.06	0.34	0.21	0.27	0.19	**0.02**	0.34	0.29	0.30	0.40	0.68	**0.01**	**0.01**	0.06	**0.01**		0.26	**0.04**
WD	0.18	0.06	0.24	0.10	0.41	**0.00**	0.53	0.44	0.06	0.95	**0.00**	0.11	**0.00**	0.37	0.24	**0.00**	**0.03**	0.26		**0.00**
CP	**0.01**	0.71	0.85	**0.01**	0.43	**0.00**	0.05	**0.00**	0.85	0.52	**0.00**	0.53	**0.00**	**0.00**	**0.00**	**0.00**	0.93	**0.04**	**0.00**	

**BSi = Bead Size, BeR = Bead Ratio, BSlo = Bead Slope, FPCR = Floodplain-Channel Width Ratio, Tsin = Total Sinuosity, ACS/E = Avg Catchment Slope/Elev, HBS = High Sev Burn %, TB = Total Burn %, BuR = Burn Ratio, DrA = Drainage Area, MFP = Mixed Forest %, 16H = 16H100Y, SN = STORNHD, 1pct = 1% AEP, 50pct = 50% AEP, BD = Berm Density, MBC = Min Berm Count, WD = Wood Density, CP = Catchment Precipitation

13. APPENDIX 3 – SITE DESCRIPTIONS

Field Indicators of Connectivity

Prior to calculating functionality response metrics, indicators of connectivity and height of water table were documented in the field. These indicators of connectivity were assumed to be associated with greater bead functionality and higher response metrics. Rivers flow where the water table meets the surface of the Earth, but a high floodplain water table indicates higher lateral connectivity between adjacent uplands and the stream corridor (via groundwater) and between the channel and floodplain (via hyporheic exchange flows). Observed groundwater inputs were primarily upwellings and perched saturated surfaces (Figure 21).

Perched saturated surface in channel-adjacent wet meadow at the third bead on Beaver Creek. Flowing water feeds the creek.

Uplands water inputs flowing into the channel at the first bead on Beaver Creek.

Subsurface water inputs at the second bead on Jacks Gulch. This water feeds a channel-adjacent wet meadow.

Channel-adjacent water inputs at Fall Creek. Towards the top of the image are large, well-defined deposits associated with beaver activity.

Figure 21: Indicators of floodplain-channel connectivity photographed at various sites in the field

Upwellings were photographed at Jacks Gulch (JG2), Fall Creek, Beaver Creek (BC1), Monument Gulch, and the South Fork Poudre Tributary (SFPT1); other sites may have had additional groundwater activity that was not found during field activities. The latter two beads

appeared to have complex groundwater dynamics, wherein surface water flow disappeared into large wetlands and reappeared farther downstream in distinct channels. Groundwater and hyporheic inputs were varied in elevation, morphology, and estimated discharge. Most were small seeps with low discharge (visually estimated at <50 ml/sec) adjacent to the channel and located at or slightly above the elevation of the water surface. A particularly large upwelling with an opening of approximately 1 m and a higher discharge rate (visually estimated at ~1 L/sec) was observed in the floodplain at Jacks Gulch. Flowing conduit-type upwellings were not observed at any other site. This particular upwelling was associated with widespread floodplain inundation, although extensive beaver modification is also likely to have contributed to the higher water table and subsequent ponding and storage of water in this bead. Upwellings were associated with small clusters of different vegetation classes, particularly mosses, wildflowers, and marsh grasses.

Perched groundwater surfaces in the form of ponded wetlands located above the elevation of the primary channel were observed at Beaver Creek (BC3) and Jacks Gulch (JG6). These surfaces intersected channelized flow at the banks, resulting in an artificial knickpoint and measurable flow from the surface into the channel. Flow rates were moderate (visually estimated at 100-200 ml/sec). Flow rate variability is unknown but likely depends on precipitation, time of year, and other factors. In addition, widespread presence of wetlands in beads, particularly beaver meadows, implies the importance of these features in defining bead boundaries and impacting their ability to attenuate fluxes of water. Wetlands are also sites of biogeochemical importance, hosting diverse varieties of microbial communities and organisms that improve water quality by encouraging deposition of fine sediment and sorption of metals, pollutants, and other harmful substances impacting water quality (Ferreira et al., 2023). Groundwater dynamics

were not directly measured in this study, but the variations in groundwater connectivity and types of surface-subsurface exchange observed in beads warrant future investigation into hydrology and subsurface water storage and conveyance in these corridors.

Field Indicators of Impairment

Indicators of impairment were also observed and documented in the field prior to formal data analysis. These indicators of connectivity were assumed to be associated with lesser bead functionality and lower response metrics. Biotic and geomorphic effects associated with impairment include channel incision, loss of floodplain-channel connectivity, bank instability, and decrease in patch heterogeneity. Known or detected bead impairment did not appear to have one cause; human infrastructure (diversions, roads, construction, modification of the floodplain), ecosystem imbalance (ungulate over-browsing, loss of beaver), and disturbance-initiated changes in the sediment regime all seemed to play a role in bead evolution into an impaired state. In particular, single-thread systems with tall banks, typically in elk grasslands or relict beaver meadows, were assessed visually for signs of impaired connectivity.

Degree of channel incision was difficult to quantify in the field due to a lack of repeat visits; additionally, calculating critical bank height, or the minimum height resulting in bank instability and changes in bank morphology, is difficult and time-consuming. However, signs of connectivity loss were more easily found and documented to provide a snapshot of functionality in beads (Figure 22). Loss of floodplain-channel connectivity was most commonly observed in the field through bank instability, mass movements, and channel incision. Bank instabilities and mass movements varied in size and lateral extent. Tension cracks, which are small fissures in bank-adjacent riparian zones, are indicative of bank-related stress and are often activated following incision. Tension cracks were observed at several beads. Bank collapses of varied

sizes and geometries were also observed. Collapses were generally small and columnar in shape, but one laterally extensive bank collapse was observed at the fourth bead on Little Beaver Creek (Figure 22).

Incised river channel on Beaver Brook at Upper Beaver Meadows, RMNP.

Bank collapses on river left on the Big Thompson River at Moraine Park, RMNP.

Large block failure of left bank at fourth bead on Little Beaver Creek. Felled bank trees have created local knickpoints; tree conditions suggest this failure is recent.

Incised river corridor and exposed cut bank on river right at the sixth bead on Jacks Gulch.

Figure 22: Indicators of impairment photographed at various sites in the field. Flow direction denoted with yellow arrow.

In some cases, bank collapse fragments with cohesive and dense roots may behave as clasts, retaining their structure, diverting flow, and undergoing periodic transport depending on

their size and configuration in the channel. The erosion rates and breakdown of these fragments are unclear, but it is assumed that bank sediment will eventually be stripped away by the current, leaving behind a floating vegetation mass that can be more easily transported downstream. These fragments were observed most prominently on the Big Thompson River at Moraine Park (Figure 23), although other examples were found at several other impaired beads.

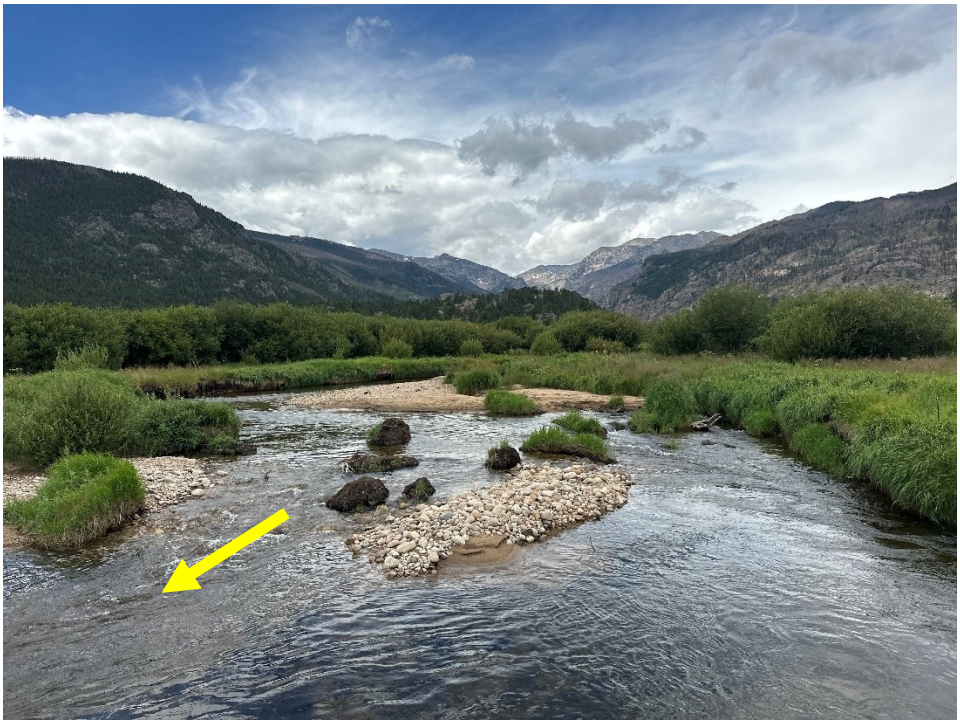

Figure 23: Cohesive bank fragments in the Big Thompson River at Moraine Park, RMNP. Note varied sizes, configurations, and states of "decay". Flow direction denoted with yellow arrow.

Beaver Modifications

Berm conditions ranged from active, intact beaver dams to fragmented and completely breached berms (Figure 24). Berms in elk grasslands with retained beaver modification signatures were breached and of short stature but often continued to exert control on river channel morphology. Berms in beaver meadows were observed to be taller – possibly less eroded – and often populated with dense willow colonies. Recent beaver activity was observed at

several sites, but recent damming was not observed at any site. Thus, nearly all of these berms were breached; like grassland berms, though, these berms still exert strong controls on river channel morphology. Breach dimensions depended on flow geometry and discharge; breaches on larger, higher-discharge channels were wider, and breaches on smaller, lower-discharge channels were narrower. Although breaches often result in a localized collapse of the berm, some breaches were small enough to resist structural instabilities in the berm for an (assumed) temporary period, creating a tunnel through the berm, referred to as a "bridge".

Breached beaver dam in floodplain of second bead on Jacks Gulch. Site appears to be abandoned. Age is unknown; satellite imagery shows episodic ponding and indicates periodic beaver occupation from pre-1985 until about 2019.

Breached beaver dam at fourth bead on Beaver Creek. Ellen Wohl for scale. Flow direction denoted with yellow arrow.

Figure 24: Breached berms in the field.

Mill Creek, the North St. Vrain at Wild Basin, the first bead on Pennock Creek, and the fifth bead on Jacks Gulch had the only intact unvegetated beaver berms (Figure 25) found in the study. The former two of these dams were located in the floodplain off the main channel,

although ponding and floodplain inundation caused by the damming propagated longitudinally and laterally within each bead. The latter two were located on the primary channel and created major knickpoints and some flow diversion, as well as the slowing and ponding of water. All beaver berms were associated with thickly bedded deposits of fine, dark, organic-rich sediment, also known as “beaver fill”. Deposition of beaver fill occurred primarily in the ponded areas adjacent to the berm. However, bank cross sections and sediment bars implied both active and relict fluvial transport of beaver fill (Figure 25).

Intact beaver dam in inundated floodplain of Mill Creek at Hollowell Park, RMNP. Dam is approximately 12-14 years old as estimated from Google Earth satellite imagery. It is unclear whether the site is active or abandoned.

Intact bank beaver dam in inundated floodplain of the North St. Vrain River at Wild Basin, RMNP. Age is unknown and it is unclear whether the site is active or abandoned, but adjacent willow chew and smaller dams on secondary channels nearby imply ongoing presence of beaver.

Intact beaver berm on primary channel at fifth bead on Jacks Gulch. Age is unknown and berm appears to be abandoned. Flow direction denoted with yellow arrow. Berm is difficult to see.

Intact beaver berm on primary channel at first bead on Pennock Creek. Age is unknown t is unclear whether berm is active or abandoned. Flow direction denoted with yellow arrow.

Figure 25: Active beaver berms from various sites.

Although berms were the only field-measured beaver modification, other varieties of channel and floodplain alterations initiated by beaver were observed and documented. Hydrologic and biotic interactions with beaver alterations can have lasting effects on the heterogeneity, flux attenuation potential, structure, and geometry of beads. Such alterations include deposition of distinct sediment sequences, loading of carbon-rich soils into the fluvial corridor, addition of downed wood into the channel and floodplain, introduction of topographic variations in vegetation, construction of narrow secondary channels in the floodplain ("beaver canals"), floodplain inundation, and the creation, draining, and infilling of ponded zones (Figure 25). Thus, noting the presence of beaver habitats documented additional varieties of bead complexity.

Deposits associated with beaver chew on river left at Lower Elkhorn Creek. Chewed wood and layered deposits of light-colored fluvially-transported sands/fines and dark, organic-rich beaver fill.

Floodplain beaver-chewed stumps and felled log at the fifth bead on Jacks Gulch.

Cross-sectional view of large breached berm at Boulder Brook, RMNP. Note extensive willow colonization on top of the berm. Ellen Wohl for scale.

Relict beaver canal in the floodplain at Fall Creek. Satellite imagery and field exploration suggest that beaver are not presently active at this cite. Canal outlined in white dashed lines.

Figure 20: Other varieties of beaver modification noted and photographed in the field.

Channel morphology in beads can also be controlled by active and relict beaver modification. Beaver fill is especially resistant to erosion, often initiating channel rerouting and a subsequent breach of the least cohesive segment, typically towards the valley edges (Figure 23). River bend geometry and presence of straight segments running perpendicular to valley length were often used to delineate berms in the field; beaver-initiated changes in river morphology appeared to persist beyond the breaching of the dam and loss of the topographic signal of the berm. Beaver fill is also an efficient storer of water due to its high organic carbon content and richness in clays and silts, and the persistence of berms and beaver fill deposits appeared to have a powerful and lasting effect on bead hydrology by structurally facilitating the ponded and entrapment of water both in the surface and subsurface.

Figure 21: Beaver fill, wet and almost mulch-like, from a berm on Swamp Creek (left). Aeolian deposition of silt and clay contributes to low permeability of this material. Pen for scale. Aerial view of unusual river morphology associated with this particular berm (right), including a nearly 90-degree turn and a straight segment.

14. APPENDIX 4 – ADDITIONAL FIELD PHOTOS

First large logjam on river right on the South Fork Poudre River at Lazy D Ranch. Jam diverts but does not block flow. Field personnel for scale. Flow direction denoted with yellow arrow.

Mostly intact beaver berm spanning the width of the second bead on Swamp Creek. Note berm breach in foreground and retention of ponded water and dark, organic-rich sediment. Flow direction denoted with yellow arrow.

Second large logjam on the South Fork Poudre River at Lazy D Ranch. Jam spans entire channel and has accumulated additional material over several years. Field personnel for scale. Flow direction denoted with yellow arrow.

Aerial view of SFP2 Jam. Photo credit Larimer Conservation District. Flow direction denoted with yellow arrow.

Second active beaver berm on primary channel at the first bead on Pennock Creek. Flow direction denoted with yellow arrow.